Role of Cardiac Catecholamines in Embryos and Adults Under Stress

2014

Candice Baker
University of Central Florida

ROLE OF CARDIAC CATECHOLAMINES IN EMBRYOS AND ADULTS UNDER STRESS

by

CANDICE BAKER
B.S. University of Central Florida, 2007
M.S. University of Central Florida, 2011

A dissertation submitted in partial fulfillment of the requirements
for the degree of Doctor of Philosophy
in the Burnett School of Biomedical Sciences
in the College of Graduate Studies
at the University of Central Florida
Orlando, Florida

Fall Term
2014

Major Professor: Steven N. Ebert

ABSTRACT

Cardiovascular disease is responsible for the loss of one life every 38 seconds and accounts for 26.6 percent of all infants that die of congenital birth defects. Adrenergic hormones are critically important regulators of cardiovascular physiology in embryos and adults. They are key mediators of stress responses and have profound stimulatory effects on cardiovascular function, and dysregulation of adrenergic function has been associated with many adverse cardiac conditions, including congenital malformations, arrhythmias, ischemic heart disease, heart failure, and sudden cardiac death. Despite intensive study, the specific roles these hormones play in the developing heart is not well-understood. Further, there is little information available regarding how these important hormones mediate stress responses in adult females (before and after menopause) in comparison to males. My thesis thus has two major foci: (1) What role(s) do catecholamines play in the embryonic heart?, and (2) Do catecholamines differentially influence cardiac function in aging male and female hearts?

Initially, we sought to uncover the roles of adrenergic hormones in the embryonic heart by utilizing an adrenergic-deficient (*Dbh*$^{-/-}$) mouse model. We found that adrenergic hormones influence heart development by stimulating expression of the gap junction protein, connexin 43, facilitating atrioventricular conduction, and helping to maintain cardiac rhythm. As development progresses, cardiac energy demands increase substantially, and oxidative

phosphorylation becomes vital. Adrenergic hormones regulate metabolism in adults, thus we hypothesized they may stimulate energy metabolism during the embryonic/fetal transition period. We examined ATP, ADP, oxygen consumption rate, and extracellular acidification rates and found these metabolic indices were significantly decreased in *Dbh*$^{-/-}$ hearts compared to *Dbh*$^{+/+}$ controls. We employed transmission electron microscopy of embryonic cardiomyocytes and found the mitochondria were significantly larger in *Dbh*$^{-/-}$ hearts compared to controls, and had more branch points. Taken together, these results suggest adrenergic hormones play a major role mediating the shift from predominantly anaerobic to aerobic metabolism during the embryonic/fetal transition period.

Since there are known differential cardiac responses due to sex, age, and menopause to stress, we used echocardiography to measure left ventricular (LV) function in adult (9, 18 and 21 month) male and female mice (pre and postmenopausal) in response to epinephrine, and immobilization stress to investigate the roles of these factors. My results show 9-month premenopausal female mice display significantly decreased LV responsiveness to epinephrine compared to males, and an increased response to epinephrine due to age, especially in the premenopausal females. Similar LV function was also observed between postmenopausal females and males, and this pattern persisted after immobilization stress. I also investigated anatomical differences in the distribution of adrenergic cells within the heart comparing age, sex, and menopausal status. Notably, the density of cells derived from an adrenergic

lineage in the heart was significantly increased in postmenopausal mice compared to age-matched males and cycling females. The selective re-appearance of adrenergic cells in the heart following menopause may provide an explanation for the differential stress responses observed in our system, and could have important clinical ramifications for stress-induced cardiomyopathies.

To my parents who have been a constant support system as I entered this amazing adventure.

ACKNOWLEDGEMENTS

This work was supported by NIH grants to SNE (HL078716) and JH (5RO1EB005459), and a postdoctoral fellowship (DGT) from the American Heart Association (0825395E) and funds from the College of Medicine at the University of Central Florida. I would like to thank my dissertation committee members; Drs. Ebert, Bossy-Wetzel, Lambert, and Siddiqi. I also offer my sincere gratitude to additional faculty members who have assisted with my research and training; Drs. Parthasarathy, Khaled, Estevez, Altomare, Davidson, Zhao, Samsam and King.

TABLE OF CONTENTS

LIST OF FIGURES

LIST OF TABLES

LIST OF ABBREVIATIONS

ADP	Adenosine diphosphate
ATP	Adenosine triphosphate
APX	Apex of ventricle
AV	Atrio-ventricular
AVJ	Atrio-ventricular junction
BPM	Beats per minute
CO	Cardiac output
Cx43	Connexin 43
Dbh	Dopamine β-hydroxylase
ECAR	Extracellular acidification rate
EF	Ejection Fraction
EPI	Epinephrine (adrenaline)
GRK2	G protein-coupled receptor kinase 2
Hcn4	Hyperpolarization-activated cyclic nucleotide-modulated channel isoform 4
HF	Heart failure
ICA	Intrinsic cardiac adrenergic (cells)
IMO	Immobilization
I.p.	Intraperitoneal
ISO	Isoproterenol
LV	Left ventricular

MEA	Microelectrode array
mtDNA	Mitochondrial DNA
NE	Norepinephrine (noradrenaline)
OCR	oxygen consumption rate
OT	Outflow Tract
OXPHOS	Oxidative phosphorylation
PKA	protein kinase A
Pnmt	Phenylethanolamine n-methyltransferase
SAN	Sinoatrial node
SAR	Sinoatrial region
SV	Stroke volume
TEM	Transmission electron microscopy
TTS	Takotsubo Syndrome
VCD	4-Vinycyclohexane diepoxide
V(d)	End diastolic volume
V(s)	End systolic volume

CHAPTER ONE: INTRODUCTION

Adrenergic hormones and embryonic electrophysiology

The mammalian cardiac conduction system is comprised of the SA and AV nodes, bundle of His, and Purkinje fibers (Christoffels and Moorman, 2009; Moorman et al., 1998). The electrical signal is propagated in the SAN and travels to the AVN where there is a significant delay. The signal then travels to the bundle of His, located in the interventricular septum, where it is then passed to the interventricular Purkinje fibers to initiate ventricular muscular contractions (Keith and Flack, 1907).

The mouse primitive embryonic heart begins to display contractions at approximately embryonic (E)7.5 (~22 days in humans). This is considerably earlier than sympathetic innervation of the heart is seen, E16-17 in rat (Shigenobu et al., 1988). The adrenergic hormone synthesizing enzyme phenylethanolamine-n-methyltransferase (PNMT) (Figure 1), however, was found to be present as early as E9.5 in the rat heart (~E8.5 in mouse) (Ebert et al., 1996). Similar findings of this and other catecholamine biosynthesis enzymes (ie. tyrosine hydroxylase and dopamine β-hydroxylase) have been shown in the chick and even human heart (Huang et al., 1996; Ignarro and Shideman, 1968a, b).

The localization of these “Intrinsic Cardiac Adrenergic” (ICA) cells is intriguing as they are found to colocalize with regions of the AV canal and the dorsal venous valve cusp at rat E11.5 (Ebert et al., 1996). These regions of the

embryonic heart further develop into the AV node and SA node, respectively (Viragh and Challice, 1977, 1980, 1982). These cells are seemingly transitory and later at E16.5 (rat) large clusters where observed in the crest of the interventricular septum, the sight of the bundle of His and Purkinje fibers (Ebert et al., 1996). In addition, at E15.5 (mouse) co-staining was observed between historical staining of adrenergic cells and *Hyperpolarization-activated cyclic nucleotide-modulated channel isoform 4* (HCN4) (Ebert et al., 2004) a protein associated with pacemaker properties found in the SA node (Stieber et al., 2003).

While there is strong evidence for colocalization of ICA cells with key pacemaker and conduction regions of the heart few studies have investigated the relationship between adrenergic hormones and the electrophysiology of the embryonic heart and the necessity of these hormones for proper function of the conduction system. Here we explore the roles of adrenergic hormones in the development of the embryonic conduction system.

Adrenergic hormones and embryonic energy metabolism

The primary source of adenosine triphosphate (ATP) during fetal development is commonly reported to be from glycolysis and lactate production, with a ‘fetal-shift’ occurring at birth where the primary source of ATP production ‘shifts’ to oxidative phosphorylation in the mitochondria (Duncan, 2011; Madrazo and Kelly, 2008; Makinde et al., 1998). A typical example of this notion from the

literature is stated as follows (Duncan, 2011; Madrazo and Kelly, 2008): '…metabolic programming often is referred to as a 'fetal' shift because the myocardium of the developing embryo relies mostly on glycolysis and lactate metabolism for its ATP production'. It has been known for more than 40 years, however, that mammalian hearts show an increase in the importance of oxidative phosphorylation for ATP production during the embryonic development (Cox and Gunberg, 1972; Ellington, 1987; Shepard et al., 1970). Additionally, there is accumulating evidence from targeted genetic studies in mice showing embryonic lethality due to disruption of genes associated with the mitochondria and/or dysfunctional oxidative phosphorylation. Moreover, cardiovascular development has been well studied using transgenic mice demonstrating embryonic lethality occurring around the time of mitochondrial maturation during organogenesis (Conway et al., 2003; Porter et al., 2011). Organogenesis begins around embryonic day 8.0 (E8.0) in mice, which is equivalent to about day 17–19 (Carnegie Stage 8) in humans (O'Rahilly, 1979; Theiler, 1972).

Interestingly, this is approximately the stage of development when increased embryonic lethality due to the genetic disruption of mitochondrial associated genes occurs (Figure 2) thereby demonstrating that embryonic mitochondrial function is indeed critical for embryonic and fetal development *in utero*. In support of this genetic evidence, electron microscopy has shown an obvious maturation of mitochondria and cristae development between E10–12 in rat embryos (equivalent to E9.0–E10.0 in mice) (Shepard et al., 1998). Further,

the inhibition of glycolysis using the drug 2-deoxyglucose did not show a decrease in E9.0 mouse ATP concentrations, indicating an alternative mechanism of energy production (e.g. oxidative phosphorylation) (Hunter and Tugman, 1995). Until recently, the study of oxidative phosphorylation and mitochondrial maturation *in utero* had not been thoroughly investigated, but a new mechanism for the induction of mitochondrial maturation was proposed involving the closure of the mitochondrial permeability transition pore (mPTP) beginning at E9.5 in mouse cardiomyocytes (Hom et al., 2011). The closure of the mPTP led to increased oxidative phosphorylation and decreased ROS production in the E9.5 mouse heart, and has thus been proposed as a key mechanism in the maturation of mitochondrial function in the developing embryo at a time when the embryo becomes dependent on aerobic metabolism (Hom et al., 2011).

Here, my studies show a link between adrenergic-hormones and mitochondrial functional maturation during embryogenesis. Adrenergic stimulation is known to regulate metabolism in adult organs, including the heart and liver, however, this is the first study to carefully examine adrenergic regulation of embryonic energy metabolism in the developing embryonic heart.

Adrenergic hormones, stress, age and gender

The impacts of emotional stress on health have been generally recognized since ancient times, but only in relatively recent years have scientists and

clinicians started to gain an understanding of the pathophysiological mechanisms linking emotional stress to specific dysfunctions within the cardiovascular system. In contrast, biological manifestations of physical stress are much more extensively characterized, and broadly include hypertension, ischemic heart disease (including myocardial infarction and its consequences), myocarditis, cardiomyopathies, heart failure, arrhythmias, and sudden cardiac death (Steptoe and Kivimaki, 2012). While emotional stress may also contribute to these conditions, the specific pathophysiologic manifestations of emotional stress are only beginning to emerge.

Takotsubo Syndrome is a prototypical stress-induced cardiomyopathy. The first clinical cases of this stress cardiomyopathy were reported in Japan in 1990 (H. Sato, 1990). Early reports described a transient hypokinesis or akinesis in the apex of the LV in patients suffering from acute emotional stress (Bybee and Prasad, 2008; Hurst et al., 2010; Tsuchihashi et al., 2001). The unusual shape of the heart in these patients bore a striking resemblance to a Japanese octopus trap, and hence, it was named “takotsubo”, meaning octopus trap in Japanese (Dote et al., 1991; H. Sato, 1990; Tsuchihashi et al., 2001). Takotsubo Syndrome is also referred to as “Broken Heart Syndrome” (due to the emotional stress connection), “Ampulla Cardiomyopathy” (due to the peculiar shape of the heart), or “Apical Ballooning Syndrome” (to describe one of the most pronounced clinical features commonly observed in these patients) (Hurst et al., 2010). Takotsubo Syndrome is also referred to as a “Stress-Induced Cardiomyopathy”

or more simply, “Stress Cardiomyopathy”. These terms have become essentially interchangeable when describing this syndrome (Sharkey et al., 2011). For this purpose, we will use the historical “Takotsubo Cardiomyopathy (TTC)” designation as the prototype clinical form of stress-induced cardiomyopathies. It is important to note, however, that stress induction for TTC need not be exclusively emotional or psychological, but can also be precipitated by physical stressors such as pharmacological challenge with adrenaline and other adrenergic agonists (Abraham et al., 2009; Litvinov et al., 2009), complications from other diseases (e.g., pheochromocytoma) (Marcovitz et al., 2010; Naderi et al., 2012), physical trauma from injury or surgery, and a wide variety of other physical stressors (Ennezat et al., 2005; Patel et al., 2013).

The common feature of both physical and psychological stress responses in these contexts is elevated plasma catecholamines (Akashi et al., 2004; Ito et al., 2003; Kume et al., 2008; Wittstein et al., 2005). Indeed, studies examining plasma catecholamine concentrations in TTC patients have shown high levels of circulating catecholamines compared to those from control groups (Shao et al., 2013a; Wittstein et al., 2005). The fact that exogenously administered catecholamines can induce TTC-like symptoms in patients and animal models further supports adrenergic mediation of this syndrome (Abraham et al., 2009; Izumi et al., 2009; Shao et al., 2013a; Shao et al., 2013b). TTC symptoms have also been reported in some patients with pheochromocytoma, which results in abnormally high concentrations of circulating endogenous catecholamines

secreted from adrenal medullary tumors (Kim et al., 2010). TTC symptoms have responded favorably to pharmacological intervention with beta-blockers in some cases (Bybee and Prasad, 2008). Taken together, these observations strongly implicate the major peripheral catecholamines, adrenaline and noradrenaline, as key players in acute precipitation of TTC.

We hypothesize the pathogenesis of TTC is due (in part) to a local release of catecholamines that overload adrenergic receptor signaling systems in specific regions of the heart (Kume et al., 2008; Osuala et al., 2011), however the other prevailing hypothesis include coronary microspasms and increased β-adrenergic receptor densities (Figure 3). During stress, there is input from sympathetic nerves as well as circulating catecholamines, but there are also autocrine/paracrine actions of catecholamines from stores within the heart itself (Armour et al., 1997; Ebert et al., 1996; Ebert and Taylor, 2006; Ebert and Thompson, 2001; Elayan et al., 1990; Huang et al., 1996; Osuala et al., 2011; Papka, 1974). As mentioned earlier, sympathetic nerve input is not uniform throughout the LV. There is much greater nerve terminal density in the base compared to mid or apical sections of the LV (Angelakos, 1965; Pierpont et al., 1984). Kume et al, 2008 measured catecholamines from two locations representing base (aortic root, Ao) and apex (coronary sinus, CS) in five confirmed cases of TTC. In all five cases, concentrations of noradrenaline and dopamine were elevated in CS compared to Ao, whereas adrenaline concentrations were unchanged or slightly decreased. These results suggested

there may indeed be differential local catecholamine concentrations in apical and basal regions of the left ventricular myocardium.

Another piece of evidence comes from recent studies in the mouse heart showing cells marked by expression of the adrenaline biosynthetic enzyme, phenylethanolamine n-methyltransferase (Pnmt), were found to be concentrated on the left side of the adult heart (Osuala et al., 2011). More specifically, Pnmt+ cells were localized to swaths or finger-like projections into left ventricular myocardium at the apex, mid, and basal regions (Osuala et al., 2011). These data suggest there may be an anatomical substrate for regional catecholamine production differences in the heart. Nearly 90% of Pnmt-derived cells were found to be localized to the left side of the heart, which could, in theory, help to explain why left ventricular function is selectively influenced in TTC. Moreover, the regional variations within the LV could likewise help to explain how those areas could be susceptible to local surges in catecholamines. It is also possible that local presence of catecholamines in these regions during development may influence the expression and functional sensitivities of adrenergic receptor subtype distributions in the LV. Although this has not been explicitly demonstrated in the heart, there are numerous studies showing that innervation and adrenergic receptor expression is influenced by catecholamine exposure (Clarke et al., 2010; Habecker et al., 1996; Lau et al., 1982).

Notably, many of the Pnmt-derived cells in the adult mouse heart appear to be myocytes, though neuronal-like and immature embryonic-like Pnmt-derived

cells were also identified in these regions (Osuala et al., 2011). Clear examples of striated myocardial cells marked with XGAL to denote Pnmt expression were observed in the LV (Ebert et al., 2008; Osuala et al., 2011). These results suggest there may be autocrine or paracrine actions of local catecholamines from non-neuronal as well as neuronal sources. This idea is not new (Kimura et al., 2012; Kloberg and Fritsche, 2002; Slavikova et al., 2003), but is often overlooked in modern studies and textbooks. The classic work of Spurgeon et al. (Spurgeon et al., 1974) showed that cardiac adrenaline concentrations remain relatively high in the heart following surgical and chemical (6-hydroxydopamine, 6-OHDA) denervation, while noradrenaline concentrations were nearly completely eradicated by these procedures. The authors concluded that cardiac noradrenaline content was mostly neuronal while only ~50% of the adrenaline content was neuronal. They hypothesized that cardiac adrenaline "is held in non-neuronal stores either in chromaffin cells, in the specialized cells themselves or in cardiac analogs of chromaffin cells" (Spurgeon et al., 1974). There is ample evidence for these from a wide variety of species (Abrahamsson et al., 1979; Ellison and Hibbs, 1974; Forsgren et al., 1990; Padbury et al., 1981), including humans (Dail and Palmer, 1973), suggesting their presence is highly conserved and, therefore, likely critical for survival. It remains to be determined if these cells truly play a significant role in TTC, but they certainly represent a potential local source of adrenaline that could contribute to regional variations in adrenergic stimulation within the LV.

To investigate this further I performed longitudinal high-resolution echocardiography on male and female mice ranging from 9 to 21 months old. Additionally, to test if menopausal status affects left ventricular heart function ovarian follicle failure was induced and echocardiographs were repeated. The effect of stress on heart function was tested by the injection of epinephrine and immobilization. Lastly, adrenergic cell distributions patterns within the heart were determined using X-gal staining.

Figures

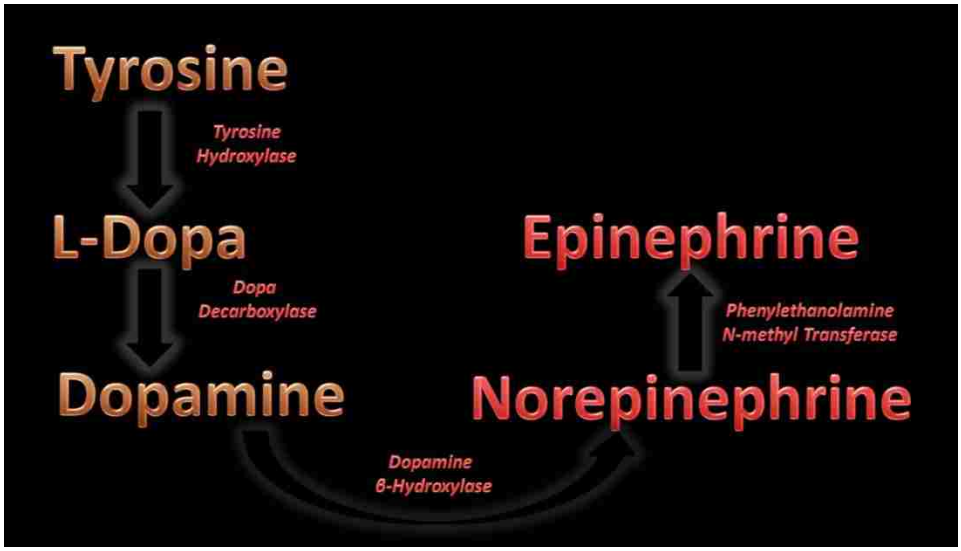

Figure 1 Catecholamine biosynthetic pathway

Catecholamine biosynthetic pathway with enzymes next to arrows.

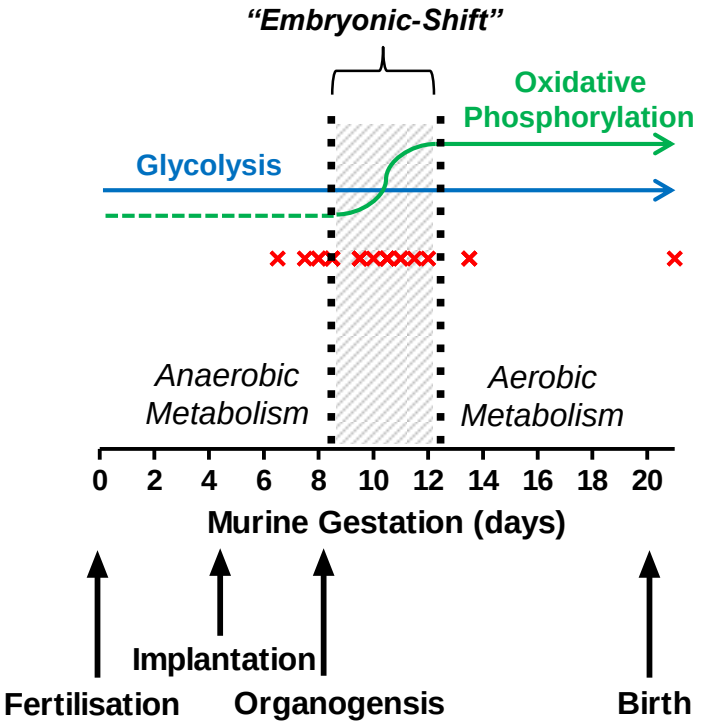

Figure 2 Timeline of attrition in genetic knock-out models that affect mitochondrial function

' X' represents a model of mitochondrial-associated lethality; vertical dashed lines indicate timing of 'embryonic-shift' from anaerobic to aerobic metabolism. Please note that arrows depicting timelines of activity for 'glycolysis' and 'oxidative phosphorylation' are qualitative and mainly serve to indicate the relative importance of glycolysis (and subsequent lactic acid formation through anaerobic means) and oxidative phosphorylation in mitochondria for proper embryonic and foetal development.

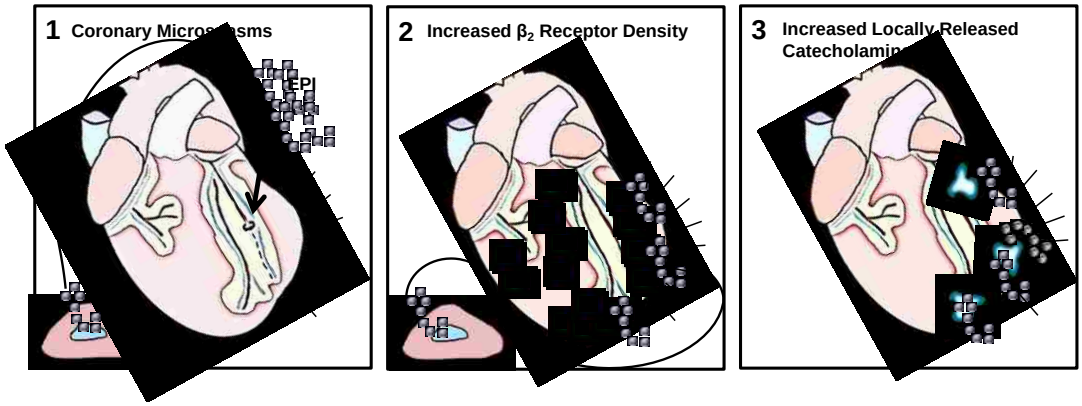

Figure 3 Schematic illustrations of three distinctive models proposed to explain TTC mechanisms.

1. Coronary Microspasms: In this model, stress-induced surges in catecholamines trigger coronary microspasms, which then lead to decreased blood flow and regional myocardial inactivity. 2. Increased β_2-Receptor Density: This model proposes that β_2-adrenergic receptors are more concentrated at the apex compared to the base. High concentrations of adrenaline cause these receptors to switch from G_s to G_i, which results in myocardial stunning in affected regions that would appear as akinetic or hypokinetic sections of LV during systole. 3. Increased Local Catecholamine Release: In this hypothesis, adrenaline and/or noradrenaline are released locally in the apex, mid, and/or basal regions of the LV from non-neuronal resident adrenergic cell populations (depicted by the highlighted blue areas). This local release overstimulates adrenergic receptors that are already near saturation from circulating adrenaline and sympathetic nerves (NA). Abbreviations: HPA, Hypothalamic-Pituitary-Adrenal (axis); A, adrenaline; NA, noradrenaline

List of References

Abraham, J., Mudd, J.O., Kapur, N.K., Klein, K., Champion, H.C., and Wittstein, I.S. (2009). Stress cardiomyopathy after intravenous administration of catecholamines and beta-receptor agonists. Journal of the American College of Cardiology *53*, 1320-1325.

Abrahamsson, T., Jonsson, A.C., and Nilsson, S. (1979). Catecholamine synthesis in the chromaffin tissue of the African lungfish, Protopterus aethiopicus. Acta physiologica Scandinavica *107*, 149-151.

Akashi, Y.J., Nakazawa, K., Sakakibara, M., Miyake, F., Musha, H., and Sasaka, K. (2004). 123I-MIBG myocardial scintigraphy in patients with "takotsubo" cardiomyopathy. Journal of nuclear medicine : official publication, Society of Nuclear Medicine *45*, 1121-1127.

Angelakos, E.T. (1965). Regional Distribution of Catecholamines in the Dog Heart. Circulation research *16*, 39-44.

Armour, J.A., Murphy, D.A., Yuan, B.X., Macdonald, S., and Hopkins, D.A. (1997). Gross and microscopic anatomy of the human intrinsic cardiac nervous system. The Anatomical record *247*, 289-298.

Bybee, K.A., and Prasad, A. (2008). Stress-related cardiomyopathy syndromes. Circulation *118*, 397-409.

Christoffels, V.M., and Moorman, A.F. (2009). Development of the cardiac conduction system: why are some regions of the heart more arrhythmogenic than others? Circulation Arrhythmia and electrophysiology *2*, 195-207.

Clarke, G.L., Bhattacherjee, A., Tague, S.E., Hasan, W., and Smith, P.G. (2010). ss-adrenoceptor blockers increase cardiac sympathetic innervation by inhibiting autoreceptor suppression of axon growth. The Journal of neuroscience : the official journal of the Society for Neuroscience *30*, 12446-12454.

Conway, S.J., Kruzynska-Frejtag, A., Kneer, P.L., Machnicki, M., and Koushik, S.V. (2003). What cardiovascular defect does my prenatal mouse mutant have, and why? Genesis *35*, 1-21.

Cox, S.J., and Gunberg, D.L. (1972). Metabolite utilization by isolated embryonic rat hearts in vitro. J Embryol Exp Morphol *28*, 235-245.

Dail, W.G., Jr., and Palmer, G.C. (1973). Localization and correltion of catecholamine-containing cells with adenyl cyclase nd phosphodiesterase activities in the human fetal heart. The Anatomical record *177*, 265-287.

Dote, K., Sato, H., Tateishi, H., Uchida, T., and Ishihara, M. (1991). [Myocardial stunning due to simultaneous multivessel coronary spasms: a review of 5 cases]. Journal of cardiology *21*, 203-214.

Duncan, J.G. (2011). Peroxisome proliferator activated receptor-alpha (PPARalpha) and PPAR gamma coactivator-1alpha (PGC-1alpha) regulation of cardiac metabolism in diabetes. Pediatr Cardiol *32*, 323-328.

Ebert, S.N., Baden, J.M., Mathers, L.H., Siddall, B.J., and Wong, D.L. (1996). Expression of phenylethanolamine n-methyltransferase in the embryonic rat heart. Journal of molecular and cellular cardiology *28*, 1653-1658.

Ebert, S.N., Rong, Q., Boe, S., and Pfeifer, K. (2008). Catecholamine-synthesizing cells in the embryonic mouse heart. Annals of the New York Academy of Sciences *1148*, 317-324.

Ebert, S.N., Rong, Q., Boe, S., Thompson, R.P., Grinberg, A., and Pfeifer, K. (2004). Targeted insertion of the Cre-recombinase gene at the phenylethanolamine n-methyltransferase locus: a new model for studying the developmental distribution of adrenergic cells. Dev Dyn *231*, 849-858.

Ebert, S.N., and Taylor, D.G. (2006). Catecholamines and development of cardiac pacemaking: an intrinsically intimate relationship. Cardiovascular research *72*, 364-374.

Ebert, S.N., and Thompson, R.P. (2001). Embryonic epinephrine synthesis in the rat heart before innervation: association with pacemaking and conduction tissue development. Circulation research *88*, 117-124.

Elayan, H.H., Kennedy, B.P., and Ziegler, M.G. (1990). Cardiac atria and ventricles contain different inducible adrenaline synthesising enzymes. Cardiovascular research *24*, 53-56.

Ellington, S.K. (1987). In vitro analysis of glucose metabolism and embryonic growth in postimplantation rat embryos. Development *100*, 431-439.

Ellison, J.P., and Hibbs, R.G. (1974). Catecholamine-containing cells of the guinea pig heart: an ultrastructural study. Journal of molecular and cellular cardiology *6*, 17-26.

Ennezat, P.V., Pesenti-Rossi, D., Aubert, J.M., Rachenne, V., Bauchart, J.J., Auffray, J.L., Logeart, D., Cohen-Solal, A., and Asseman, P. (2005). Transient left ventricular basal dysfunction without coronary stenosis in acute cerebral disorders: a novel heart syndrome (inverted Takotsubo). Echocardiography *22*, 599-602.

Forsgren, S., Moravec, M., and Moravec, J. (1990). Catecholamine-synthesizing enzymes and neuropeptides in rat heart epicardial ganglia; an immunohistochemical study. The Histochemical journal *22*, 667-676.

H. Sato, H.T., K. Dote, T. Uchida, M. Ishihara (1990). Tako-tsubo-like left ventricular dysfunction due to multivessel coronary spasm (Kagakuhyoronsha Publishing Co., Tokyo), pp. 56-64.

Habecker, B.A., Malec, N.M., and Landis, S.C. (1996). Differential regulation of adrenergic receptor development by sympathetic innervation. The Journal of neuroscience : the official journal of the Society for Neuroscience *16*, 229-237.

Hom, J.R., Quintanilla, R.A., Hoffman, D.L., de Mesy Bentley, K.L., Molkentin, J.D., Sheu, S.S., and Porter, G.A., Jr. (2011). The permeability transition pore controls cardiac mitochondrial maturation and myocyte differentiation. Dev Cell *21*, 469-478.

Huang, M.H., Friend, D.S., Sunday, M.E., Singh, K., Haley, K., Austen, K.F., Kelly, R.A., and Smith, T.W. (1996). An intrinsic adrenergic system in mammalian heart. The Journal of clinical investigation *98*, 1298-1303.

Hunter, E.S., 3rd, and Tugman, J.A. (1995). Inhibitors of glycolytic metabolism affect neurulation-staged mouse conceptuses in vitro. Teratology *52*, 317-323.

Hurst, R.T., Prasad, A., Askew, J.W., 3rd, Sengupta, P.P., and Tajik, A.J. (2010). Takotsubo cardiomyopathy: a unique cardiomyopathy with variable ventricular morphology. JACC Cardiovasc Imaging *3*, 641-649.

Ignarro, L.J., and Shideman, F.E. (1968a). Appearance and concentrations of catecholamines and their biosynthesis in the embryonic and developing chick. The Journal of pharmacology and experimental therapeutics *159*, 38-48.

Ignarro, L.J., and Shideman, F.E. (1968b). Norepinephrine and epinephrine in the embryo and embryonic heart of the chick: uptake and subcellular distribution. The Journal of pharmacology and experimental therapeutics *159*, 49-58.

Ito, K., Sugihara, H., Katoh, S., Azuma, A., and Nakagawa, M. (2003). Assessment of Takotsubo (ampulla) cardiomyopathy using 99mTc-tetrofosmin

myocardial SPECT--comparison with acute coronary syndrome. Annals of nuclear medicine *17*, 115-122.

Izumi, Y., Okatani, H., Shiota, M., Nakao, T., Ise, R., Kito, G., Miura, K., and Iwao, H. (2009). Effects of metoprolol on epinephrine-induced takotsubo-like left ventricular dysfunction in non-human primates. Hypertension research : official journal of the Japanese Society of Hypertension *32*, 339-346.

Keith, A., and Flack, M. (1907). The Form and Nature of the Muscular Connections between the Primary Divisions of the Vertebrate Heart. Journal of anatomy and physiology *41*, 172-189.

Kim, S., Yu, A., Filippone, L.A., Kolansky, D.M., and Raina, A. (2010). Inverted-Takotsubo pattern cardiomyopathy secondary to pheochromocytoma: a clinical case and literature review. Clinical cardiology *33*, 200-205.

Kimura, K., Ieda, M., and Fukuda, K. (2012). Development, maturation, and transdifferentiation of cardiac sympathetic nerves. Circulation research *110*, 325-336.

Kloberg, A.J., and Fritsche, R. (2002). Catecholamines are present in larval Xenopus laevis: a potential source for cardiac control. The Journal of experimental zoology *292*, 293-303.

Kume, T., Kawamoto, T., Okura, H., Toyota, E., Neishi, Y., Watanabe, N., Hayashida, A., Okahashi, N., Yoshimura, Y., Saito, K.*, et al.* (2008). Local release of catecholamines from the hearts of patients with tako-tsubo-like left ventricular dysfunction. Circulation journal : official journal of the Japanese Circulation Society *72*, 106-108.

Lau, C., Burke, S.P., and Slotkin, T.A. (1982). Maturation of sympathetic neurotransmission in the rat heart. IX. Development of transsynaptic regulation of cardiac adrenergic sensitivity. The Journal of pharmacology and experimental therapeutics *223*, 675-680.

Litvinov, I.V., Kotowycz, M.A., and Wassmann, S. (2009). Iatrogenic epinephrine-induced reverse Takotsubo cardiomyopathy: direct evidence supporting the role of catecholamines in the pathophysiology of the "broken heart syndrome". Clinical research in cardiology : official journal of the German Cardiac Society *98*, 457-462.

Madrazo, J.A., and Kelly, D.P. (2008). The PPAR trio: regulators of myocardial energy metabolism in health and disease. J Mol Cell Cardiol *44*, 968-975.

Makinde, A.O., Kantor, P.F., and Lopaschuk, G.D. (1998). Maturation of fatty acid and carbohydrate metabolism in the newborn heart. Molecular and cellular biochemistry *188*, 49-56.

Marcovitz, P.A., Czako, P., Rosenblatt, S., and Billecke, S.S. (2010). Pheochromocytoma presenting with Takotsubo syndrome. Journal of interventional cardiology *23*, 437-442.

Moorman, A.F., de Jong, F., Denyn, M.M., and Lamers, W.H. (1998). Development of the cardiac conduction system. Circulation research *82*, 629-644.

Naderi, N., Amin, A., Setayesh, A., Pouraliakbar, H., Mozaffari, K., and Maleki, M. (2012). Pheochromocytoma-induced reverse tako-tsubo with rapid recovery of left ventricular function. Cardiology journal *19*, 527-531.

O'Rahilly, R. (1979). Early human development and the chief sources of information on staged human embryos. Eur J Obstet Gynecol Reprod Biol *9*, 273-280.

Osuala, K., Telusma, K., Khan, S.M., Wu, S., Shah, M., Baker, C., Alam, S., Abukenda, I., Fuentes, A., Seifein, H.B.*, et al.* (2011). Distinctive left-sided distribution of adrenergic-derived cells in the adult mouse heart. PloS one *6*, e22811.

Padbury, J.F., Diakomanolis, E.S., Lam, R.W., Hobel, C.J., and Fisher, D.A. (1981). Ontogenesis of tissue catecholamines in fetal and neonatal rabbits. Journal of developmental physiology *3*, 297-303.

Papka, R.E. (1974). A study of catecholamine-containing cells in the hearts of fetal and postnatal rabbits by fluorescence and electron microscopy. Cell and tissue research *154*, 471-484.

Patel, S.M., Chokka, R.G., Prasad, K., and Prasad, A. (2013). Distinctive clinical characteristics according to age and gender in apical ballooning syndrome (takotsubo/stress cardiomyopathy): an analysis focusing on men and young women. Journal of cardiac failure *19*, 306-310.

Pierpont, G.L., DeMaster, E.G., and Cohn, J.N. (1984). Regional differences in adrenergic function within the left ventricle. The American journal of physiology *246*, H824-829.

Porter, G.A., Jr., Hom, J., Hoffman, D., Quintanilla, R., de Mesy Bentley, K., and Sheu, S.S. (2011). Bioenergetics, mitochondria, and cardiac myocyte differentiation. Prog Pediatr Cardiol *31*, 75-81.

Shao, Y., Redfors, B., Scharin Tang, M., Mollmann, H., Troidl, C., Szardien, S., Hamm, C., Nef, H., Boren, J., and Omerovic, E. (2013a). Novel rat model reveals important roles of beta-adrenoreceptors in stress-induced cardiomyopathy. International journal of cardiology.

Shao, Y., Redfors, B., Stahlman, M., Tang, M.S., Miljanovic, A., Mollmann, H., Troidl, C., Szardien, S., Hamm, C., Nef, H.*, et al.* (2013b). A mouse model reveals an important role for catecholamine-induced lipotoxicity in the pathogenesis of stress-induced cardiomyopathy. European journal of heart failure *15*, 9-22.

Sharkey, S.W., Lesser, J.R., Maron, M.S., and Maron, B.J. (2011). Why not just call it tako-tsubo cardiomyopathy: a discussion of nomenclature. Journal of the American College of Cardiology *57*, 1496-1497.

Shepard, T.H., Muffley, L.A., and Smith, L.T. (1998). Ultrastructural study of mitochondria and their cristae in embryonic rats and primate (N. nemistrina). Anat Rec *252*, 383-392.

Shepard, T.H., Tanimura, T., and Robkin, M.A. (1970). Energy metabolism in early mammalian embryos. Symp Soc Dev Biol *29*, 42-58.

Shigenobu, K., Tanaka, H., and Kasuya, Y. (1988). Changes in sensitivity of rat heart to norepinephrine and isoproterenol during pre- and postnatal development and its relation to sympathetic innervation. Developmental pharmacology and therapeutics *11*, 226-236.

Slavikova, J., Kuncova, J., Reischig, J., and Dvorakova, M. (2003). Catecholaminergic neurons in the rat intrinsic cardiac nervous system. Neurochemical research *28*, 593-598.

Spurgeon, H.A., Priola, D.V., Montoya, P., Weiss, G.K., and Alter, W.A., 3rd (1974). Catecholamines associated with conductile and contractile myocardium of normal and denervated dog hearts. The Journal of pharmacology and experimental therapeutics *190*, 466-471.

Steptoe, A., and Kivimaki, M. (2012). Stress and cardiovascular disease. Nature reviews Cardiology *9*, 360-370.

Stieber, J., Herrmann, S., Feil, S., Loster, J., Feil, R., Biel, M., Hofmann, F., and Ludwig, A. (2003). The hyperpolarization-activated channel HCN4 is required for the generation of pacemaker action potentials in the embryonic heart. Proceedings of the National Academy of Sciences of the United States of America *100*, 15235-15240.

Theiler, K. (1972). The house mouse; development and normal stages from fertilization to 4 weeks of age (Berlin, New York,: Springer-Verlag).

Tsuchihashi, K., Ueshima, K., Uchida, T., Oh-mura, N., Kimura, K., Owa, M., Yoshiyama, M., Miyazaki, S., Haze, K., Ogawa, H.*, et al.* (2001). Transient left ventricular apical ballooning without coronary artery stenosis: a novel heart syndrome mimicking acute myocardial infarction. Angina Pectoris-Myocardial Infarction Investigations in Japan. J Am Coll Cardiol *38*, 11-18.

Viragh, S., and Challice, C.E. (1977). The development of the conduction system in the mouse embryo heart. II. Histogenesis of the atrioventricular node and bundle. Developmental biology *56*, 397-411.

Viragh, S., and Challice, C.E. (1980). The development of the conduction system in the mouse embryo heart. Developmental biology *80*, 28-45.

Viragh, S., and Challice, C.E. (1982). The development of the conduction system in the mouse embryo heart. Developmental biology *89*, 25-40.

Wittstein, I.S., Thiemann, D.R., Lima, J.A., Baughman, K.L., Schulman, S.P., Gerstenblith, G., Wu, K.C., Rade, J.J., Bivalacqua, T.J., and Champion, H.C. (2005). Neurohumoral features of myocardial stunning due to sudden emotional stress. The New England journal of medicine *352*, 539-548.

CHAPTER TWO:
ADRENERGIC DEFICIENCY LEADS TO IMPAIRED ELECTRICAL CONDUCTION AND INCREASED ARRHYTHMIC POTENTIAL IN THE EMBRYONIC MOUSE HEART

Abstract

The adrenergic hormones, epinephrine and norepinephrine, are produced by cardiac cells in the pacemaking and conduction system, as well as other portions of the heart during a critical period of embryonic development when adrenergic action is essential for survival. The underlying mechanisms of adrenergic action in the embryonic heart, however, are not well-understood. To determine if adrenergic hormones play a critical role in the functional development of the cardiac pacemaking and conduction system, we employed a mouse model where adrenergic hormone production was blocked due to targeted disruption of the *dopamine β-hydroxylase* (*Dbh*) gene. Immunofluorescent histochemical evaluation of the major gap junction protein, connexin 43, revealed that its expression was substantially decreased in adrenergic-deficient ($Dbh^{-/-}$) mouse hearts relative to adrenergic-competent ($Dbh^{+/+}$ and $Dbh^{+/-}$) at embryonic day 10.5 (E10.5), whereas pacemaker and structural protein staining appeared similar. To evaluate cardiac electrical conduction in these hearts, we cultured them on microelectrode arrays (8x8, 200 µm apart). Our results show a significant slowing of atrioventricular conduction in adrenergic-deficient hearts compared to controls (31.4 ± 6.4 vs. 15.4 ± 1.7 ms, respectively, $p < 0.05$). To determine if the absence of adrenergic hormones affected heart rate and rhythm,

mouse hearts from adrenergic-competent and deficient embryos were cultured *ex vivo* at E10.5, and heart rates were measured before and after challenge with the β-adrenergic receptor agonist, isoproterenol (500 nM). On average, all hearts showed increased heart rate responses following isoproterenol challenge, but a significant ($p < 0.05$) 225% increase in the arrhythmic index (AI) was observed only in adrenergic-deficient hearts. These results show that adrenergic hormones may influence heart development by stimulating connexin 43 expression, facilitating atrioventricular conduction, and helping to maintain cardiac rhythm during a critical phase of embryonic development.

Introduction

Mice that lack the ability to produce the adrenergic hormones, norepinephrine (NE) and epinephrine (EPI), due to targeted disruption of the *dopamine β-hydroxylase* (*Dbh*) gene die at mid-gestation from apparent heart failure (Thomas et al., 1995). Structural formation of the heart was not markedly perturbed in the adrenergic-deficient embryos, though subtle abnormalities such as dilated atria and disorganized ventricular myofibrils were observed in the deficient group. In addition, blood pooling in major organs and slower *in vivo* heart rates led to the conclusion that heart failure was the likely cause of death in adrenergic-deficient embryos. The mechanism of action appears to be primarily through β-adrenergic receptor activation because isoproterenol (β-agonist) but not L-phenylephrine (α-agonist) could rescue the adrenergic-deficient ($Dbh^{-/-}$)

mouse embryos when supplied via the maternal drinking water (Thomas and Palmiter, 1998). Despite a relatively wide body of data on adrenergic mechanisms in the adult heart, only rudimentary information exists regarding adrenergic actions in the embryonic heart. A major gap in our current knowledge is how embryonic activation of β-adrenergic signaling specifically affects cardiac function and embryonic survival at these critical formative stages of development.

Independent studies have shown that the heart itself is a source of adrenergic hormones during early development (Ebert et al., 1996; Ebert and Thompson, 2001; Huang et al., 1996). "Intrinsic Cardiac Adrenergic" (ICA) cells appear in the heart at about the time that it first starts to beat (Ebert et al., 1996; Huang et al., 1996). There is a transient clustering of ICA cells in regions of the heart progressively associated with development of the cardiac pacemaking and conduction system, including the pacemaker cells in the sinoatrial node, the atrioventricular node, bundle of His, and Purkinje fibers (Ebert and Thompson, 2001). Some of these transient ICA cells appear to differentiate into cardiac myocytes, including the specialized myocytes that serve as pacemaker cells in the sinoatrial and atrioventricular nodes as well as extensive labeling of myocytes throughout the ventricular conduction system (Ebert et al., 2004). These observations have led us to hypothesize that NE and/or EPI play a critical role in the embryonic development of the cardiac pacemaking and conduction system (Ebert and Taylor, 2006).

In the present study, we utilized the *Dbh* knockout mouse model to test the hypothesis that NE and EPI play a critical role in the development of the cardiac pacemaking and conduction systems. Our initial experiments evaluated the *in situ* expression of a key pacemaker channel protein, the hyperpolarization-activated cyclic nucleotide-modulated channel isoform 4 (Hcn4) (Stieber et al., 2003), and a major gap junction protein responsible for fast ventricular conduction, connexin 43 (Cx43) (van Veen et al., 2001), in adrenergic-competent and deficient embryos. We then used microelectrode arrays (MEAs) to evaluate electrical conduction, and videomicroscopy to examine heart rate and rhythm. Our results indicate that while pacemaking activity appeared relatively unaffected by the absence or presence of adrenergic hormones, electrical conduction was impaired and susceptibility to arrhythmias was increased in adrenergic-deficient hearts relative to controls.

Materials and Methods

Animals

The *Dbh* mouse strain and collection of embryos used in this study has been described previously [25]. All animal procedures were performed in accordance with NIH guidelines and were approved by the University of Central Florida Animal Care and Use Committee. Most of our analyses were performed using embryonic day 10.5 (E10.5) mouse embryos because E10.5 is the latest stage of development when adrenergic-deficient embryos are still largely asymptomatic

(Thomas et al., 1995). Since various secondary and other indirect effects of adrenergic deficiency may occur as a consequence of heart failure at later developmental stages, we confined our analyses to E10.5 and earlier stages in an attempt to identify more direct mechanisms of adrenergic action in the developing heart.

Immunofluorescence histochemistry

Dual immunofluorescent histochemical staining of hearts was performed essentially as described previously (Ebert et al., 2004; Ebert and Thompson, 2001).

Ex vivo embryonic mouse heart cultures

E10.5 mouse hearts were isolated under aseptic conditions and cultured in Dubelcco's modified Eagle's medium (DMEM) containing 10% fetal bovine serum (Hyclone Labs, Logan, UT) that had been charcoal-stripped to remove catecholamine and steroid hormones (Natarajan et al., 2004). The media was additionally supplemented with the following (final concentrations given): D-glucose (25 mM), sodium pyruvate (1 mM), penicillin G (100,000 U/L), streptomycin (100 mg/L), β-mercaptoethanol (55 μM), l-glutamine (2 mM), and 1% 100x α-minimum nonessential amino acids (Ebert et al., 2007). Hearts were cultured for 20-24 hours prior to any measurements of beating activity or conduction properties.

Microelectrode arrays (MEAs)

General MEA procedures were similar to those described previously (Pillekamp et al., 2006), with the exceptions described here. Freshly isolated E10.5 hearts were placed in the center of gelatin-coated 8x8 MEAs (#200/10iR-Ti, Multichannel Systems, Reutlingen, Germany) with the flat ventral surface in contact with electrodes (i.e., outflow tract projecting upward). A representative video of an E10.5 spontaneously beating mouse heart on a MEA is shown in Supplemental Video 3. Electrodes were 10 µm in diameter and 200 µm apart. MEA analysis was performed using Clampfit v10.0.0.61 (Molecular Devices, Sunnyvale, CA). The first depolarizing atrial electrode was considered the sinoatrial region (SAR). The electrode with the largest depolarization in the atrioventricular region was considered the atrioventricular junction (AVJ), and the ventricular apex (APX) was identified both by location and bifurcation of impulse propagation to the distal Purkinje fibers. Within the AVJ and APX regions, adjacent electrodes depolarized usually near-simultaneously (<0.5 ms of each other). Conduction time was measured between field potential minimums (FP_{min}) (Halbach et al., 2003; Reppel et al., 2004).

Beating rate and rhythmicity measurements

Beating rate and rhythmicity measurements were performed as described previously (Fink et al., 2009; Natarajan et al., 2004). Arrhythmic index (AI) was

calculated as the median cycle length divided by the standard deviation (Fink et al., 2009).

Statistics

Data are expressed as mean ± S.E.M. Student *t*-tests were performed to compare means, with $p < 0.05$ required to reject the null hypothesis. No significant differences were observed between wild-type (*Dbh*$^{+/+}$) and heterozygous (*Dbh*$^{+/-}$) hearts at E10.5 in any examined parameter. Since there was no significant difference between *Dbh*$^{+/+}$ and *Dbh*$^{+/-}$ embryos (Thomas et al., 1995), these two genotypes were combined into a single group referred to as "adrenergic-competent." In contrast, homozygous knockout (*Dbh*$^{-/-}$) mice were designated as "adrenergic-deficient" due to their inability to produce NE or EPI (Thomas et al., 1995).

Results

Since ICA cells have previously been identified in regions of the developing heart associated with conduction and pacemaking function (Ebert et al., 2004; Ebert and Thompson, 2001), we employed immunofluorescent histochemical staining to evaluate a key pacemaking protein (Hcn4) and a major gap junction protein (Cx43) important for the generation and propagation, respectively, of electrical signaling in adrenergic-competent and deficient embryonic hearts. As shown in Fig. 4, our results indicate that Cx43 immunofluorescent staining intensity in adrenergic-deficient hearts was

substantially less than that observed in adrenergic-competent hearts (compare red fluorescence in panels a and b). In this example, co-immunofluorescent staining with Hcn4 showed similar distribution and intensity in both groups. Higher magnification of the dual immunofluorescent staining in the SAN region is shown in panels c and d. The arrowhead points to red Cx43-expressing cells while the arrow indicates the Hcn4-expressing cells shown in green. Cx43-expressing cells showed only marginal overlap with Hcn4-positive cells in the SAN region, but were found in the adjacent atrial myocardial cells and extending into the myocardium of the ventricle and outflow tract regions as well. This was true for both adrenergic-competent and deficient E10.5 hearts, though the intensity of the Cx43 staining in the deficient hearts was much less than that seen in the competent hearts (compare panels c and d). This effect appeared to be specific for Cx43 since anti-sarcomeric α-actinin staining in adjacent sections showed similar intensity and distribution for both adrenergic-competent and deficient hearts (compare red staining in panels e and f). Further, since the same secondary antibody source and concentration were used for both sarcomeric α-actinin and Cx43, the relative decrease in Cx43 staining intensity was probably not due to differential effects of the secondary antibody, but instead likely reflects changes in Cx43 expression resulting from lack of adrenergic stimulation.

We similarly analyzed other regions of the heart, and found that Cx43 immunofluorescent histochemical staining was also decreased in the

atrioventricular (A-V) area of adrenergic-deficient compared to adrenergic-competent E10.5 embryos (Fig. 5). Low-magnification views of sarcomeric α–actinin immunofluorescent staining in adrenergic-competent and deficient hearts (panels a and b) are provided to aid in orientation of the higher-magnification views of Cx43 staining in these same sections, as shown in panels c-f. When camera exposure times and image processing were optimized for viewing of Cx43 in adrenergic-competent E10.5 mouse hearts, virtually no Cx43 staining was observed in the A-V junctional region of adrenergic-deficient hearts using equivalent image acquisition and processing settings (compare panels c and d, “dim”). Cx43 was not entirely absent from the A-V region of the adrenergic-deficient hearts, however, as it can be seen when image processing was adjusted to increase sensitivity. Equivalent processing of the images from adrenergic-competent hearts led to overexposure of Cx43 immunofluorescent staining, though the comparison with the deficient example under the same conditions (“bright”) still clearly demonstrate the disparity of staining intensities between adrenergic-competent and deficient E10.5 in the A-V regions (compare panels e and f). These results further demonstrate that Cx43 expression is selectively diminished in E10.5 adrenergic-deficient myocardium relative to that found in adrenergic-competent hearts at this stage of development.

When examined one day earlier in development (E9.5), however, Cx43 staining intensity and distribution appeared similar in adrenergic-competent and deficient mouse hearts (Fig. 6). Hcn4 immunostaining was also similar between

these groups at E9.5 (compare panels a and b). Comparative views of Cx43 are shown at low (panels c and d) and high (panels e and f) magnification. These results demonstrate that the Cx43 immunofluorescent staining is not inherently diminished in adrenergic-deficient hearts throughout development, suggesting that decreased Cx43 expression occurs after E9.5.

To determine if the electrical properties of the developing embryonic heart were altered as a result of adrenergic-deficiency, we cultured isolated E10.5 adrenergic-competent and deficient hearts on MEAs and measured extracellular field potentials from different regions of the heart. These included the sinoatrial region (SAR) near the SAN (sinoatrial node), the interchamber atrioventricular junction region (AVJ), and ventricular apex (APX), as illustrated in Fig. 7. Representative field potential traces from adrenergic-competent and deficient hearts are shown from simultaneous MEA recordings at the SAR and APX electrodes, indicating a general lengthening of the conduction time from SAR to APX in deficient hearts. MEA measurements were thus obtained for a series of these *ex vivo* embryonic heart preparations, and the combined results are summarized in Table 1, where it can be seen that the atrioventricular conduction time (AVJ-APX), which includes transmission time through the AVJ, was roughly twice the duration in adrenergic-deficient hearts compared with competent control hearts (31±6 vs. 15±2 ms, respectively, n=5/6, $p < 0.05$). In contrast, atrial conduction times (SAR-AVJ) were not significantly altered between the groups. The adrenergic-deficient hearts displayed slightly slower intrinsic heart

rates and longer SAR-APX conduction times than adrenergic-competent controls on average, but these differences were not significant. These data suggest that there was a selective slowing of atrioventricular conduction velocity in adrenergic-deficient E10.5 hearts whereas atrial conduction and average beating rates were not significantly altered under these conditions.

To determine if adrenergic-deficient embryonic mouse hearts show increased susceptibility to arrhythmia, we cultured adrenergic-deficient and adrenergic-competent hearts *ex vivo* following isolation at E9.5 and E10.5. Heart rate and rhythmicity were measured at baseline and after challenge with the β-adrenergic receptor agonist, isoproterenol (500 nM). This challenge resulted in consistent 30-40% increase in heart rates for all groups within 2 minutes after drug application (Fig. 8a). Baseline and isoproterenol-induced heart rates were not significantly different between adrenergic-deficient and competent hearts at either E9.5 or E10.5 (Supplemental Table). Arrhythmic index (AI) was used to measure the rhythmicity of these isolated hearts before and after isoproterenol treatment as previously reported and described in the Materials and Methods section [9]. A significant ($p < 0.05$) 225% increase in AI from the adrenergic-deficient E10.5 mouse hearts was observed following the isoproterenol challenge (Fig. 8b). Representative examples of adrenergic-competent (rhythmic beating) and adrenergic-deficient (arrhythmic beating) hearts are provided in Supplemental Videos 1 and 2, respectively. Relatively small non-significant ($p > 0.05$) increases in AI (< 50%) were observed for adrenergic-competent hearts at

E10.5, and no significant differences were observed in AI for either group at E9.5 (Fig. 8b). These results demonstrate that by E10.5, adrenergic-deficient mouse hearts were significantly more arrhythmic compared with adrenergic-competent controls following acute challenge with isoproterenol.

Discussion

In the present study, we showed that adrenergic deficiency during embryonic development leads to increased susceptibility for cardiac arrhythmias, slowed atrioventricular conduction, and decreased expression of the major cardiac gap junction protein, Cx43. We also showed that sarcomeric α-actinin and Hcn4 expression patterns and intensities were similar in adrenergic-competent and deficient hearts, thereby suggesting that myocardial and pacemaker cell development are grossly normal in the absence of NE and EPI. These results are supported by the finding that heart rates were not significantly different in adrenergic-competent and deficient hearts. Taken together, these results suggest that adrenergic hormones are not required for the development of cardiac pacemaking activity through E10.5 in the mouse, but instead function to stimulate Cx43 expression, facilitate atrioventricular conduction, and maintain cardiac rhythmicity.

Initially, we aimed to examine protein staining intensity and distribution patterns for Cx43 and Hcn4 to determine if these are altered in adrenergic-deficient embryonic hearts around the time of their demise. Cx43 staining was

less intense relative to that for sarcomeric α-actinin and Hcn4 in adrenergic-deficient hearts compared with competent controls at E10.5. Our co-immunofluorescent histochemical staining data show that was not true one day earlier at E9.5, where Cx43 expression was not diminished in adrenergic-deficient hearts relative to controls or to sarcomeric α-actinin and Hcn4 staining. These results indicate that Cx43 appears to develop normally through E9.5 in adrenergic-deficient hearts, but that it either becomes down-regulated or fails to be up-regulated due to the lack of NE and EPI, such that by E10.5, Cx43 expression was substantially lower in adrenergic-deficient hearts than in controls. The pattern of Cx43 distribution, which remained diffuse and spotty, as has been seen in other studies at these early developmental stages (Coppen et al., 2003; Delorme et al., 1997; Fromaget et al., 1992; Peters et al., 1994), did not appear to be altered in adrenergic-deficient mouse hearts, but the intensity of the staining for Cx43 was substantially reduced compared with equivalent staining in the control group.

Disruption of both Cx43 alleles (*Cx43*$^{-/-}$) results in lethality at birth due to cardiac malformation resulting from swelling and blockage of the right outflow tract (Reaume et al., 1995). Surprisingly, cardiac conduction speeds were not altered much at E12.5, the earliest developmental timepoint measured in *Cx43*$^{-/-}$ hearts, though significant slowing became apparent by E15.5 and continued to lengthen thereafter (Vaidya et al., 2001). Cardiac-restricted Cx43 knockouts survive through birth, but die within the first two months of life from sudden

cardiac death due to severe arrhythmias (Gutstein et al., 2001). Ventricular conduction velocity was also markedly slowed in these animals. Additionally, cultured embryonic myocytes derived from *Cx43*$^{-/-}$ hearts show dramatic reductions in conduction speeds relative to *Cx43*$^{+/-}$ or *Cx43*$^{+/+}$ controls (Beauchamp et al., 2004). Thus, it is well-established that Cx43 plays a critical role in mediating ventricular conduction through the fetal and early postnatal periods. At earlier stages of embryonic development, it may be less critical as compensation by Cx40 and Cx45 appear to help ameliorate conduction slowing due to the absence of Cx43 (Vaidya et al., 2001), though there is evidence suggesting that expression and activity may also be compromised in *Cx43*$^{-/-}$ myocytes (Beauchamp et al., 2004; Johnson et al., 2002; Kirchhoff et al., 2000; Xie et al., 2009). These caveats notwithstanding, lowered Cx43 expression in adrenergic-deficient hearts could contribute to the observed slowing of atrioventricular conduction. We expect to find additional targets of embryonic adrenergic hormone action in the developing heart that will also likely contribute to the slowed atrioventricular conduction and arrhythmogenic phenotype of adrenergic-deficient mice.

Microelectrode arrays provided *ex vivo* heart rate and conduction analysis of cultured adrenergic-competent and deficient embryonic hearts. One of the limitations of the MEA analysis, however, was the relatively large electrode-electrode distance (200 µm) compared to the small heart (~600 x ~800 µm). In addition, the 2-dimensional MEA surface could only examine the ventral plane of

the 3-dimensional heart. Despite these limitations, the data from the MEA experiments demonstrated that atrioventricular conduction was slower in adrenergic-deficient hearts. Of note, it has been reported that E10.5 is approximately the stage of development in the mouse when ventricular conduction transitions from a base-to-apex to an apex-to-base pattern of excitation (Rentschler et al., 2002). It is therefore conceivable that adrenergic hormones could play a role in mediating this transition in the developing heart. Future experiments are needed to further explore the underlying molecular mechanisms that mediate adrenergic influence on the development of atrioventricular conduction.

Failure to complete this transition in a coordinated and timely manner could have critical consequences for heart development and embryonic survival if the myocardium becomes more susceptible to arrhythmogenesis. Adrenergic-competent and deficient embryonic hearts did not show a difference in basal AI; however, isoproterenol challenge did induce significantly increased AI in adrenergic-deficient E10.5 hearts compared to controls. This indicates that in *ex vivo* cultured conditions adrenergic hormones help maintain a balance of rhythmic beating even after increased stimulation. Other mechanisms of β-adrenergic regulation, such as synchronization of intracellular Ca^{2+} oscillations (Song et al., 2001), may also impact arrhythmia susceptibility in adrenergic-deficient hearts. Consequently, we cannot say for certain if the altered Cx43 expression and slowed atrioventricular conduction observed in adrenergic-

deficient hearts were contributory to the increased propensity for arrhythmias. If such arrhythmias are triggered *in vivo*, they could certainly contribute to the observed heart failure and fetal lethality in adrenergic-deficient mice, but further study is required to make that determination.

In summary, we have shown that adrenergic deficiency led to decreased Cx43 in E10.5 but not E9.5 mouse hearts. We have also for the first time shown that atrioventricular conduction is significantly slower in adrenergic-deficient hearts, and that arrhythmic activity was significantly induced in adrenergic-deficient hearts compared with adrenergic-competent controls. In contrast, pacemaking cell development and gross cardiac structural development of the early muscle chambers appear relatively normal in adrenergic-deficient embryos through E10.5. Thus, our data do not support the hypothesis that adrenergic hormones are critical for development of cardiac pacemaking, but they are supportive of a role for adrenergic hormones in stimulating Cx43 expression, facilitating atrioventricular conduction, and helping to maintain cardiac rhythm during a critical early period of embryonic heart development.

Acknowledgements

This work was supported by NIH grants to SNE (HL078716) and JH (5RO1EB005459), and a postdoctoral fellowship (DGT) from the American Heart Association (0825395E).

Tables

Table 1 Summary of MEA data from E10.5 mouse hearts.

	Adrenergic-Competent	**Adrenergic-Deficient**
Heart Rate (bmp)	148.6 ± 10.7 (11)	120.7 ± 6.7 (6)
Conduction Time: SAR-APX (ms)	52.1 ± 4.0 (11)	64.8 ± 9.1 (6)
Conduction Time: SAR-AVJ (ms)	33.8 ± 3.0 (6)	29.8 ± 4.8 (5)
Conduction Time: AVJ-APX (ms)	15.4 ± 1.7 (6)	**31.4 ± 6.4 * (5)**

*, $p < 0.05$

Table 2 Values for heart rate and arrhythmic index responses to isoproterenol challenge in adrenergic-competent and deficient embryonic mouse hearts isolated at E9.5 (a) and E10.5 (b).

Heart rate and arrhythmic index at baseline and in response to isoproterenol in E9.5 adrenergic-competent and deficient embryos.

	Adrenergic-competent (5)		Adrenergic-deficient (4)	
	Baseline	Isoproterenol	Baseline	Isoproterenol
Heart Rate (bpm)	119.6 ± 9.8	160.0 ± 14.6	137.3 ± 7.8	177.5 ± 6.6
Arrhythmic Index	0.03 ± 0.01	0.02 ± 0.001	0.04 ± 0.03	0.02 ± 0.003

Heart rate and arrhythmic index at baseline and in response to isoproterenol in E10.5 adrenergic-competent and deficient embryos.

	Adrenergic-competent (17)		Adrenergic-deficient (5)	
	Baseline	Isoproterenol	Baseline	Isoproterenol
Heart Rate (bpm)	112.7 ± 10.1	159.6 ± 12.6	148.8 ± 15.2	206.4 ± 16.1
Arrhythmic Index	0.06 ± 0.01	0.05 ± 0.01	0.04 ± 0.02	0.08 ± 0.02

Figures

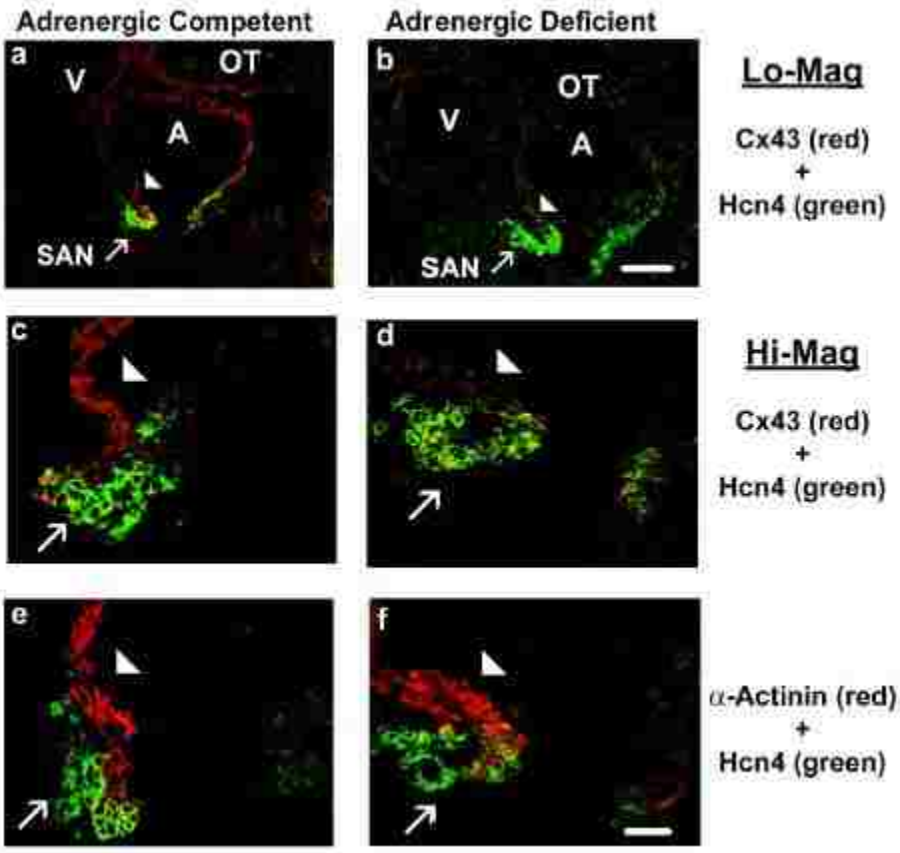

Figure 4 Immunofluorescent histochemical evaluation of Cx43 relative to Hcn4 and sarcomeric α-actinin expression in adrenergic-competent and deficient E10.5 mouse hearts.

(a,b) Low-magnification (Lo-Mag, 20X objective) views of adrenergic-competent and deficient mouse hearts, respectively, for Cx43 (red) and Hcn4 (green). Co-localized areas appear yellow. Scale bar for panels a-b, 0.1 mm. (c,d) High-magnification (Hi-Mag, 60X objective) views of the corresponding SAN regions (arrows) depicted in panels a and b, respectively, for adrenergic-competent and deficient hearts stained for Cx43 and Hcn4. (e,f) Hi-Mag view of an adjacent section co-stained for sarcomeric α-actinin (red) and Hcn4 (green) in adrenergic-competent and deficient hearts. Arrow indicates Hcn4 staining (a-f), and arrowhead indicates either Cx43 (a-d) or α-actinin (e,f) in approximately equivalent regions of each heart. Scale bar for panels c-f, 25 µm.

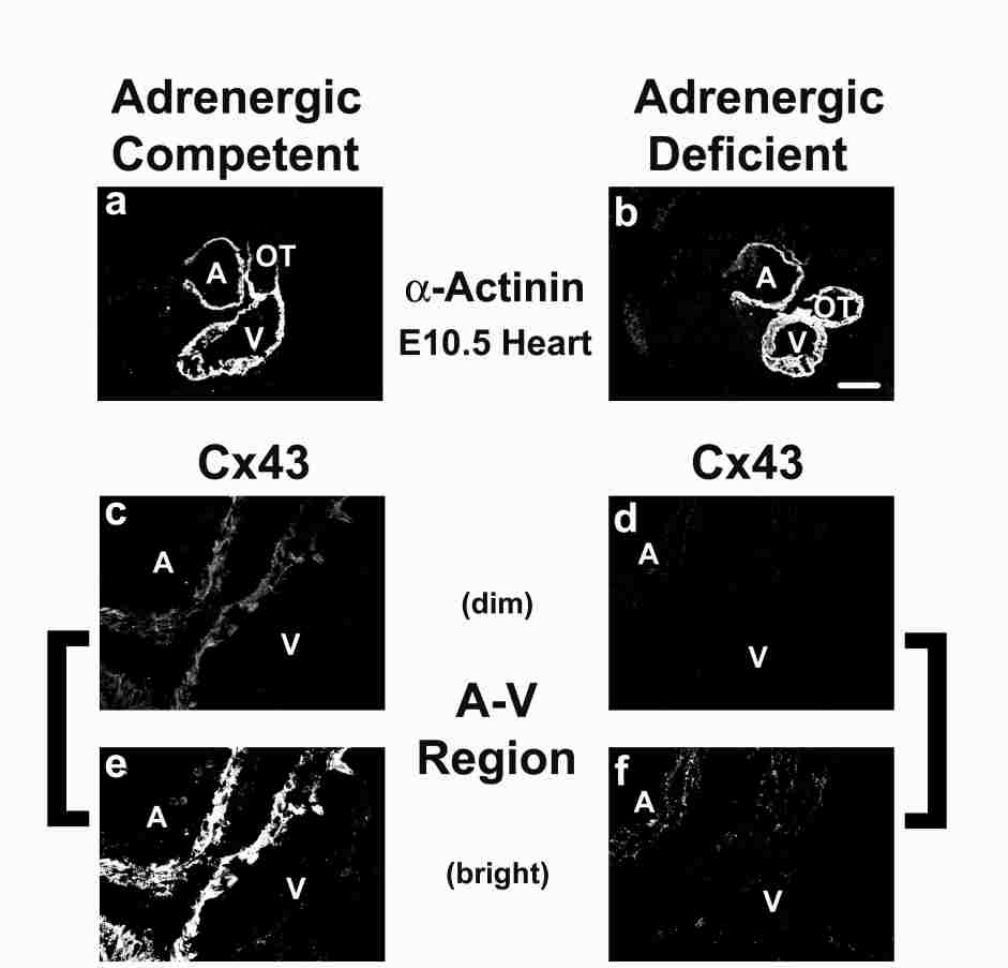

Figure 5 Immunofluorescent histochemical evaluation of Cx43 expression in the A-V junction region of adrenergic-competent and deficient E10.5 mouse hearts.

(a, b) Low magnification (10X) objective of adrenergic-competent and deficient heart sections stained for sarcomeric α-actinin. Scale bar for a-b 200 µm. (c,d) Cx43 staining in the A-V junction region when pixel levels are optimized for staining in the adrenergic-competent specimens ("dim"). (e, f) Same image as in panels c and d, respectively but shown under "bright" conditions to optimize for Cx43 appearance in the adrenergic-deficient specimens. Scale bar for c-f, 50 µm.

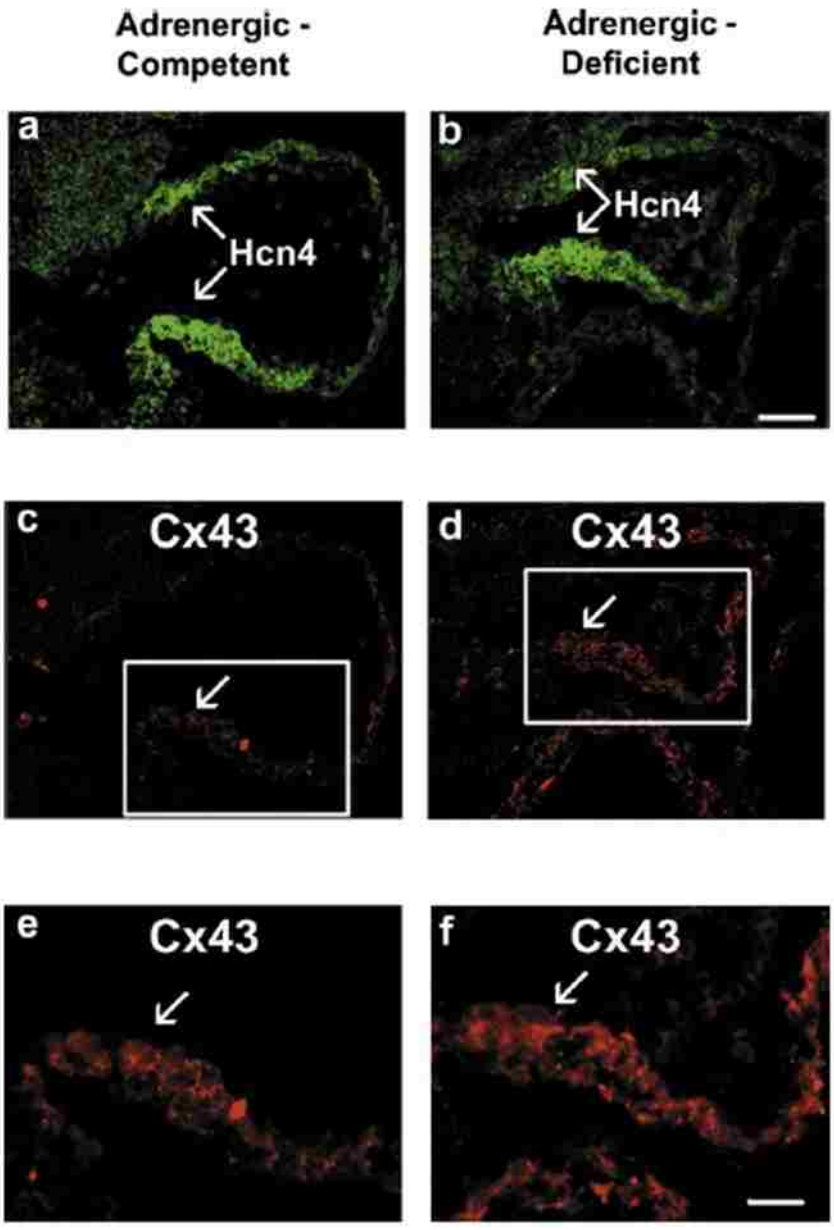

Figure 6 Immunofluorescent histochemical evaluation of Cx43 and Hcn4 expression in adrenergic-competent and deficient E9.5 mouse hearts.

(a,b) Hcn4 (green) staining (arrows) in adrenergic-competent and deficient hearts, respectively. (c,d) Cx43 (red) staining (arrow) in adrenergic-competent and deficient hearts, respectively. Scale bar for a-d, 50 μm. (e,f) Expanded view of the Cx43 (boxed insets from panels c and d) in adrenergic-competent and deficient hearts, respectively. Scale bar for e-f, 25 μm.

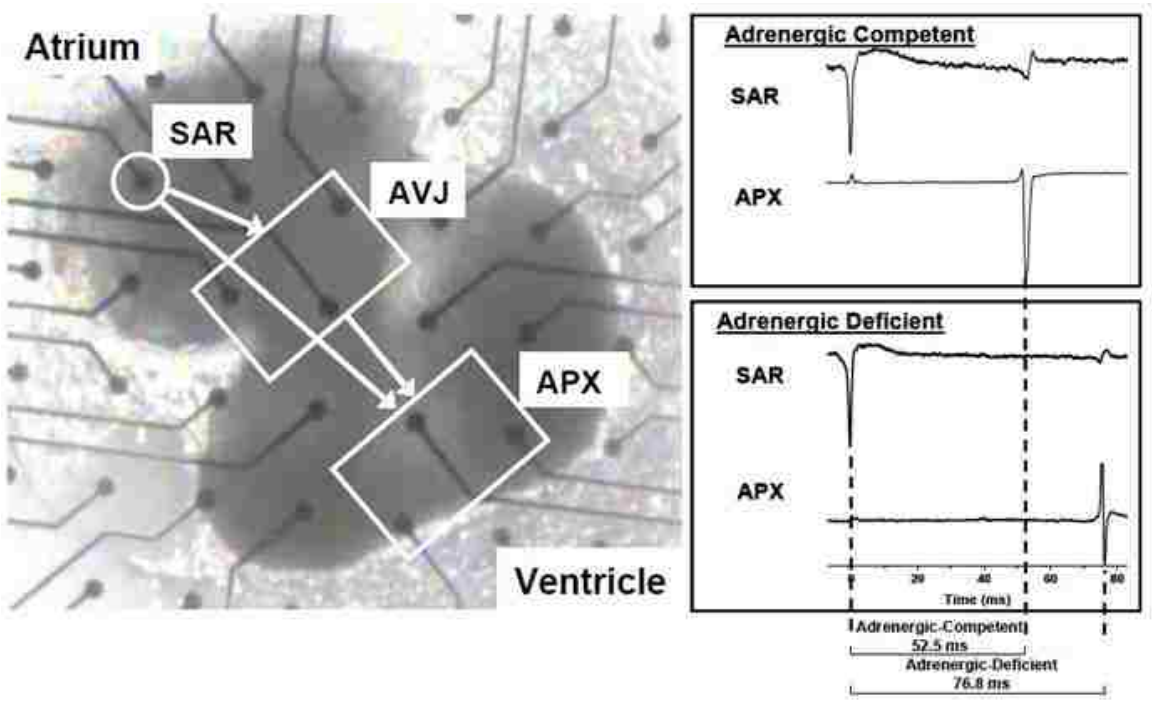

Figure 7 Illustrative conduction paths and representative field potential traces from adrenergic-competent and deficient E10.5 mouse hearts cultured *ex vivo* on MEAs.

(a) Representative heart shown without anchoring grid for visual clarity. Circle indicates first electrode to depolarize in the sinoatrial region (SAR). Boxes indicate electrodes depolarizing near-simultaneously (within 0.5 ms of each other) in the atrioventricular junction region (AVJ) and ventricular apex (APX). Arrows display overall evaluated conduction paths. (b,c) Representative field potential recordings were aligned and compared from the SAR and APX regions of adrenergic-competent and deficient hearts, respectively. Vertical dashed lines were drawn to show how conduction times were measured from the FP_{min} (see Materials and Methods for more details on how these measurements were performed) [9]. Cumulative data from several experiments is shown in Table 1. Figure contributed courtesy of Dr. David Taylor.

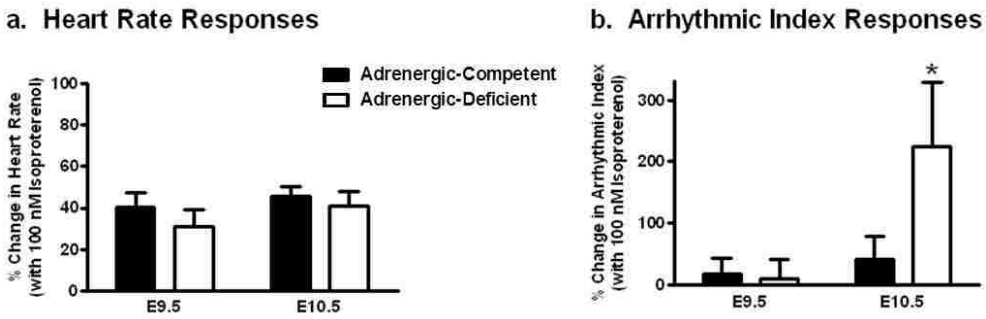

Figure 8 Heart rate and arrhythmic index responses to isoproterenol challenge in adrenergic-competent (black columns) and adrenergic-deficient (white columns) embryonic mouse hearts isolated at E9.5 and E10.5.

(a) Percent change in heart rates following acute (2-min) challenge with 0.5 μM isoproterenol. (b) Percent change in arrhythmic index (AI) in response to acute isoproterenol (0.5 μM) challenge in adrenergic-competent and deficient embryonic mouse hearts. *, $p < 0.05$ relative to control adrenergic-competent E10.5 hearts.

List of References

Beauchamp, P., Choby, C., Desplantez, T., de Peyer, K., Green, K., Yamada, K.A., Weingart, R., Saffitz, J.E., and Kleber, A.G. (2004). Electrical propagation in synthetic ventricular myocyte strands from germline connexin43 knockout mice. Circulation research *95*, 170-178.

Coppen, S.R., Kaba, R.A., Halliday, D., Dupont, E., Skepper, J.N., Elneil, S., and Severs, N.J. (2003). Comparison of connexin expression patterns in the developing mouse heart and human foetal heart. Molecular and cellular biochemistry *242*, 121-127.

Delorme, B., Dahl, E., Jarry-Guichard, T., Briand, J.P., Willecke, K., Gros, D., and Theveniau-Ruissy, M. (1997). Expression pattern of connexin gene products at the early developmental stages of the mouse cardiovascular system. Circulation research *81*, 423-437.

Ebert, S.N., Baden, J.M., Mathers, L.H., Siddall, B.J., and Wong, D.L. (1996). Expression of phenylethanolamine n-methyltransferase in the embryonic rat heart. Journal of molecular and cellular cardiology *28*, 1653-1658.

Ebert, S.N., Rong, Q., Boe, S., Thompson, R.P., Grinberg, A., and Pfeifer, K. (2004). Targeted insertion of the Cre-recombinase gene at the phenylethanolamine n-methyltransferase locus: a new model for studying the developmental distribution of adrenergic cells. Dev Dyn *231*, 849-858.

Ebert, S.N., and Taylor, D.G. (2006). Catecholamines and development of cardiac pacemaking: an intrinsically intimate relationship. Cardiovascular research *72*, 364-374.

Ebert, S.N., Taylor, D.G., Nguyen, H.L., Kodack, D.P., Beyers, R.J., Xu, Y., Yang, Z., and French, B.A. (2007). Noninvasive tracking of cardiac embryonic stem cells in vivo using magnetic resonance imaging techniques. Stem cells *25*, 2936-2944.

Ebert, S.N., and Thompson, R.P. (2001). Embryonic epinephrine synthesis in the rat heart before innervation: association with pacemaking and conduction tissue development. Circulation research *88*, 117-124.

Fink, M., Callol-Massot, C., Chu, A., Ruiz-Lozano, P., Izpisua Belmonte, J.C., Giles, W., Bodmer, R., and Ocorr, K. (2009). A new method for detection and quantification of heartbeat parameters in Drosophila, zebrafish, and embryonic mouse hearts. BioTechniques *46*, 101-113.

Fromaget, C., el Aoumari, A., and Gros, D. (1992). Distribution pattern of connexin 43, a gap junctional protein, during the differentiation of mouse heart myocytes. Differentiation; research in biological diversity *51*, 9-20.

Gutstein, D.E., Morley, G.E., Tamaddon, H., Vaidya, D., Schneider, M.D., Chen, J., Chien, K.R., Stuhlmann, H., and Fishman, G.I. (2001). Conduction slowing and sudden arrhythmic death in mice with cardiac-restricted inactivation of connexin43. Circulation research *88*, 333-339.

Halbach, M., Egert, U., Hescheler, J., and Banach, K. (2003). Estimation of action potential changes from field potential recordings in multicellular mouse cardiac myocyte cultures. Cellular physiology and biochemistry : international journal of experimental cellular physiology, biochemistry, and pharmacology *13*, 271-284.

Huang, M.H., Friend, D.S., Sunday, M.E., Singh, K., Haley, K., Austen, K.F., Kelly, R.A., and Smith, T.W. (1996). An intrinsic adrenergic system in mammalian heart. The Journal of clinical investigation *98*, 1298-1303.

Johnson, C.M., Kanter, E.M., Green, K.G., Laing, J.G., Betsuyaku, T., Beyer, E.C., Steinberg, T.H., Saffitz, J.E., and Yamada, K.A. (2002). Redistribution of connexin45 in gap junctions of connexin43-deficient hearts. Cardiovascular research *53*, 921-935.

Kirchhoff, S., Kim, J.S., Hagendorff, A., Thonnissen, E., Kruger, O., Lamers, W.H., and Willecke, K. (2000). Abnormal cardiac conduction and morphogenesis in connexin40 and connexin43 double-deficient mice. Circulation research *87*, 399-405.

Natarajan, A.R., Rong, Q., Katchman, A.N., and Ebert, S.N. (2004). Intrinsic cardiac catecholamines help maintain beating activity in neonatal rat cardiomyocyte cultures. Pediatr Res *56*, 411-417.

Peters, N.S., Severs, N.J., Rothery, S.M., Lincoln, C., Yacoub, M.H., and Green, C.R. (1994). Spatiotemporal relation between gap junctions and fascia adherens junctions during postnatal development of human ventricular myocardium. Circulation *90*, 713-725.

Pillekamp, F., Reppel, M., Brockmeier, K., and Hescheler, J. (2006). Impulse propagation in late-stage embryonic and neonatal murine ventricular slices. Journal of electrocardiology *39*, 425 e421-424.

Reaume, A.G., de Sousa, P.A., Kulkarni, S., Langille, B.L., Zhu, D., Davies, T.C., Juneja, S.C., Kidder, G.M., and Rossant, J. (1995). Cardiac malformation in neonatal mice lacking connexin43. Science *267*, 1831-1834.

Rentschler, S., Zander, J., Meyers, K., France, D., Levine, R., Porter, G., Rivkees, S.A., Morley, G.E., and Fishman, G.I. (2002). Neuregulin-1 promotes formation of the murine cardiac conduction system. Proceedings of the National Academy of Sciences of the United States of America *99*, 10464-10469.

Reppel, M., Pillekamp, F., Lu, Z.J., Halbach, M., Brockmeier, K., Fleischmann, B.K., and Hescheler, J. (2004). Microelectrode arrays: a new tool to measure embryonic heart activity. Journal of electrocardiology *37 Suppl*, 104-109.

Song, L.S., Wang, S.Q., Xiao, R.P., Spurgeon, H., Lakatta, E.G., and Cheng, H. (2001). beta-Adrenergic stimulation synchronizes intracellular Ca(2+) release during excitation-contraction coupling in cardiac myocytes. Circulation research *88*, 794-801.

Stieber, J., Herrmann, S., Feil, S., Loster, J., Feil, R., Biel, M., Hofmann, F., and Ludwig, A. (2003). The hyperpolarization-activated channel HCN4 is required for the generation of pacemaker action potentials in the embryonic heart. Proceedings of the National Academy of Sciences of the United States of America *100*, 15235-15240.

Thomas, S.A., Matsumoto, A.M., and Palmiter, R.D. (1995). Noradrenaline is essential for mouse fetal development. Nature *374*, 643-646.

Thomas, S.A., and Palmiter, R.D. (1998). Examining adrenergic roles in development, physiology, and behavior through targeted disruption of the mouse dopamine beta-hydroxylase gene. Adv Pharmacol *42*, 57-60.

Vaidya, D., Tamaddon, H.S., Lo, C.W., Taffet, S.M., Delmar, M., Morley, G.E., and Jalife, J. (2001). Null mutation of connexin43 causes slow propagation of ventricular activation in the late stages of mouse embryonic development. Circulation research *88*, 1196-1202.

van Veen, A.A., van Rijen, H.V., and Opthof, T. (2001). Cardiac gap junction channels: modulation of expression and channel properties. Cardiovascular research *51*, 217-229.

Xie, L.J., Huang, G.Y., Zhao, X.Q., Qi, C.H., Peng, T., and Zhou, G.M. (2009). [Spatio-temporal expression of connexion (Cx) 40 and Cx45 in Cx43 knockout embryonic mouse hearts]. Zhonghua yi xue za zhi *89*, 686-689.

CHAPTER THREE:
IMPAIRED CARDIAC ENERGY METABOLISM IN EMBRYOS LACKING ADRENERGIC STIMULATION

Abstract

We hypothesize that adrenergic hormones play a vital role in development by providing critical stimulation of energy metabolism during the embryonic/fetal transition period. To test this hypothesis, we examined ATP and ADP concentrations in mouse embryos lacking the ability to produce the adrenergic hormones, norepinephrine and epinephrine, due to targeted disruption of the essential *dopamine β-hydroxylase* (*Dbh*) gene. Our results show that embryonic ATP concentrations decreased dramatically while ADP concentrations rose such that the ATP/ADP ratio in the adrenergic-deficient group was nearly 50-fold less than that found in littermate controls by embryonic day 11.5. We also found that extracellular acidification and oxygen consumption rates were significantly decreased, and mitochondria were drastically larger and more branched in adrenergic-deficient hearts. Metabolic deficiencies in $Dbh^{-/-}$ embryos were prevented by administration of the β-adrenergic agonist, isoproterenol. These data demonstrate that adrenergic hormones stimulate cardiac energy metabolism during a critical period of embryonic development.

Introduction

The adrenergic hormones, epinephrine (EPI) and norepinephrine (NE), are key mediators of stress responses and sympathetic nervous system activities in adult mammals. NE, in particular, is also essential for embryonic development. Targeted disruption of the gene *dopamine β-hydroxylase* (*Dbh*), which codes for the enzyme that converts dopamine into NE, led to a loss of NE and EPI, and embryonic lethality due to heart failure in mice (Thomas et al., 1995). In contrast, disruption of the subsequent enzymatic step catalyzed by *phenylethanolamine n-methyltransferase* (*Pnmt*) led to the loss of EPI without concomitant developmental phenotypes (Ebert et al., 2004). Thus, while EPI may contribute to adrenergic activity in the embryo, NE is clearly of critical importance for heart development.

How NE influences heart development in utero is not fully understood. In $Dbh^{-/-}$ embryos signs of cardiac distress begin to appear on embryonic day 10.5 (E10.5), and approximately 50% of the $Dbh^{-/-}$ embryos die by E11.5 (Thomas et al., 1995). Remarkably, the heart appears to develop and function normally up to this point, but then deteriorates rapidly into heart failure within 24h of the first symptoms, which include sluggish cardiac contractions, arrhythmia, and asynchrony as observed via echocardiography in utero (Osuala et al., 2012). Recent work has shown that $Dbh^{-/-}$ hearts display significantly delayed conduction speed across the atrioventricular junction relative to age-matched littermate controls (Baker et al., 2012). These results suggest important

adrenergic influences on the development of cardiac structure and function, but do not fully explain how NE affects them.

At these early embryonic stages of development, there is no sympathetic innervation of the heart, and the adrenal glands have not yet formed. Instead, NE is produced in the embryonic heart itself, as well as outside of the heart in primordial sympathetic ganglia and brainstem neurons (Ebert et al., 1996; Ebert et al., 2004; Ebert and Thompson, 2001). With respect to heart function, NE appears to be acting primarily through β-adrenergic receptors since *Dbh*$^{-/-}$ embryos could be rescued by providing the β-agonist, isoproterenol, in the maternal drinking water, whereas the α-agonist, l-phenylephrine, was ineffective at rescuing the heart failure and lethality (Thomas and Palmiter, 1998). These results established that NE stimulates cardiovascular functions during the early embryonic period primarily through β-adrenergic receptors. But what are the important downstream pathways and targets affected by β-adrenergic receptor stimulation in the embryonic heart?

To gain insight about adrenergic actions in cardiac development, we recently performed a genome-wide expression screen of *Dbh*$^{-/-}$ and *Dbh*$^{+/+}$ embryonic hearts. A key finding from this screen demonstrated the largest category of differentially expressed genes (~31% of total) were those involved in metabolism (Osuala et al., 2012). In adult mammals, adrenergic hormones are known to have profound and widespread influences on metabolism. In the liver, for example, β-adrenergic stimulation inhibits glycolysis, promotes

gluconeogenesis, and stimulates breakdown of glycogen (Berthet et al., 1957; Sutherland and Wosilait, 1955). In cardiac and skeletal muscle, glycolysis and oxidative phosphorylation (OXPHOS) are increased in response to β-adrenergic stimulation to produce more available energy during stress. Free fatty acids are released from adipose tissue, and these serve as the primary fuel source for cardiac metabolism in adult mammals, but prior to birth the heart principally uses carbohydrates (Bing et al., 1954; Carlsten et al., 1961; Cox and Gunberg, 1972; Ellington, 1987; Gordon and Cherkes, 1956; Neely and Morgan, 1974; Shepard et al., 1970). The shift from carbohydrate to lipid metabolism in the heart occurs shortly after birth and is often referred to as the "fetal-shift" in cardiac metabolism (Duncan, 2011; Madrazo and Kelly, 2008; Makinde et al., 1998). Surprisingly little, however, is known regarding adrenergic influences on cardiac metabolism during the embryonic period.

There is compelling evidence indicating that aerobic metabolism in the mitochondria becomes increasingly important as the heart transitions from embryonic to fetal stages of development. For example, genetic mutations that decrease or disrupt OXPHOS often result in heart failure and embryonic lethality (Humble et al., 2013; Larsson et al., 1998; Li et al., 2000). Furthermore, mutations that disrupt mitochondrial structure and function also interfered with cardiomyocyte differentiation and development(Chen et al., 2003; Chen et al., 2011; Davies et al., 2007; Wakabayashi et al., 2009), and many of these ultimately succumbed to heart failure and embryonic lethality. Thus, there

appears to be an “embryonic-shift” from primarily anaerobic to aerobic metabolic mechanisms in the heart during the embryonic-fetal transition period of development (Baker and Ebert, 2013).

We hypothesize that adrenergic hormones play a critical role in facilitating the metabolic shift towards aerobic oxidative phosphorylation in cardiac mitochondria during embryonic development. Here, we test this hypothesis by examining metabolic profiles of ATP, ADP, and ATP/ADP ratios in *Dbh*$^{-/-}$ and control embryos. In parallel, we also examine other metabolic indices, including cardiac oxygen consumption rate (OCR) and extracellular acidification rate (ECAR) as estimators of aerobic and anaerobic metabolism, respectively. In addition, we performed detailed ultrastructural analysis of mitochondria in adrenergic-deficient and control hearts. As described in the next section, our results show that both anaerobic and aerobic metabolism are compromised in *Dbh*$^{-/-}$ hearts.

Materials and Methods

Mice

All procedures and handling of mice were conducted in accordance with The University of Central Florida Institutional Animal Care and Use Committees. The *Dbh* mouse strain was kindly provided by Dr. Richard Palmiter (University of Washington, Seattle, WA) (Thomas et al., 1995) and maintained as previously described (Baker et al., 2012; Osuala et al., 2012). Timed pregnancies were

determined by the presence of a vaginal plug (denoted as E0.5) and further confirmed by high-resolution ultrasound (Vevo 2100 instrument with 40 MHz transducer; Visualsonics, Inc.) at E8.5. For isoproterenol rescue, maternal drinking water was supplemented with 0.02 mg/ml isoproterenol and 2.0 mg/ml vitamin C beginning at E8.5, as previously described (Thomas and Palmiter, 1998).

Reagents

Chemical reagents were purchased from Sigma-Aldrich, St. Louis, MO, unless otherwise noted. Electron microscopy grade reagents for TEM were purchased from Electron Microscopy Sciences, Hatfield, PA. Cell culture reagents were purchased from Invitrogen, Grand Island, NY.

Embryonic tissue collections

All embryos used in this study appeared to be healthy and viable at the time of isolation as judged by their size (crown-rump lengths), color, texture, morphology, and overall appearance. Microscopic examination confirmed a beating heart and bright red blood coursing through the embryonic circulation. Unhealthy and dead embryos were discarded. From the living specimens collected, no apparent differences were observed between adrenergic-deficient and control embryos based on these gross examinations at the time of isolation. Upon isolation, the heads were removed and used for genotyping. For enzyme assays, trunks were flash-frozen in liquid nitrogen and stored at -80ºC. For some

experiments, E10.5 and E11.5 mouse hearts were isolated under aseptic conditions and cultured in DMEM containing 10% fetal bovine serum (Hyclone Labs) that had been charcoal-stripped to remove catecholamine and steroid hormones (Natarajan et al., 2004). The media was additionally supplemented with penicillin G (100,000 U/L) and streptomycin (100 mg/L). Hearts were cultured for 24 hours prior to any measurements of oxygen consumption or extracellular acidification rates.

ATP and ADP measurements

ATP and ADP measurements were performed with an Aposensor™ ATP/ADP Ratio Bioluminescence Assay Kit (Biovision) as per manufacturer's instructions. Briefly, embryonic tissue was homogenized in 6% trichloroacetic acid (TCA) for 1 min then centrifuged at 6,000 g for 5 min at 4ºC. The supernatant was then removed, and TCA was neutralized with tris-acetate as previously described (Cosen-Binker et al., 2006). ATP measurements were performed with ATPlite™ Bioluminescence Assay (Perkin Elmer) as instructed by the manufacturers' protocol. Standard curves were generated with known concentrations of ATP. Luminescence was detected in an Envision Multilabel plate reader (Perkin Elmer), and ATP measurements were normalized to total protein concentrations.

Lactate measurements

Embryos were homogenized in 8% perchloric acid for 1 min then centrifuged at 6,000 g for 4 min. Absorbance readings at 340 nm before and after addition of L-

lactate dehydrogenase was performed as described (Bergmeyer, 1974). The supernatants for lactate measurements were combined with NAD solution (2.5 M NAD, 0.2 M Glycine buffer, and 100 µL ≥500 units/mg protein L-lactate dehydrogenase from bovine heart). Increase in absorbance at 340 nm was compared to a standard curve of known lactate concentrations. Lactate measurements were normalized to total protein concentrations.

Glucose measurements

Glucose was measured in triplicate using a WaveSense Presto blood glucose monitoring system and compared to a standard curve of known D-glucose concentrations.

Oxygen consumption rate and Extracellular acidification rate measurements

Hearts were isolated and cultured, as described above, in Seahorse Biosciences XF24 Islet Capture Microplate with mesh grids placed on top of the specimen to prevent it from floating and from probe interference. After 24 hrs culture media was removed and replaced with serum free Seahorse XF Assay media and basal oxygen consumption and extracellular acidification rates were simultaneously measured with a Seahorse XF^e system (Seahorse Biosciences) at 10-min intervals over a period of 2 hrs. Rotenone (0.5 µM) and antimycin A (2 µM) were added through separate injection ports (Zhang et al., 2012).

Transmission Electron Microscopy

Experiments were performed as previously described (Song et al., 2011). Briefly, isolated embryonic hearts were placed in Karnovsky's fixative (2% paraformaldehyde, 2.5% glutaraldehyde and 0.1 M sodium cacodylate) for 1 hour. Samples were then rinsed in 0.1 M sodium cacodylate with 3 µM $CaCl_2$ and post-fixed in a 1% osmium tetroxide, 0.8% potassium ferrocyanide and 3 µM $CaCl_2$ solution. Samples were en bloc stained with 2% uranyl acetate and dehydrated in graded ethanol solutions. Samples were embedded in Durcupan, and thin sections were cut at 80nm using a Leica UTC Ultramicrotome and diamond knife, and then mounted on copper grids. Thin sections were stained with routine TEM double stain: Four minutes in 4% Uranyl Acetate. Four minutes in Reynolds Lead Citrate. Thin Sections were examined using an FEI 268D TEM at 50Kv, and digital images recorded using an AMT XR-60 digital camera. Mitochondrial morphometric analyses were performed with ImageJ software (NIH).

JC-1 dye

Myocytes were isolated and cultured on coverglass (for microscopy) or 48-well plates (for flow cytometry) as described previously (Maltsev et al., 1994). Cardiomyocytes were cultured for 48 hours before staining with 5 µg/mL JC-1 dye (Invitrogen) for 20 min. Dye was washed with PBS and samples were either viewed using a Perkin Elmer Spinning Disk confocal microscope or quantified

using a BDFacs Canto flow cytometer (BD Biosciences, Inc.). Gates were set with unstained cells and carbonyl cyanide-*p*-trifluoromethoxyphenylhydrazone (FCCP, 50 µM) treated controls and quantified emission filters appropriate for Alexa Fluor® 488 nm and R-phycoerythrin. Data were analyzed using FCSExpress software (DeNovo).

Gene Expression

RNA was isolated using TRIzol reagent, and converted to cDNA using High Capacity cDNA reverse Transcription Kit (Invitrogen). Real-time PCR was performed using SYBR Green Fast reagent in an AB7500 machine (Applied Biosystems). Genes of interest were normalized to the housekeeping gene GAPDH. Forward and reverse primers were as follows: *Pgc-1α*, 5'-TATGGAGTGACATAGAGTGTGCT-3' and 5'-CCACTTCAATCCACCCAGAAAG-3' Primer Bank ID 6679433a1, *Tfam,* 5'-GAGCGTGCTAAAAGCACTGG-3' and 5'-CCACAGGGCTGCAATTTTCC-3' (Lagouge et al., 2006), *Sirt*1, 5'-TGTGAAGTTACTGCAGGAGTGTAAA-3' and 5'-GCATAGATACCGTCTCTTGATCTGA-3'(Lagouge et al., 2006), G*apdh,* 5'-CCATCACCATCTTCCAGGAGCG-3' and 5'-AGAGATGACCCTTTTGGC-3' (Osuala et al., 2012). mtDNA content was measured as described previously (Park et al., 2012).

Oil Red O Staining

Oil Red O (5 mg/mL in isopropanol) stock stain was diluted to the working solution (30 ml of the stock stain diluted with 20 ml of distilled water), and used to stain for fat droplets, as previously described (Sengupta et al., 2013). Briefly, the slides were air-dried, fixed in formalin, and briefly washed with running tap water for 1 min. They were then rinsed with 60% isopropanol, stained with freshly prepared Oil Red O working solution for 15-min. The staining solution was then removed and the samples were rinsed with 60% isopropanol, rinsed further with distilled water, and mounted using Vectashield mounting medium (Vector Labs). Digital micrographs were obtained using a Leica DM2000 microscope, and images were analyzed for lipid droplets using NIH ImageJ software.

Free Fatty Acid Quantification

Fatty Acids were measured using the Free Fatty Acid Quantification Colorimetric/Fluorometric Kit (Biovision) according to the manufacturer's instructions. Briefly, flash-frozen embryos were homogenized for 30-sec then centrifuged at 12,000 g for 1 min. 100 µL 1% Triton-X 100 in chloroform was added to the supernatant. Samples were centrifuged at 12,000 g for 10 min and lower phase was transferred and allowed to air dry, pellets were then resuspended in fatty acid buffer. After following manufacturer's protocol fluorescence readings were conducted in an Envision Multilabel plate reader

(Perkin Elmer) (Excitation: 535nm and Emission: 590 nm) and compared to palmitic acid standard curve. Samples were measured in duplicate.Statistics Data are expressed as mean ± SEM. Student *t*-tests were performed to compare means, with $p < 0.05$ required to reject the null hypothesis.

Results

ATP is depleted in adrenergic-deficient embryos

To determine if adrenergic deficiency affects embryonic metabolism, we measured ATP and ADP concentrations in adrenergic-competent (*Dbh*$^{+/-}$ and *Dbh*$^{+/+}$) and deficient (*Dbh*$^{-/-}$) embryos. Throughout this and previous studies, we observed no significant difference in *Dbh*$^{+/+}$ and *Dbh*$^{+/-}$ embryos for any assays employed, and these genotypes are phenotypically indistinguishable. Thus we have combined *Dbh*$^{+/+}$ and *Dbh*$^{+/-}$ mice into a single group that we will hereafter refer to as “adrenergic-competent”. *Dbh*$^{-/-}$ mice fail to produce NE or EPI, and most will succumb to heart failure and embryonic lethality between E10.5-E15.5(Thomas et al., 1995) unless rescued by maternal supplementation of alternative catecholamine substrates(Thomas et al., 1995) or β-adrenergic agonists, such as isoproterenol (ISO) (Thomas and Palmiter, 1998).

In the absence of any rescue, ATP concentrations begin to show significant decreases in adrenergic-deficient embryos as early as E10.5, and decline precipitously by E11.5 (Figure 9A). Conversely, ADP concentrations increased over the same time period in the *Dbh*$^{-/-}$ group relative to controls

(Figure 9B). Notably, both ATP and ADP concentrations were unchanged at E9.5 relative to adrenergic-competent controls (Figure 9A, and 9B). Absolute ATP, ADP, and ATP/ADP values, generated from known ATP and ADP standard curve concentrations, are shown in Table 3 for adrenergic-competent and deficient embryos.

This is seen most clearly by examining the ATP/ADP ratio. At E9.5, for example, ATP/ADP ratios were virtually identical in adrenergic-competent and deficient embryos, but then diverge dramatically over the next two days. In control embryos, the ATP/ADP ratio steadily increases over this time period, but in *Dbh*$^{-/-}$ embryos, this ratio drops by 50% at E10.5 and by >95% (~48-fold reduction) at E11.5 (Figure 9C). It is important to note all embryos collected for these analyses appeared healthy and viable, as described in the Supplemental Methods section. In other words, the *Dbh*$^{-/-}$ embryos used throughout this study were phenotypically indistinguishable from controls at the time of isolation. These results demonstrate that *Dbh*$^{-/-}$ embryos exhibited an energy deficit beginning around E10.5 that rapidly became much more severe within 24h (E11.5).

To determine if the observed energy depletion was due to the absence of β-adrenergic stimulation, we attempted to rescue the phenotype by providing ISO in the maternal drinking water beginning at E8.5. When the experiment was repeated under these conditions, the ATP deficits disappeared (Figure 9D). We observed a 1.8-fold increase in ATP concentrations at E10.5 and a 4.5-fold

increase in E11.5 *Dbh*$^{-/-}$ ATP concentrations after ISO treatment compared to those observed without the addition of ISO. These results demonstrate that β-adrenergic stimulation was effective at preventing the energy loss resulting from adrenergic deficiency in developing mouse embryos.

Influence of adrenergic hormones on embryonic carbohydrate and lipid metabolism

Carbohydrate metabolism is the principle source of energy for the developing heart prior to birth (Cox and Gunberg, 1972; Ellington, 1987; Shepard et al., 1970). To determine if key carbohydrate metabolites were altered in adrenergic-deficient embryos, we measured glucose, glycogen, and lactate concentrations in embryos isolated at E10.5 and E11.5 (Table 4). No significant differences were observed in the concentrations of these carbohydrate metabolites at these ages. However, lactate concentrations appeared slightly elevated, on average, in adrenergic-deficient embryos at both E10.5 and E11.5, but these differences were also not statistically significant. Glycogen concentrations trended lower in the deficient group, but the results were variable and again not found to be significantly different. The biochemical results for glycogen were corroborated by image analysis of glycogen granules from transmission electron microscopy (TEM) micrographs, which showed a similar insignificant downward trend in glycogen granules at E11.5 for the adrenergic-deficient group (Table 4). We also measured free fatty acid concentrations and lipid droplets, but found no significant differences in these either, though there

was a downward trend in the deficient group for lipid droplets, which were predominantly located in the liver at these stages of development. Despite these trends, steady-state levels of free fatty acids as well as glucose, glycogen, and lactate were relatively unchanged (no significant differences) in adrenergic-deficient embryos compared to age-matched littermate controls at E10.5 and E11.5 (Table 4).

When we examined the rate of glycolysis, however, significant differences were observed. To perform these measurements, we isolated and cultured whole beating hearts from E10.5-E11.5 *Dbh*$^{-/-}$ and littermate controls, and recorded the extracellular acidification rate (ECAR) at various intervals over a 40-min period. Similar beating rates were observed in the adrenergic-competent and deficient samples at both ages (Figure 9). At E10.5, there was little difference in ECAR from adrenergic-deficient and control samples over the entire 40-mins (Figure 10A). At E11.5, however, adrenergic-deficient and control ECARs were similar initially, but began to decline in the adrenergic-deficient group after about 10-mins and continued to decline further over the next 30-mins such that it was less than half the initial rate by 40-mins (Figure 10B). This decline was prevented by the addition of ISO in the maternal drinking water (Figure 10C). These results suggest that glycolysis was compromised in adrenergic-deficient hearts by E11.5.

Oxygen consumption rate (OCR) decrease due to absence of β-adrenergic stimulation

Mitochondria begin to play an increasingly important role in the heart at these early embryonic stages of development. To determine if adrenergic hormones influence mitochondrial respiration, oxygen consumption rates (OCRs) were measured in beating embryonic hearts isolated and cultured from E10.5 and E11.5 adrenergic-deficient and age-matched littermate control samples. At both ages, OCR was significantly lower in the adrenergic-deficient hearts over a 35-min period as shown in Figure 12 (panels A & B). To confirm the oxygen consumption was from mitochondrial function, we administered rotenone (0.5 μM) and antimycin A (2 μM) to adrenergic-competent isolated hearts to block complexes I and III, which significantly decreased the overall OCR (Figure 13). OCR increased similarly in adrenergic-deficient and competent hearts between E10.5 and E11.5 (compare panels A & B, Figure 12), but the adrenergic-deficient group nevertheless continued to lag significantly below the control group through E11.5. It is important to note that hearts appeared similar and were beating spontaneously at comparable slow but steady rates in both adrenergic-deficient and competent hearts during the ex vivo culture period. Thus, despite the lack of any clear differences in outward appearance or behavior, adrenergic-deficient hearts consumed oxygen at significantly lower rates than control hearts, thereby indicating their ability to carry out OXPHOS was significantly and substantially decreased relative to adrenergic-competent controls. To verify this effect was

due to the absence of adrenergic hormones, we show that rescue with ISO restored OCRs in adrenergic-deficient hearts (Figure 12 panels C & D).

Mitochondrial biogenesis not affected by the loss of adrenergic-hormones

In theory, the lowered OCR and ATP/ADP could be due to fewer mitochondria resulting from compromised mitochondrial biogenesis in adrenergic-deficient hearts. To test this hypothesis, we measured expression of key mitochondrial biogenesis genes; however, no significant alterations in mRNA for *Pgc-1α* (p=0.58), *Tfam* (p=0.47), and *Sirt1* (p=0.65) were found in E10.5 isolated hearts when normalized to the housekeeping gene *Gapdh* (Figure 14A). Similar results were found at E11.5. We also measured mitochondrial DNA (mtDNA) content present in adrenergic-deficient and control hearts, but no significant differences were observed (Figure 14B). Although not significant, there was a small apparent increase in mtDNA at E10.5, which may be related to the similar upward trend seen in *Pgc-1α* from this group (compare Figure 14A and 14B). These results suggest that mitochondrial biogenesis is not likely a limiting factor in adrenergic-deficient embryos at these early stages.

Adrenergic-deficient myocytes have intact mitochondrial membranes

The decreased OCR in adrenergic-deficient hearts suggests that mitochondrial function may be impaired. To properly function, mitochondria must maintain membrane potentials sufficient to drive the proton gradients necessary for OXPHOS in their inner membrane space. The fluorescent dye JC-1 can

distinguish between mitochondria with intact membranes and those with compromised membrane potentials via differential fluorescence emissions(Reers et al., 1991). For example, red fluorescence (~590 nm) detects aggregates and is indicative of healthy intact membranes, while green fluorescence (~529 nm) detects monomers associated with perturbed mitochondrial potentials. We employed JC-1 staining with flow cytometry in combination with laser-scanning confocal fluorescence microscopy to assess mitochondrial membrane potential integrity in cardiomyocytes isolated from E10.5 and E11.5 adrenergic-competent and deficient hearts. Flow cytometry for red (aggregates) and green (monomers) showed no difference between adrenergic-deficient and control samples at E10.5 (Figure 15A) or E11.5 (Figure 15C). Quantification of the stained primary cardiomyocyte culture showed a red to green ratio of 3.4 ± 0.7; n=9 in the E10.5 deficient samples and 3.1 ± 0.6; n=9 in controls (Figure 15B). Similar results were observed in the E11.5 primary cardiomyocyte cultures with the red to green ratio of 3.4 ± 1.3; n=4 in the deficient group and 2.5 ± 0.8; n=4 in the control group (Figure 15D). Representative mitochondrial staining with JC-1 is shown in Figure 15E for adrenergic-competent and deficient myocytes isolated from E11.5 hearts. Despite the fact there were no significant differences in the ratio of red/green staining in these specimens, the mitochondrial staining pattern in the adrenergic-deficient group appeared to be less densely clustered and less well-organized within myocytes than those typically found in age-matched adrenergic-competent littermates, indicating there may be structural abnormalities in

mitochondria from adrenergic-deficient embryos. At this resolution, however, it was difficult to determine if there were truly structural anomalies in the mitochondria, so we employed transmission electron microscopy (TEM) for these evaluations as described below.

Mitochondrial morphology altered in adrenergic-deficient hearts

To obtain a more detailed view and assessment of mitochondrial structure in adrenergic-deficient and control embryonic hearts, we analyzed cardiac tissue specimens using TEM. Our results show that mitochondria within E10.5 adrenergic-deficient myocardium were enlarged and appeared swollen (Figure 16B) relative to adrenergic-competent controls (Figure 16A). Similar results were observed in E11.5 adrenergic-deficient hearts, demonstrating elongated mitochondria (Figure 16F) compared to adrenergic-competent samples (Figure 16E). Additionally, multiple mitochondria showed a branching and swollen appearance (Figure 16C and 16G arrowheads). Tracings of the abnormal shaped mitochondria observed in adrenergic-deficient hearts are shown for E10.5 (Figure 16D) and E11.5 hearts (Figure 16H). Like E10.5 adrenergic-deficient samples, E11.5 mutants had a significantly ($p<0.05$) decreased number of mitochondria per micrograph as compared to E11.5 adrenergic-competent hearts (Table 5). While there was a decreased number of mitochondria, the length of those present was considerably increased ($p<0.0001$) in the adrenergic-deficient samples versus controls (Table 5). Consequently, increased ($p<0.001$)

overall mitochondrial surface area was observed within myocytes for the adrenergic-deficient samples when compared to controls (Table 5). These results clearly show that mitochondrial structure is significantly altered in adrenergic-deficient embryos. On average, the mitochondria were longer, had greater surface area, and displayed more abnormal shapes such as branch points, curvatures, and budding bulges in their membranes compared with their control counterparts.

Discussion

Anaerobic glycolysis is the predominant mode of metabolism of the heart during early embryonic development, but aerobic mitochondrial metabolism becomes an increasingly important and essential mode of energy production at late embryonic to early fetal stages of development (Cox and Gunberg, 1972; Ellington, 1987; Shepard et al., 1970). For example, classic studies showed that isolated embryonic rat hearts utilized glycolytic mechanisms through E11; however, glycolysis was not sufficient to maintain maximal heart rates at E12 or E13 (Cox and Gunberg, 1972). Further, energy metabolism was unaffected by the presence of oxygen at E11 in the rat, but was significantly and progressively elevated by oxygen in E12 and E13 hearts. This embryonic-shift in metabolic capability between E11-E12 in the rat roughly corresponds to the end of the organogenesis period of embryonic development and the beginning of fetal development. In the mouse, the equivalent stages of development are

approximately E9.5-E10.5 (Theiler, 1972). It is at this embryonic/fetal juncture when metabolic deficiencies first become apparent in *Dbh*$^{-/-}$ mouse embryos, which lack the ability to produce the adrenergic hormones, NE and EPI.

At E9.5, there was no discernible difference in ATP or ADP concentrations in adrenergic-deficient and control embryos, but ATP/ADP ratios began to decline at E10.5 and much more dramatically so at E11.5 in adrenergic-deficient embryos. It seems unlikely this decline in ATP/ADP can be fully ascribed to glycolysis since no significant differences were observed in key glycolytic metabolites including glucose, pyruvate, and lactate at E10.5 or E11.5. In addition, glycolytic rates (ECAR) were virtually identical at E10.5 in adrenergic-deficient and control embryos. By E11.5, however, ECAR began to decline in the adrenergic-deficient group, indicating that glycolytic rate was compromised. The decline was not apparent immediately, but developed over a 15-30 min period, and could be prevented by supplying the β-agonist, isoproterenol. At present, it is not yet clear how β-adrenergic stimulation influences glycolytic rates in the embryo. Potential targets include Protein Kinase A (PKA)-mediated phosphorylation of glycolytic and glycogenolysis enzymes (Krebs and Fischer, 1956). Further study is required to determine which enzymes or other factors may be influenced by adrenergic hormones in the embryonic condition.

As we have shown, OCR was also significantly decreased in adrenergic-deficient hearts at E10.5 and E11.5 relative to littermate controls. These results indicate that aerobic metabolism was compromised in these embryos. In fact, it

appeared that basal OCRs in adrenergic-deficient hearts lagged about a day behind adrenergic-competent hearts, and were only about 50% of control levels at E10.5 and E11.5. These effects were extinguished by supplying isoproterenol in the maternal drinking water, thereby indicating the absence of β-adrenergic stimulation was responsible for the declining OCRs in *Dbh*$^{-/-}$ embryos. These results suggest that oxidative phosphorylation was impaired in adrenergic-deficient embryos.

Consistent with these observations, we found that mitochondrial structure was significantly altered in adrenergic-deficient embryos. TEM analyses showed that mitochondria were enlarged and more frequently displayed branching or budding membranes in adrenergic-deficient hearts at E10.5 and E11.5. Despite the abnormal mitochondrial morphology in these hearts, the membranes appeared to be intact with well-formed cristae. Further, no significant alterations in red/green fluorescence ratios were observed following application of the mitochondrial membrane potential-sensitive dye, JC-1, in adrenergic-deficient hearts compared with controls. These findings suggest that although the mitochondria were larger and abnormally shaped, the observed structural changes may represent compensatory mechanisms to try and increase ATP production in energy-starved *Dbh*$^{-/-}$ hearts (Gomes et al., 2011; Mao et al., 2013). Indeed, enlarged mitochondria have been associated with enhanced metabolic output while smaller fragmented mitochondria have generally been associated with decreased metabolic output (Knott et al., 2008; Palorini et al., 2013; Tasseva

et al., 2013). In the present study, however, we observed enlarged mitochondria with apparent decreased metabolic output. The phenomenon of elongated mitochondria with diminished function has been demonstrated previously in other models of mitochondrial dysfunction (Benard et al., 2007; Chen et al., 2003; Mortiboys et al., 2008).

We speculated the *Dbh*$^{-/-}$ embryos may be starved for substrate metabolites, but as indicated above, little change was observed in key carbohydrate or lipid substrates. This result was not entirely unexpected since glucose is known to pass freely from maternal blood supply to the embryo (Takata et al., 1994). These results suggest that metabolic substrates did not appear to be depleted in adrenergic-deficient embryos. It is possible, however, the rate of substrate transport into cells and/or inner membrane space of mitochondria could be a limiting factor in the embryos, and this will likely be an important target for future investigations. The inability of the embryo to increase nutrient supply and subsequently increase metabolic rate provides an explanation for the differences observed in the embryonic versus adult *Dbh*$^{-/-}$ mice, which compensate by increasing food intake and basic metabolic rates through mechanisms that are not fully understood (Thomas and Palmiter, 1997).

The pathophysiology of adult heart failure is commonly characterized by mitochondrial dysfunction, indicated by decreased energy production (Ingwall and Weiss, 2004; Ventura-Clapier et al., 2004; Ventura-Clapier et al., 2011). However, in the *Dbh*$^{-/-}$ embryos the signs of energy starvation are seen before

any outward precursor of heart failure. Indeed, metabolic deficiencies were observed in *Dbh*$^{-/-}$ embryos that were otherwise phenotypically indistinguishable from adrenergic-competent controls at the time of isolation in terms of size, morphology, color, texture, and cardiac beating activity. These results suggest that metabolic defects likely contribute to the subsequent heart failure and embryonic lethality in this model.

The results presented here open the door for exploration of the mechanisms responsible for the observed energy deficits in embryos lacking the ability to produce adrenergic hormones. Potential targets for adrenergic-mediated regulation of aerobic metabolism include, but are not limited to, electron transport chain enzymes in mitochondria such as complex I or IV, which have both been shown to be substrates for PKA-mediated phosphorylation (Acin-Perez et al., 2011; De Rasmo et al., 2011; Papa et al., 2012). Alternatively, proteins that regulate mitochondrial structure by promoting fission or fusion (Drp1 and Mfn2) have also been shown to be subject to PKA-mediated phosphorylation (Chang and Blackstone, 2007; Cribbs and Strack, 2007; Zhou et al., 2010), and alterations in their activities may also be crucial for mitochondrial function in these embryos. Yet other avenues for investigation here include ATP utilization rates (Ingwall, 2006; Luptak et al., 2005), the creatine kinase system (De Sousa et al., 1999; Nascimben et al., 1996), other subunits of the electron transport chain (Chung et al., 2007; Spitkovsky et al., 2004), and regulation of the closing of the mitochondrial transition pore, which naturally occurs at similar stages of

development (~E10.5) in embryonic mouse hearts (Drenckhahn, 2011; Halestrap and Pasdois, 2009; Hom et al., 2011). The G protein-coupled receptor kinase 2 (GRK2) is another attractive target since it is activated by β-adrenergic stimulation, is essential for heart development and embryonic survival, and appears to be an important signaling intermediary in the regulation of mitochondrial metabolism (Chen et al., 2013; Fusco et al., 2012; Jaber et al., 1996; Lymperopoulos et al., 2013). Future experiments are needed to distinguish between these various possibilities.

In summary, we have shown that adrenergic hormones fulfill a critical developmental role by serving to provide the growing embryo with sufficient chemical energy in the form of ATP to enable successful transition from embryonic to fetal stages. Further, our results demonstrate that adrenergic hormones are necessary to maintain sufficient ATP/ADP, ECAR, and OCR during late periods of embryonic development in preparation for the transition to the fetal period. The discovery of these influential regulatory connections between adrenergic hormones and embryonic energy metabolism opens new paths for the study of cardiovascular development that could give rise to novel therapeutic targets and strategies for treating congenital heart defects (Chin et al., 2012; Krebs et al., 2011) as well as adult forms of heart disease.

Acknowledgements

This work was supported by a grant to S.N.E. from the National Heart, Lung, and Blood Institute (R01HL-78716), and funds from the College of Medicine at the University of Central Florida.

Tables

Table 3 ATP, ADP, and ATP/ADP ratio values of adrenergic-deficient and control embryos.

		[ATP] (nmol/mg protein)	[ADP] (nmol/mg protein)	ATP/ADP Ratio (AU)	Number of samples
E9.5	Competent	40.6 ± 10.7	19.8 ± 6.6	3.9 ± 1.2	12
	Deficient	32.4 ± 8.3	10.8 ± 2.9	3.8 ± 1.2	6
E10.5	Competent	26.8 ± 3.1	9.1 ± 1.9	5.1 ± 1.0	13
	Deficient	19.5 ± 7.3	9.9 ± 4.1	2.6 ± 0.8	5
E11.5	Competent	7.6 ± 0.5	0.8 ± 0.06	9.4 ± 1.3	8
	Deficient	1.0 ± 0.4***	4.3 ± 1.3**	0.2 ± 0.03***	4

Values obtained from standard curve of known ATP and ADP concentrations. Data are represented as mean±SEM. **, p<0.05; **, p<0.01; ***, p<0.001*

Table 4 Carbohydrate and Lipid Metabolite Concentrations.

	E10.5			E11.5		
	Competent	**Deficient**	***p*-value**	**Competent**	**Deficient**	***p*-value**
Glucose (nmol/mg protein)	**313±17 n=10**	**260±26 n=9**	**0.09**	**436±27 n=8**	**421±44 n=7**	**0.77**
Glycogen (nmol/mg protein)	**5.8±1.4 n=4**	**7.5±1.5 n=4**	**0.45**	**9.9±6.5 n=4**	**4.3±2.2 n=3**	**0.51**
Glycogen Granules (% per nm^2)	**5.0±0.6 n=32**	**6.2±0.9 n=46**	**0.30**	**4.8±1.0 n=18**	**3.3±0.7 n=23**	**0.20**
Lactate (nmol/mg protein)	**250±50 n=6**	**422±107 n=6**	**0.17**	**293±37 n=6**	**416±78 n=6**	**0.18**
Lipid (liver) Droplets (per sq. mm)	**5015±677 n=10**	**3528±416 n=14**	**0.06**	**5866±598 n=16**	**3988±869 n=16**	**0.09**
Free Fatty Acids (nmol/mg protein)	**1.6±0.2 n=10**	**1.5±0.2 n=10**	**0.86**	**1.5±0.1 n=8**	**1.5±0.3 n=7**	**0.92**

Values obtained from standard curve of known concentrations. Data are represented as mean±SEM.

Table 5 Quantification of transmission electron microscopy.

	E10.5 Adrenergic-Competent	E10.5 Adrenergic-Deficient	E11.5 Adrenergic-Competent	E11.5 Adrenergic-Deficient
Number per 17.5 μm^2	**12.3 ± 0.5 n=59**	**10.4 ± 0.4** n=103**	**13.9 ± 1.1 n=38**	**11.0 ± 0.7* n=38**
Length (nm)	**715.9 ± 13.7 n=701**	**775.9 ± 14.6** n=1074**	**637.5 ± 17.4 n=529**	**888.5 ± 27.9*** n=418**
Surface Area (μm^2)	**245 ± 10.4 n=171**	**324.9 ± 21.1*** n=140**	**204.8 ± 10.6 n=166**	**362.8 ± 28.7*** n=127**

Data are expressed mean ± sem. *, $p<0.05$; **, $p<0.01$; ***, $p<0.001$

Figures

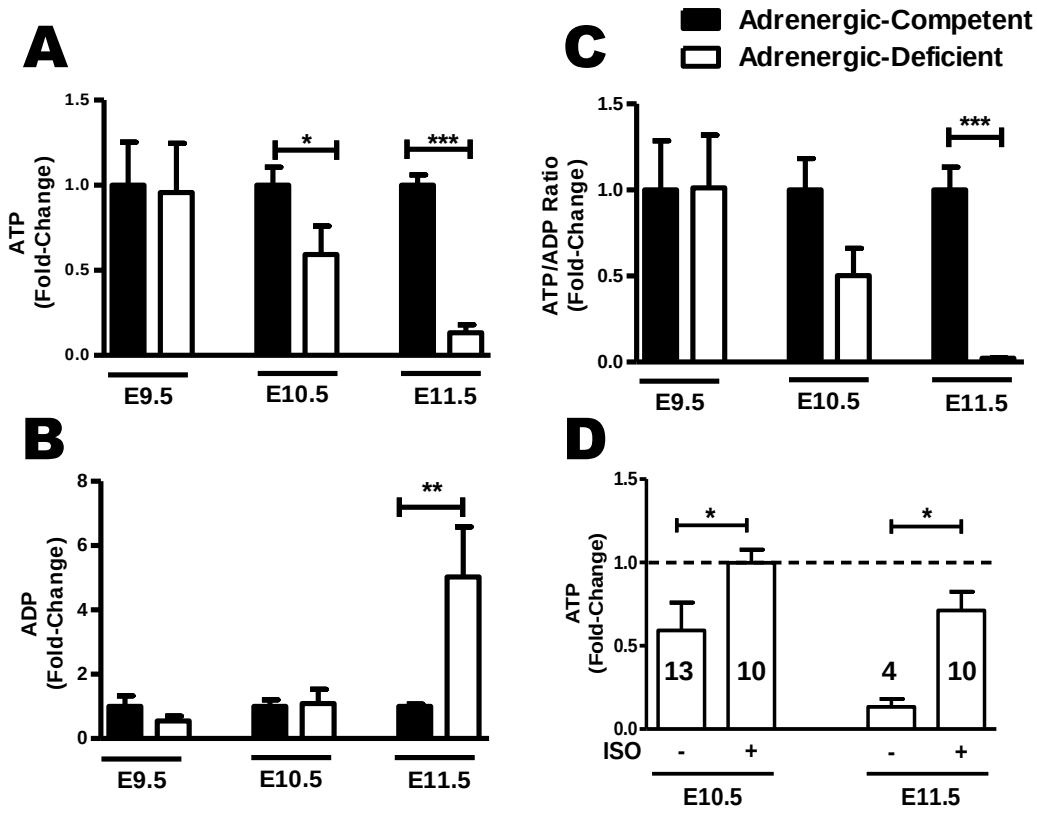

Figure 9 ATP, ADP and ATP/ADP measurements in adrenergic-deficient embryos compared to controls.

(A) ATP, (B) ADP, and (C) ATP/ADP ratio measurements at E9.5, E10.5, and E11.5 in adrenergic-competent (black bars) and adrenergic-deficient littermates (white bars). (D) ATP measurements at E10.5 (n≥10) and E11.5 (n≥4) in adrenergic-deficient embryos with and without isoproterenol. Fold-change calculations were generated from steady-state ATP and ADP concentrations. **, p<0.05; **p<0.005; ***, p<0.001*.

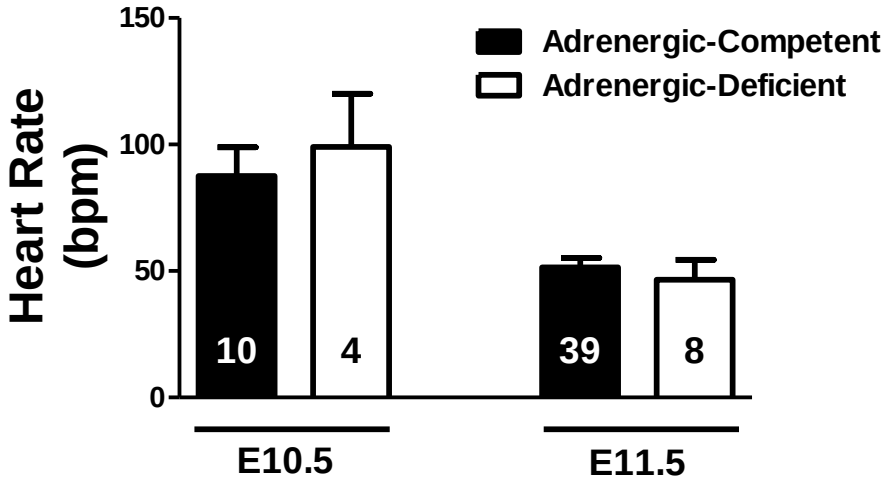

Figure 10 Beating rates of embryonic mouse hearts after 24-hrs of ex vivo culture.

Data are presented as mean ± SEM.

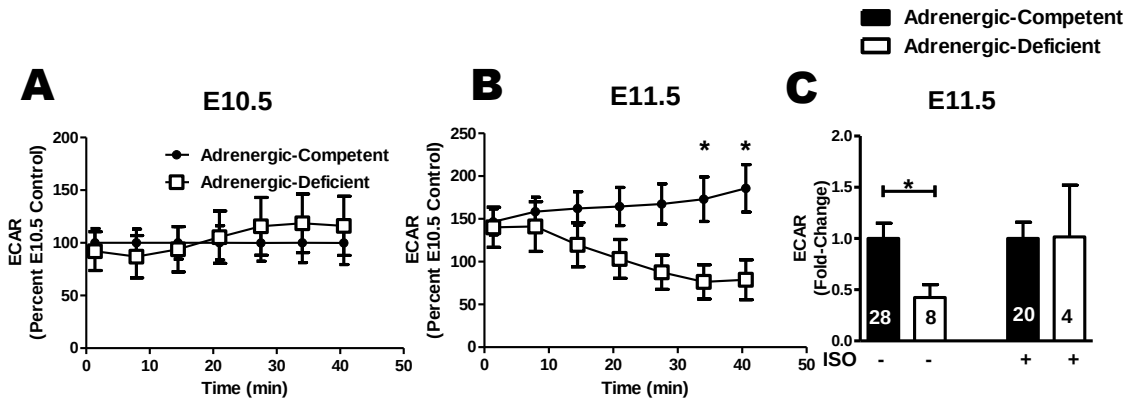

Figure 11 Effects of adrenergic-deficiency on glycolytic ECAR.

(A-B) ECAR in E10.5 and E11.5 adrenergic-competent (closed circles) and deficient (open squares) isolated beating hearts. For E10.5 adrenergic-competent, n= 15 and deficient, n=9. For E11.5 adrenergic-competent, n=28 and deficient, n=8. (C) ECAR fold-change at 40-min between adrenergic-competent (black bars) and deficient (white bars) E11.5 isolated hearts with and without isoproterenol in maternal drinking water. Mean ± SEM values at the final (40-min) timepoint are shown. **, p<0.05*.

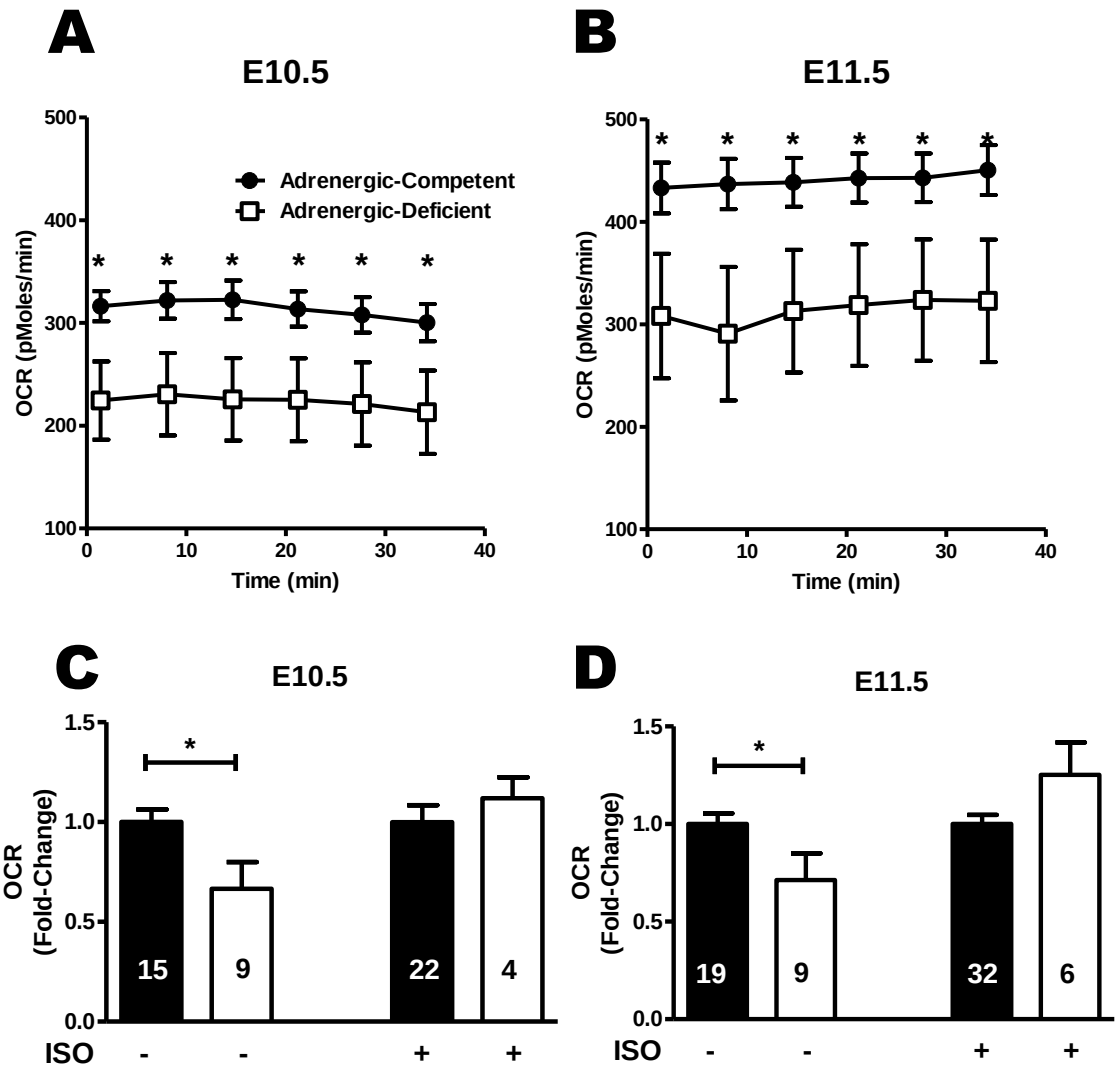

Figure 12 Effects of adrenergic-deficiency on OCR in isolated embryonic hearts.

(A-B) OCR in E10.5 and E11.5 adrenergic-competent (closed circles) and deficient (open squares) hearts. Numerical values in the columns refer to the number (n) of samples analyzed. For E10.5 adrenergic-competent, n= 15 and deficient, n=9. For E11.5 adrenergic-competent, n=20 and deficient, n=9. (C-D) OCR fold-change at 15-min between adrenergic-competent (black bars) and deficient (white bars) E10.5 and E11.5 isolated hearts with and without isoproterenol. Data are represented as mean ± SEM. **, p<0.05*.

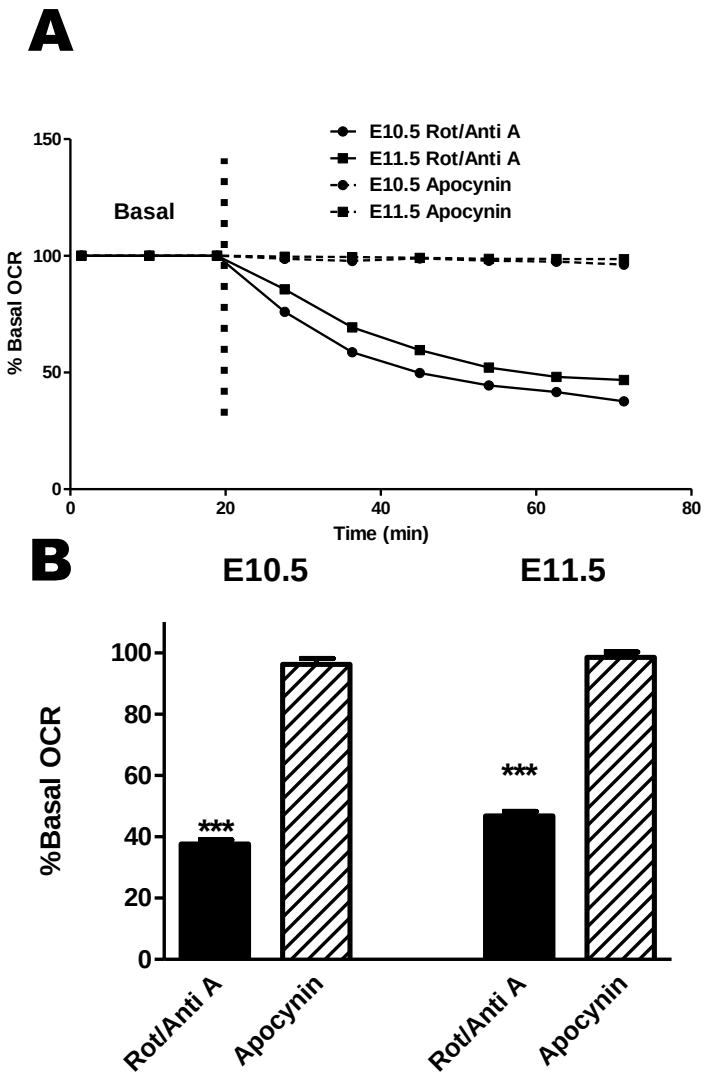

Figure 13 OCR is due to mitochondrial function in isolated embryonic hearts.

(A) OCR E10.5 (circles) and E11.5 (squares) adrenergic-competent hearts treated with rotenone and antimycin A. (B) OCR in E10.5 (n=9) and E11.5 (n=7) adrenergic-competent hearts before (black bars) and after (lined bars) rotenone and antimycin A treatment. Data are represented as mean±SEM. *, *p<0.05;* ***, *p<0.001*

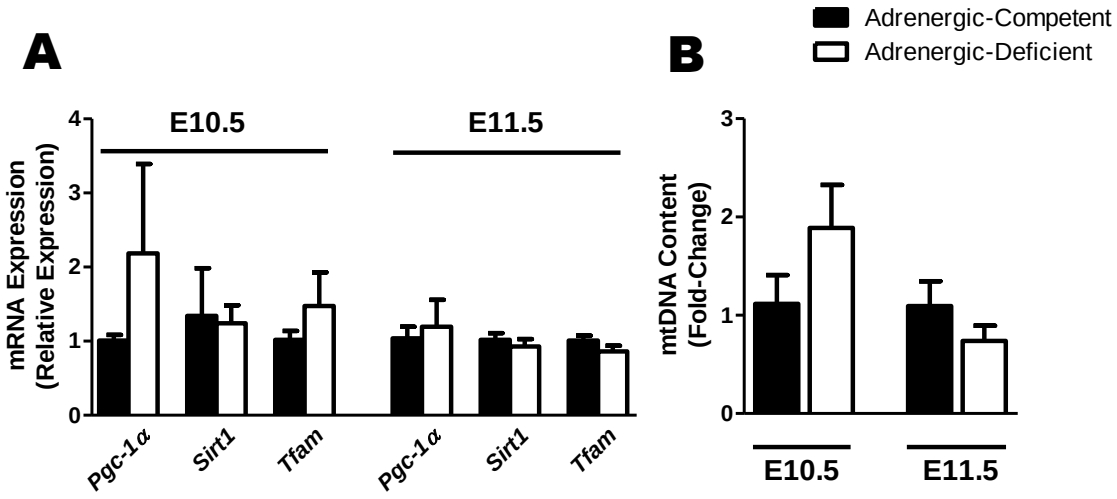

Figure 14 Mitochondrial biogenesis gene expression and mtDNA content in adrenergic-deficient versus control hearts.

(A) Fold-change of key mitochondrial biogenesis genes between adrenergic-competent and deficient mRNA from E10.5 (n=5) and E11.5 (n=6) hearts as measured by quantitative RT-PCR analysis. (B) Mitochondrial DNA (mtDNA) content fold-change between E10.5 and E11.5 adrenergic-competent (black bars) and deficient (white bars) hearts. Numerical values in the columns refer to the number (n) of samples analyzed.

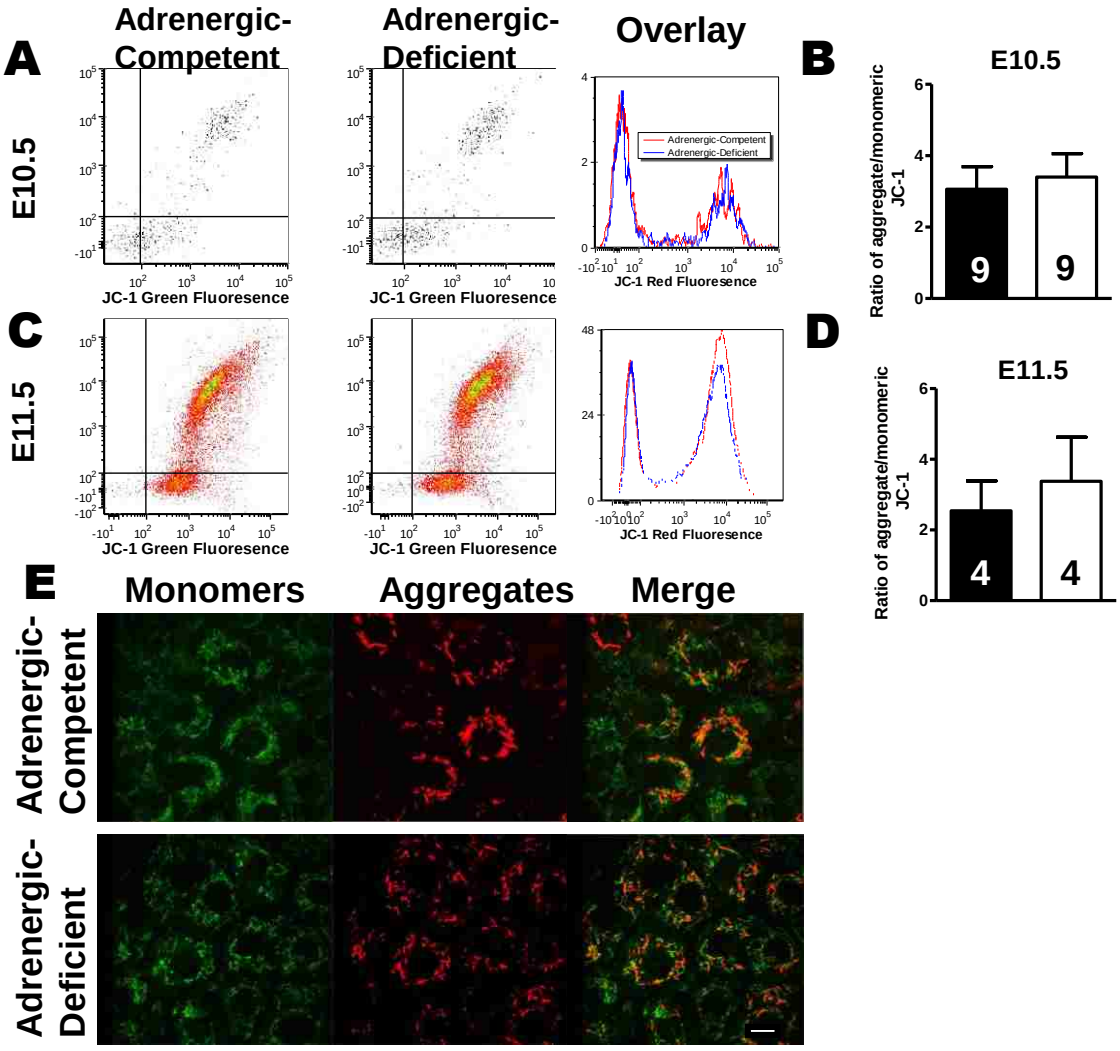

Figure 15 Analysis of mitochondrial membrane potentials in adrenergic-deficient and control myocytes using flow cytometry and fluorescence microscopy with JC-1 dye.

(A and C) Representative scatter plots of flow cytometry with red and green fluorescence from JC-1 dye in adrenergic-deficient and adrenergic-competent E10.5 and E11.5 embryonic primary cardiomyocytes. Adrenergic-competent samples (red) and adrenergic-deficient samples (blue) in histogram overlay. (B and D) Ratio of red/green fluorescence in E10.5 and E11.5 adrenergic-competent (white bars) and deficient (black bars) samples. Numerical values in the columns refer to the number (n) of samples analyzed. (E) Representative scanning laser confocal microscopy of JC-1 dye in E11.5 primary cardiomyocytes. Scale bar, 10 μm.

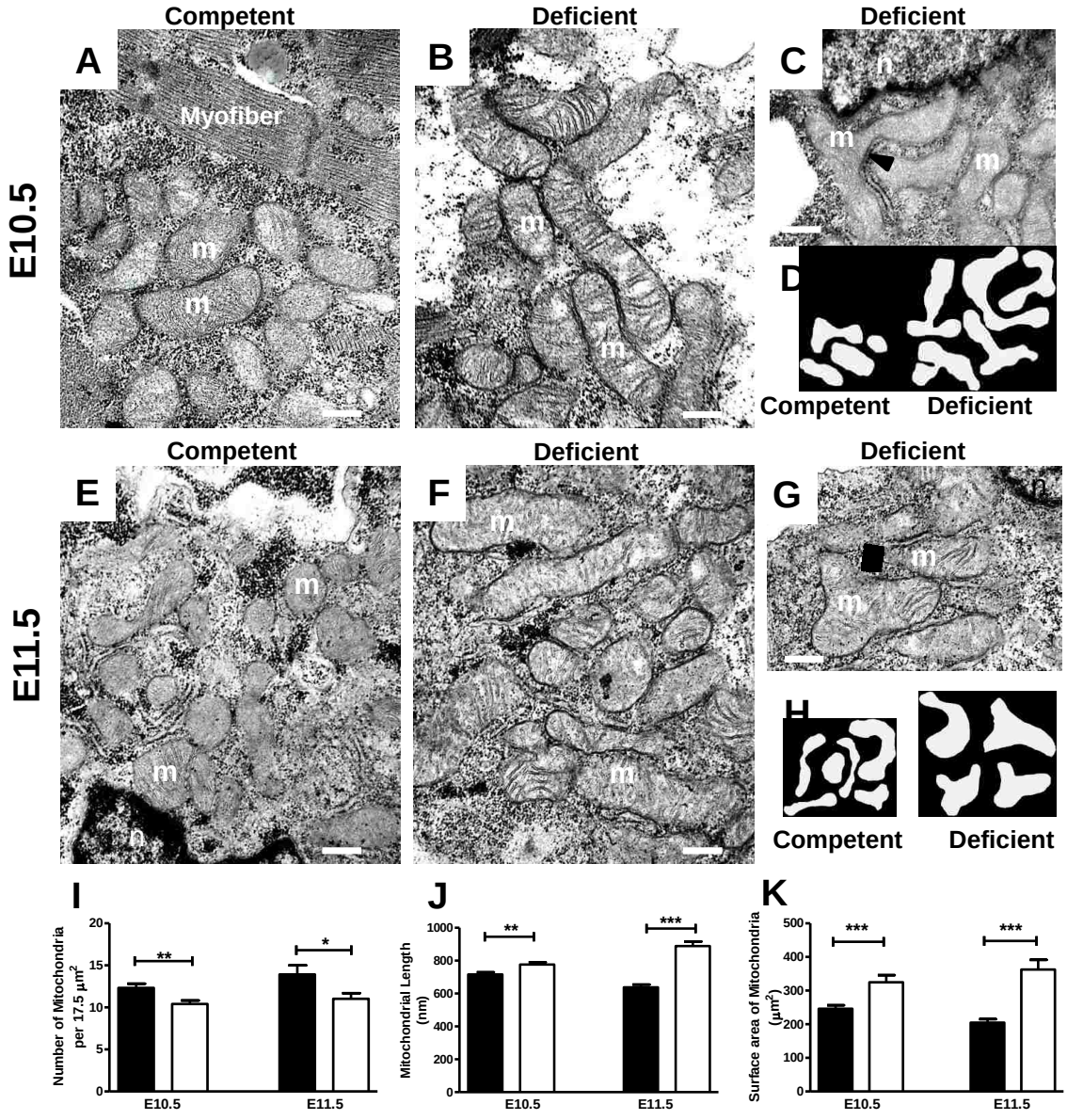

Figure 16 Ultrastructural analysis of mitochondria in adrenergic-deficient and control hearts following evaluation of TEM images.

Mitochondrial morphology in adrenergic-competent and deficient E10.5 (compare A and B) and E11.5 (compare E and F) myocytes. (C and G) Branched (arrowheads) and swollen mitochondria in adrenergic-deficient samples. (D and H) Representative tracings of abnormally shaped mitochondria in adrenergic-deficient samples. (I) Number of mitochondria per defined micrograph area (17.5 μm^2) in E10.5 and E11.5 adrenergic-competent (black bars) and deficient (white

bars) samples. (J) Mitochondrial length in E10.5 and E11.5 adrenergic-competent (black bars) and deficient (white bars) samples. (K) Surface area of mitochondria in E10.5 and E11.5 adrenergic-competent (black bars) and deficient (white bars) samples. Abbreviations: m=mitochondria; n=nucleus. **, p<0.05; **, p<0.01; ***, p<0.001*. Scale bar= 500 nm.

List of References

Acin-Perez, R., Gatti, D.L., Bai, Y., and Manfredi, G. (2011). Protein phosphorylation and prevention of cytochrome oxidase inhibition by ATP: coupled mechanisms of energy metabolism regulation. Cell metabolism *13*, 712-719.

Baker, C., Taylor, D.G., Osuala, K., Natarajan, A., Molnar, P.J., Hickman, J., Alam, S., Moscato, B., Weinshenker, D., and Ebert, S.N. (2012). Adrenergic deficiency leads to impaired electrical conduction and increased arrhythmic potential in the embryonic mouse heart. Biochem Biophys Res Commun *423*, 536-541.

Baker, C.N., and Ebert, S.N. (2013). Development of aerobic metabolism *in utero*: requirement for mitochondrial function during embryonic and foetal periods. Open Access Biotechnology *2*.

Benard, G., Bellance, N., James, D., Parrone, P., Fernandez, H., Letellier, T., and Rossignol, R. (2007). Mitochondrial bioenergetics and structural network organization. J Cell Sci *120*, 838-848.

Bergmeyer, H., Bernt, E. (1974). In Methods of Enzymatic Analysis (New York, NY: Academic Press), pp. 574-579.

Berthet, J., Rall, T.W., and Sutherland, E.W. (1957). The relationship of epinephrine and glucagon to liver phosphorylase. IV. Effect of epinephrine and glucagon on the reactivation of phosphorylase in liver homogenates. The Journal of biological chemistry *224*, 463-475.

Bing, R.J., Siegel, A., Ungar, I., and Gilbert, M. (1954). Metabolism of the human heart. II. Studies on fat, ketone and amino acid metabolism. Am J Med *16*, 504-515.

Carlsten, A., Hallgren, B., Ja Genbur, G.R., Svanborg, A., and Werko, L. (1961). Myocardial metabolism of glucose, lactic acid, amino acids and fatty acids in healthy human individuals at rest and at different work loads. Verhandlungen der Deutschen Gesellschaft fur Kreislaufforschung *27*, 195-196.

Chang, C.R., and Blackstone, C. (2007). Cyclic AMP-dependent protein kinase phosphorylation of Drp1 regulates its GTPase activity and mitochondrial morphology. The Journal of biological chemistry *282*, 21583-21587.

Chen, H., Detmer, S.A., Ewald, A.J., Griffin, E.E., Fraser, S.E., and Chan, D.C. (2003). Mitofusins Mfn1 and Mfn2 coordinately regulate mitochondrial fusion and are essential for embryonic development. J Cell Biol *160*, 189-200.

Chen, M., Sato, P.Y., Chuprun, J.K., Peroutka, R.J., Otis, N.J., Ibetti, J., Pan, S., Sheu, S.S., Gao, E., and Koch, W.J. (2013). Prodeath signaling of G protein-coupled receptor kinase 2 in cardiac myocytes after ischemic stress occurs via extracellular signal-regulated kinase-dependent heat shock protein 90-mediated mitochondrial targeting. Circulation research *112*, 1121-1134.

Chen, Y., Liu, Y., and Dorn, G.W., 2nd (2011). Mitochondrial fusion is essential for organelle function and cardiac homeostasis. Circulation research *109*, 1327-1331.

Chin, A.J., Saint-Jeannet, J.P., and Lo, C.W. (2012). How insights from cardiovascular developmental biology have impacted the care of infants and children with congenital heart disease. Mech Dev *129*, 75-97.

Chung, S., Dzeja, P.P., Faustino, R.S., Perez-Terzic, C., Behfar, A., and Terzic, A. (2007). Mitochondrial oxidative metabolism is required for the cardiac differentiation of stem cells. Nat Clin Pract Cardiovasc Med *4 Suppl 1*, S60-67.

Cosen-Binker, L.I., Binker, M.G., Cosen, R., Negri, G., and Tiscornia, O. (2006). Relaxin prevents the development of severe acute pancreatitis. World J Gastroenterol *12*, 1558-1568.

Cox, S.J., and Gunberg, D.L. (1972). Metabolite utilization by isolated embryonic rat hearts in vitro. J Embryol Exp Morphol *28*, 235-245.

Cribbs, J.T., and Strack, S. (2007). Reversible phosphorylation of Drp1 by cyclic AMP-dependent protein kinase and calcineurin regulates mitochondrial fission and cell death. EMBO Rep *8*, 939-944.

Davies, V.J., Hollins, A.J., Piechota, M.J., Yip, W., Davies, J.R., White, K.E., Nicols, P.P., Boulton, M.E., and Votruba, M. (2007). Opa1 deficiency in a mouse model of autosomal dominant optic atrophy impairs mitochondrial morphology, optic nerve structure and visual function. Hum Mol Genet *16*, 1307-1318.

De Rasmo, D., Gattoni, G., Papa, F., Santeramo, A., Pacelli, C., Cocco, T., Micelli, L., Sardaro, N., Larizza, M., Scivetti, M.*, et al.* (2011). The beta-adrenoceptor agonist isoproterenol promotes the activity of respiratory chain complex I and lowers cellular reactive oxygen species in fibroblasts and heart myoblasts. Eur J Pharmacol *652*, 15-22.

De Sousa, E., Veksler, V., Minajeva, A., Kaasik, A., Mateo, P., Mayoux, E., Hoerter, J., Bigard, X., Serrurier, B., and Ventura-Clapier, R. (1999). Subcellular creatine kinase alterations. Implications in heart failure. Circulation research *85*, 68-76.

Drenckhahn, J.D. (2011). Heart development: mitochondria in command of cardiomyocyte differentiation. Dev Cell *21*, 392-393.

Duncan, J.G. (2011). Peroxisome proliferator activated receptor-alpha (PPARalpha) and PPAR gamma coactivator-1alpha (PGC-1alpha) regulation of cardiac metabolism in diabetes. Pediatr Cardiol *32*, 323-328.

Ebert, S.N., Baden, J.M., Mathers, L.H., Siddall, B.J., and Wong, D.L. (1996). Expression of phenylethanolamine n-methyltransferase in the embryonic rat heart. Journal of molecular and cellular cardiology *28*, 1653-1658.

Ebert, S.N., Rong, Q., Boe, S., Thompson, R.P., Grinberg, A., and Pfeifer, K. (2004). Targeted insertion of the Cre-recombinase gene at the phenylethanolamine n-methyltransferase locus: a new model for studying the developmental distribution of adrenergic cells. Dev Dyn *231*, 849-858.

Ebert, S.N., and Thompson, R.P. (2001). Embryonic epinephrine synthesis in the rat heart before innervation: association with pacemaking and conduction tissue development. Circulation research *88*, 117-124.

Ellington, S.K. (1987). In vitro analysis of glucose metabolism and embryonic growth in postimplantation rat embryos. Development *100*, 431-439.

Fusco, A., Santulli, G., Sorriento, D., Cipolletta, E., Garbi, C., Dorn, G.W., 2nd, Trimarco, B., Feliciello, A., and Iaccarino, G. (2012). Mitochondrial localization unveils a novel role for GRK2 in organelle biogenesis. Cell Signal *24*, 468-475.

Gomes, L.C., Di Benedetto, G., and Scorrano, L. (2011). During autophagy mitochondria elongate, are spared from degradation and sustain cell viability. Nature cell biology *13*, 589-598.

Gordon, R.S., Jr., and Cherkes, A. (1956). Unesterified fatty acid in human blood plasma. The Journal of clinical investigation *35*, 206-212.

Halestrap, A.P., and Pasdois, P. (2009). The role of the mitochondrial permeability transition pore in heart disease. Biochim Biophys Acta *1787*, 1402-1415.

Hom, J.R., Quintanilla, R.A., Hoffman, D.L., de Mesy Bentley, K.L., Molkentin, J.D., Sheu, S.S., and Porter, G.A., Jr. (2011). The permeability transition pore controls cardiac mitochondrial maturation and myocyte differentiation. Dev Cell *21*, 469-478.

Humble, M.M., Young, M.J., Foley, J.F., Pandiri, A.R., Travlos, G.S., and Copeland, W.C. (2013). Polg2 is essential for mammalian embryogenesis and is required for mtDNA maintenance. Hum Mol Genet *22*, 1017-1025.

Ingwall, J.S. (2006). On the hypothesis that the failing heart is energy starved: lessons learned from the metabolism of ATP and creatine. Curr Hypertens Rep *8*, 457-464.

Ingwall, J.S., and Weiss, R.G. (2004). Is the failing heart energy starved? On using chemical energy to support cardiac function. Circulation research *95*, 135-145.

Jaber, M., Koch, W.J., Rockman, H., Smith, B., Bond, R.A., Sulik, K.K., Ross, J., Jr., Lefkowitz, R.J., Caron, M.G., and Giros, B. (1996). Essential role of beta-adrenergic receptor kinase 1 in cardiac development and function. Proceedings of the National Academy of Sciences of the United States of America *93*, 12974-12979.

Knott, A.B., Perkins, G., Schwarzenbacher, R., and Bossy-Wetzel, E. (2008). Mitochondrial fragmentation in neurodegeneration. Nat Rev Neurosci *9*, 505-518.

Krebs, E.G., and Fischer, E.H. (1956). The phosphorylase b to a converting enzyme of rabbit skeletal muscle. Biochim Biophys Acta *20*, 150-157.

Krebs, P., Fan, W., Chen, Y.H., Tobita, K., Downes, M.R., Wood, M.R., Sun, L., Li, X., Xia, Y., Ding, N.*, et al.* (2011). Lethal mitochondrial cardiomyopathy in a hypomorphic Med30 mouse mutant is ameliorated by ketogenic diet. Proceedings of the National Academy of Sciences of the United States of America *108*, 19678-19682.

Lagouge, M., Argmann, C., Gerhart-Hines, Z., Meziane, H., Lerin, C., Daussin, F., Messadeq, N., Milne, J., Lambert, P., Elliott, P.*, et al.* (2006). Resveratrol improves mitochondrial function and protects against metabolic disease by activating SIRT1 and PGC-1alpha. Cell *127*, 1109-1122.

Larsson, N.G., Wang, J., Wilhelmsson, H., Oldfors, A., Rustin, P., Lewandoski, M., Barsh, G.S., and Clayton, D.A. (1998). Mitochondrial transcription factor A is necessary for mtDNA maintenance and embryogenesis in mice. Nat Genet *18*, 231-236.

Li, K., Li, Y., Shelton, J.M., Richardson, J.A., Spencer, E., Chen, Z.J., Wang, X., and Williams, R.S. (2000). Cytochrome c deficiency causes embryonic lethality and attenuates stress-induced apoptosis. Cell *101*, 389-399.

Luptak, I., Balschi, J.A., Xing, Y., Leone, T.C., Kelly, D.P., and Tian, R. (2005). Decreased contractile and metabolic reserve in peroxisome proliferator-activated receptor-alpha-null hearts can be rescued by increasing glucose transport and utilization. Circulation *112*, 2339-2346.

Lymperopoulos, A., Rengo, G., and Koch, W.J. (2013). Adrenergic nervous system in heart failure: pathophysiology and therapy. Circulation research *113*, 739-753.

Madrazo, J.A., and Kelly, D.P. (2008). The PPAR trio: regulators of myocardial energy metabolism in health and disease. J Mol Cell Cardiol *44*, 968-975.

Makinde, A.O., Kantor, P.F., and Lopaschuk, G.D. (1998). Maturation of fatty acid and carbohydrate metabolism in the newborn heart. Molecular and cellular biochemistry *188*, 49-56.

Maltsev, V.A., Wobus, A.M., Rohwedel, J., Bader, M., and Hescheler, J. (1994). Cardiomyocytes differentiated in vitro from embryonic stem cells developmentally express cardiac-specific genes and ionic currents. Circulation research *75*, 233-244.

Mao, K., Wang, K., Liu, X., and Klionsky, D.J. (2013). The scaffold protein Atg11 recruits fission machinery to drive selective mitochondria degradation by autophagy. Developmental cell *26*, 9-18.

Mortiboys, H., Thomas, K.J., Koopman, W.J., Klaffke, S., Abou-Sleiman, P., Olpin, S., Wood, N.W., Willems, P.H., Smeitink, J.A., Cookson, M.R.*, et al.* (2008). Mitochondrial function and morphology are impaired in parkin-mutant fibroblasts. Ann Neurol *64*, 555-565.

Nascimben, L., Ingwall, J.S., Pauletto, P., Friedrich, J., Gwathmey, J.K., Saks, V., Pessina, A.C., and Allen, P.D. (1996). Creatine kinase system in failing and nonfailing human myocardium. Circulation *94*, 1894-1901.

Natarajan, A.R., Rong, Q., Katchman, A.N., and Ebert, S.N. (2004). Intrinsic cardiac catecholamines help maintain beating activity in neonatal rat cardiomyocyte cultures. Pediatr Res *56*, 411-417.

Neely, J.R., and Morgan, H.E. (1974). Relationship between carbohydrate and lipid metabolism and the energy balance of heart muscle. Annu Rev Physiol *36*, 413-459.

Osuala, K., Baker, C.N., Nguyen, H.L., Martinez, C., Weinshenker, D., and Ebert, S.N. (2012). Physiological and genomic consequences of adrenergic deficiency during embryonic/fetal development in mice: impact on retinoic acid metabolism. Physiol Genomics *44*, 934-947.

Palorini, R., De Rasmo, D., Gaviraghi, M., Sala Danna, L., Signorile, A., Cirulli, C., Chiaradonna, F., Alberghina, L., and Papa, S. (2013). Oncogenic K-ras expression is associated with derangement of the cAMP/PKA pathway and forskolin-reversible alterations of mitochondrial dynamics and respiration. Oncogene *32*, 352-362.

Papa, S., Rasmo, D.D., Technikova-Dobrova, Z., Panelli, D., Signorile, A., Scacco, S., Petruzzella, V., Papa, F., Palmisano, G., Gnoni, A.*, et al.* (2012). Respiratory chain complex I, a main regulatory target of the cAMP/PKA pathway is defective in different human diseases. FEBS Lett *586*, 568-577.

Park, S.J., Ahmad, F., Philp, A., Baar, K., Williams, T., Luo, H., Ke, H., Rehmann, H., Taussig, R., Brown, A.L.*, et al.* (2012). Resveratrol ameliorates aging-related metabolic phenotypes by inhibiting cAMP phosphodiesterases. Cell *148*, 421-433.

Reers, M., Smith, T.W., and Chen, L.B. (1991). J-aggregate formation of a carbocyanine as a quantitative fluorescent indicator of membrane potential. Biochemistry *30*, 4480-4486.

Sengupta, B., Narasimhulu, C.A., and Parthasarathy, S. (2013). Novel technique for generating macrophage foam cells for in vitro reverse cholesterol transport studies. Journal of lipid research *54*, 3358-3372.

Shepard, T.H., Tanimura, T., and Robkin, M.A. (1970). Energy metabolism in early mammalian embryos. Symp Soc Dev Biol *29*, 42-58.

Song, W., Chen, J., Petrilli, A., Liot, G., Klinglmayr, E., Zhou, Y., Poquiz, P., Tjong, J., Pouladi, M.A., Hayden, M.R.*, et al.* (2011). Mutant huntingtin binds the mitochondrial fission GTPase dynamin-related protein-1 and increases its enzymatic activity. Nat Med *17*, 377-382.

Spitkovsky, D., Sasse, P., Kolossov, E., Bottinger, C., Fleischmann, B.K., Hescheler, J., and Wiesner, R.J. (2004). Activity of complex III of the mitochondrial electron transport chain is essential for early heart muscle cell

differentiation. FASEB journal : official publication of the Federation of American Societies for Experimental Biology *18*, 1300-1302.

Sutherland, E.W., Jr., and Wosilait, W.D. (1955). Inactivation and activation of liver phosphorylase. Nature *175*, 169-170.

Takata, K., Kasahara, T., Kasahara, M., Ezaki, O., and Hirano, H. (1994). Immunolocalization of glucose transporter GLUT1 in the rat placental barrier: possible role of GLUT1 and the gap junction in the transport of glucose across the placental barrier. Cell Tissue Res *276*, 411-418.

Tasseva, G., Bai, H.D., Davidescu, M., Haromy, A., Michelakis, E., and Vance, J.E. (2013). Phosphatidylethanolamine deficiency in Mammalian mitochondria impairs oxidative phosphorylation and alters mitochondrial morphology. The Journal of biological chemistry *288*, 4158-4173.

Theiler, K. (1972). The house mouse; development and normal stages from fertilization to 4 weeks of age (Berlin, New York,: Springer-Verlag).

Thomas, S.A., Matsumoto, A.M., and Palmiter, R.D. (1995). Noradrenaline is essential for mouse fetal development. Nature *374*, 643-646.

Thomas, S.A., and Palmiter, R.D. (1997). Thermoregulatory and metabolic phenotypes of mice lacking noradrenaline and adrenaline. Nature *387*, 94-97.

Thomas, S.A., and Palmiter, R.D. (1998). Examining adrenergic roles in development, physiology, and behavior through targeted disruption of the mouse dopamine beta-hydroxylase gene. Adv Pharmacol *42*, 57-60.

Ventura-Clapier, R., Garnier, A., and Veksler, V. (2004). Energy metabolism in heart failure. J Physiol *555*, 1-13.

Ventura-Clapier, R., Garnier, A., Veksler, V., and Joubert, F. (2011). Bioenergetics of the failing heart. Biochim Biophys Acta *1813*, 1360-1372.

Wakabayashi, J., Zhang, Z., Wakabayashi, N., Tamura, Y., Fukaya, M., Kensler, T.W., Iijima, M., and Sesaki, H. (2009). The dynamin-related GTPase Drp1 is required for embryonic and brain development in mice. J Cell Biol *186*, 805-816.

Zhang, J., Nuebel, E., Wisidagama, D.R., Setoguchi, K., Hong, J.S., Van Horn, C.M., Imam, S.S., Vergnes, L., Malone, C.S., Koehler, C.M.*, et al.* (2012). Measuring energy metabolism in cultured cells, including human pluripotent stem cells and differentiated cells. Nat Protoc *7*, 1068-1085.

Zhou, W., Chen, K.H., Cao, W., Zeng, J., Liao, H., Zhao, L., and Guo, X. (2010). Mutation of the protein kinase A phosphorylation site influences the anti-proliferative activity of mitofusin 2. Atherosclerosis *211*, 216-223.

CHAPTER FOUR:
ECHOCARDIOGRAPHIC ANALYSIS OF LEFT VENTRICULAR FUNCTION IN STRESS-CHALLENGED AGED MICE: EFFECTS OF GENDER (SEX) AND MENOPAUSE

Abstract

To investigate age, sex, and menopausal differences left ventricular (LV) function was evaluated using high-resolution ultrasound in age-matched male, pre- and post-menopausal female mice hearts at from nine months to 21 months old at baseline and in response to epinephrine and immobilization stress. We found a more robust response to epinephrine stimulation in males at nine months compared to females. After the induction of menopause, similarities were found between males and menopausal females with regards to end systolic and diastolic volumes, fractional shortening and cardiac output. This trend persisted when the same group of mice underwent immobilization stress. These data demonstrate that biological sex and menopause have significant influence on LV function in response to various stressors in mice. Lastly, we found the distribution of adrenergic cell population was void in the aged cycling female heart and only after the induction of menopause are adrenergic cells observed in the left heart. This indicates differential adrenergic cell populations are present in male versus females and pre- versus post-menopausal females.

Introduction

Heart failure (HF) afflicts populations across the globe with an annual mortality rate of nearly 10% of the population. Male HF patients often exhibit a reduced ejection fraction (EF) compared to a preserved EF in female patients (Hogg et al., 2004; Regitz-Zagrosek et al., 2010). Reduction in EF is correlated with an overall drop in heart function and, ultimately, survival. This interesting gender difference has been highly studied in the clinical settings (Cleland et al., 2003; Regitz-Zagrosek et al., 2007) and in animal models (Du, 2004); however, mechanistic regulation of these observed gender differences in relation to the progression and prognosis of heart failure remains obscure. These studies demonstrate a need for divergent treatment of male versus female heart failure patients.

Additionally, stress-induced cardiomyopathies, such as Takotsubo cardiomyopathy, predominantly afflict post-menopausal women (greater than 82% of such cases) who have experienced a sudden emotional shock (H. Sato, 1990). These women display left ventricular (LV) dysfunction characterized by hypo- or a-kinetic regions, particularly near the apex and often have elevated plasma catecholamines, and are at high risk of arrhythmia and sudden cardiac death if left untreated (Kume et al., 2008; Wittstein et al., 2005; Yoshida et al., 2007). At present, it is not entirely clear why only specific regions of the LV are primarily affected, nor is it understood why postmenopausal women are particularly susceptible to these types of stress cardiomyopathies (Baker, 2014).

The effects of age, sex and menopausal status on cardiovascular function have been investigated individually; however these three important factors contributing to left ventricular function have not been looked at together, nor in response to stress stimuli. Additionally, very few studies have been conducted in vivo. Myocardial response to adrenergic hormones has been extensively investigated in vitro and the effects of sex and menopause have been incorporated into these types of studies (Luczak and Leinwand, 2009; McIntosh et al., 2011; Schwertz et al., 1999; Vizgirda et al., 2002).

Recent work has shown distribution of historical and/or active intrinsic adrenergic derived myocardium in young adult mice follows a similar pattern to that seen in regions of the left heart most commonly affected in stress induced cardiomyopathy patients (Osuala et al., 2011). These areas include the base, mid and apical sections of the left heart. In addition, Kume et al. showed increased catecholamines concentrations in the apex as compared to the base in five confirmed cases of Takotsubo cardiomyopathy (Kume et al., 2008). These results suggest differential local catecholamine concentrations in apical versus basal regions of the left heart, likely originating from the intrinsic adrenergic cells located in these regions (Baker, 2014).

We hypothesized there are inherent differences between in vivo left ventricular function due to sex, age, and menopausal status and tested this hypothesis by injecting epinephrine before and after menopause induction in

mice while performing high-resolution echocardiography. Further, to recapitulate an emotional stress paradigm, immobilization stress was conducted and cardiac function was monitored using echocardiography. Upon conclusion of all functional studies, the hearts were then excised and viewed for histological distribution of adrenergic myocardium.

Materials and Methods

Mice

All procedures and handling of mice were conducted in accordance with The University of Central Florida Institutional Animal Care and Use Committees. *Pnmt*$^{Cre/Cre}$ and *ROSA26*$^{\beta gal/\beta gal}$ mice were bred and maintained as previously described. *Pnmt*$^{Cre/Cre}$ and *ROSA26*$^{\beta gal/\beta gal}$ were mated and resulting offspring (Figure 17) were aged to 9 months before the first ultrasounds were performed.

Epinephrine Injections and Echocardiography

Mice were anesthetized with 2% isoflurane for duration of epinephrine injection studies. Body temperature was maintained between 36-37ºC using a heated platform and monitored with rectal probe. Transthoracic echocardiography was performed using a Vevo® 2100 (Visual Sonics, Toronto, Canada) system equipped with a high frequency 40 MHz transducer. Recordings were conducted every 5 min for 20 min to avoid any artifact from isoflurane. Intraperitoneal epinephrine injections were administered at a dose of 50 mg/kg body weight. Recordings continued for 40 min at 5 min intervals. Calculations were made from recordings taken directly prior to injection and at peak heart rate after injection.

Immobilization and Echocardiography

Mice were anesthetized with 2% isoflurane for hair removal and baseline recordings. Body temperature was maintained using an external heating pad. Mice were restrained in the supine position with limbs secured in place with perforated tape. After baseline recordings anesthesia was removed and mice were allowed to become fully conscious. Transthoracic echocardiography was performed using a Vevo® 2100 (Visual Sonics, Toronto, Canada) system equipped with a high frequency 40 MHz transducer. Recordings were taken at 15 min, 1 hr, and 2 hr timepoints. Calculations were made from recordings taken at baseline and 2 hr.

Menopause Induction

Menopause was chemically induced using 4-vinylcyclohexane diepoxide (VCD) (160 mg/kg/day) intraperitoneal injections for 15 consecutive days as previously described (Hoyer and Sipes, 2007). Vehicle control (peanut oil) injections were performed in parallel.

Vaginal Cytology

Menopause was confirmed by persistent diestrus for 5 consecutive days using vaginal cytology in both VCD and vehicle control groups. Briefly, sterile normal saline (20 µL) was flushed in vaginal cavity and collected on microscope slide daily. Slides were examined using 10X objective light microscopy using a Leica DM2000 microscope with a Leica DFC295 camera for distribution patterns of cell

type present. Upon examination of estrous cycle of control injection females, forty percent of the mice were determined to have undergone a natural menopause. Five days of persistent diestrus was classified as menopausal, if a mouse cycled from proestrous to estrus to metestrus to diestrus then back to proestrus, this indicated a typical 4 day estrus cycle and that mouse was classified as cycling. Diestrus is characterized by primarily the presence of leukocytes, proestrus by nucleated epithelial cells, estrus by cornified anucleated cells, and metestrus by a combination of all three cell types.

Corticosterone Measurements

Plasma corticosterone levels were measured following manufacturer's protocol using an ELISA (rat/mouse) kit from IBL-America (Minneapolis, MN).

Histological Preparations

Pnmt$^{+/Cre}$ *ROSA26*$^{+/\beta gal}$ mice aged 9 months and 21 months were sacrificed by cervical dislocation or swift decapitation. The heart was rapidly removed and retrogradely perfused through the aorta with phosphate-buffered saline then 2% paraformaldehyde. Adrenal glands were removed and processed similarly as hearts. Tissue was then placed in 2% paraformaldehyde for 24 hr at 4ºC then moved to 30 % sucrose with 0.02% sodium azide for storage. For sectioning the hearts and adrenal glands were embedded in Tissue-Tek® OCT compound (EM Sciences, Hatfield, PA) and sectioned at 12 micron using a Leica (CM1850 cryostat) at -20-24ºC, sections were stored at -20 ºC for subsequent staining.

Tissue sections were stained for β-galactosidase activity as previously described. Images were taken using a Leica L2 microscope and Leica EC3 camera and quantification of blue pixels were determined using Adobe Photoshop magic wand tool.

Statistics

Data are expressed as mean ± S.E.M. Student *t*-tests were performed to compare means between two groups and ANOVA performed between three groups, with $p < 0.05$ required to reject the null hypothesis.

Results

Pre-menopausal EPI Challenge

At 9 months of age male and female mice were subjected to baseline echocardiography to assess LV function. After 20 mins epinephrine (EPI, 50 mg/kg) was injected into the intraperitoneal cavity. Baseline heart rate was significantly higher in the female mice group as compared to the males, however, the males responded more robustly to the EPI than females (Figure 18A). Baseline left ventricular end diastolic and systolic volumes were significantly greater in the males as compared to females at baseline (Figure 18B and C), most likely due to the larger size of males compared to age matched females. Notably, a higher percent change in end diastolic and systolic volumes was seen in males as compared to females after EPI injections (Figure 18F). Stroke volume was also increased in males as compared to females at baseline and after EPI injections (Figure 18D). A significant increase in stroke volume after EPI injection was also observed in males as compared to females (Figure 18F). Lastly, cardiac output was significantly higher in males than females before and after EPI injections, with both groups displaying a similar increase after the injection (Figure 18E and F). Complete echocardiographic measurements at baseline and response to EPI are shown in Table 6. These results show that males have a more robust response to EPI as compared to age matched females.

Post-menopausal EPI Challenge

After induction and confirmation of menopause, EPI injections were repeated in males and females, only the female group was divided into pre-menopausal (i.e. cycling) and post-menopausal (i.e. non-cycling) subgroups. At baseline there were no differences in heart rate between the three groups (Figure 19A). After the injection of EPI significant differences were observed between the pre-menopausal females, post-menopausal females and male heart rates (Figure 19A), though the percent increases after EPI injections were not different between the three groups (Figure 19F). In addition, end systolic and diastolic volumes were significantly different between the three groups at baseline, though end diastolic volumes varied between the groups after EPI injections (Figure 19B and C). Stroke volumes were similar between the groups at baseline and only after EPI injections were differences observed between males, cycling and menopausal females (Figure 19D). A similar pattern was observed with cardiac output, demonstrating differential effects to EPI measured between the three groups, but not at baseline (Figure 19E). Complete echocardiographic measurements at baseline and response to EPI are shown in Table 7.

Age Effects

Next, we investigated the effects of age from 9 months to 21 months in males and females when stress was induced with EPI injections. Heart rate was not significantly different when comparing males and females at nine months

versus eighteen months of age before and after EPI injections (Figure 20A and 21A). End systolic ($p<0.001$) and diastolic ($p<0.05$) volumes increased significantly only in males between nine and eighteen months, after EPI these differences were no longer measured (Figure 20B and C). Stroke volume was significantly higher in males after aging (Figure 20D). However, it was drastically decreased in females at eighteen months compared to stroke volume at nine months (Figure 21D). Cardiac output was highly similar between the ages in both genders (Figure 20E and 21E).

Sex and Menopausal Status in Response to Immobilization Stress

Immobilization stress was utilized to recapitulate the emotional stress that is typically a precipitating factor in stress-induced cardiomyopathies. Baseline heart rates were not different between males, cycling and menopausal females (Figure 22A). However, after 2 hours of immobilization stress (IMO) ANOVA statistics determined a significant ($p<0.05$) variation between the three groups. End systolic volume showed no statistically significant differences (Figure 22B) and end diastolic volume demonstrated variability only after IMO stress (Figure 22C). Stroke volume showed no difference at baseline however, after IMO cycling females had significantly lowered values as compared to males and menopausal females, which were not different from one another (Figure 22D). Similarly, cardiac output was significantly different amongst the three groups at baseline with cycling females have the lowest values (Figure 22E). All three

groups had similarly high blood corticosterone levels as compared to unstressed control mice (Figure 23), thereby confirming the mice were clearly stressed physiologically. Complete echocardiographic measurements at baseline and response to EPI are shown in Table 8.

Histological Assessment of Adrenergic Cell Distribution

To determine the localization of adrenergic-derived myocardium, we utilized X-gal staining to identify positive cell populations. At 8-9 months hearts and adrenals were excised from male and female mice and frozen sections were stained. Interestingly, the male heart sections showed a robust staining pattern in the left heart and especially in the basal regions (Figure 24B). However, little to no positive staining was observed in the female left heart; however staining was readily present in the female 9 month adrenal gland (Figure 24A). At 21 months all mice were euthanized and hearts and adrenals removed and processed as indicated in Materials and Methods section. By this age no staining was observed in the male hearts or cycling female hearts, however, blue X-gal+ cells were clearly present in the postmenopausal hearts (Figure 24C-E). Staining was observed in the adrenal gland of all 21 month mice (Figure 25). Quantification of the X-gal+ pixels shows a significant increase in staining the males at 9 months compared to aged matched females (Figure 24F). Surprisingly, these X-gal+ pixels were significantly decreased in the males at 21

months, still not present in premenopausal females and drastically increased in postmenopausal females by 21 months (Figure 24F).

Discussion

The stress-induced cardiomyopathy, Takotsubo syndrome, is characterized by predominately affecting postmenopausal women, increased circulating catecholamines, and hypo or a-kinesis of the mid and apical left ventricle (Cocco and Chu, 2007; Wittstein et al., 2005). To recapitulate this syndrome we increased catecholamine levels by injecting EPI (i.p.) and inducing emotional stress by immobilization and observed cardiac function via high-resolution echocardiography (Shao et al., 2013; Ueyama, 2004). Additionally, as age and menopause are common features of this syndrome, mice were aged past nine months and menopause was induced and cardiac function studies were repeated. Lastly, using a β-galactosidase reporter we observed the localization of intrinsic adrenergic cells

While little to no apical ballooning was observed after injection of EPI or immobilization stress was observed via high-resolution echocardiography, interesting results were found regarding differences between age, sex, and menopausal status in response to stress paradigms. We compared the effects of left ventricular function using high-resolution ultrasound before and after stress response.

In parallel with other reported cases of stress response in males versus females, male nine month mice had a more robust response to EPI stimulation as compared to females (Schouwenberg et al., 2006). Others have reported a larger response in males to adrenergic stimulation, in vivo, isolated heart

preparations, as well as skinned myocytes (Gao et al., 2003; Schwertz et al., 1999; Scott et al., 2007). Investigation into the mechanism behind the greater sensitivity in males revealed a two-fold greater beta-adrenergic receptor density in male left ventricular membranes (Vizgirda et al., 2002). However, the function of these receptors has been questioned by many (Hinojosa-Laborde et al., 1999) and never been examined in vivo experimentation.

Premenopausal female patients (less than 65) are known to have better outcomes to hypertension, aortic stenosis and hypertrophic cardiomyopathy and preserved left ventricular ejection fraction in heart failure (Regitz-Zagrosek et al., 2010). However, these statistics change drastically after the age of 65 and initiation of menopause (Luczak and Leinwand, 2009). Consequently, the role of estrogen and cardiovascular function has been extensively studied, though few studies have investigations have been conducted in vivo (Dubey and Jackson, 2001; McIntosh et al., 2011; Schaible et al., 1984). Here we show differences between males, cycling and menopausal females when measuring heart rate response, stroke volume and cardiac output to EPI stimulation.

Additionally, our results demonstrate a similar aging pattern observed previously, that males have a significant increase in left ventricular end systolic and diastolic volume with age (Grandi et al., 1992). Whereas females show left ventricular stiffness exhibited by a drastic decrease in stroke volume over nine months of age (Borlaug et al., 2013).

Our studies also investigated the effects of an emotional stress paradigm, immobilization stress, with regards to gender and menopausal status. Here we show menopausal females have similar response to stress as males with regards to heart rate response, stroke volume and cardiac output. Cycling females have a decreased stroke volume as well as cardiac output compared to age matched male and menopausal female mice.

To understand the distribution of adrenergic derived myocardium with regards to age, gender, and menopausal status hearts were excised, sectioned, and stained for X-gal+ cells. The young adult mouse (3-8 weeks) was shown to have a distinct left sided distribution of intrinsic cardiac adrenergic cells. This characteristic pattern was observed in males at nine months of age, however, little to no ICA cells were observed in the myocardium of the cycling female heart at nine months. At 21 months ICA cells were no longer observed in the male heart, interestingly though the ICA cells were not observed in the menopausal female heart. One studied examined the rate of myocyte turnover in the aging heart, revealing the human male heart loses approximately 1 gram of myocytes per year, this is not seen in female hearts (Olivetti et al., 1995).

Controversial research has been conducted on whether estrogen levels regulate adrenergic receptors receptor and expression, especially in the heart. One study showed an upregulation of the β-1 adrenergic receptor in menopausal rats (Thawornkaiwong et al., 2003). While others have shown increased beta-adrenergic responses in male left ventricles, thought to be due to increased

calcium influx (McIntosh et al., 2011). Unfortunately, there has been no research conducted in adrenergic receptor sensitivity to estrogen in whole hearts.

Here we have shown a differential left ventricular response to stressors in males and females. Interestingly, trends toward similar LV responses to stress (EPI and IMO) were seen between males and menopausal females as compared to age-matched cycling females. Additionally, a drastic reappearance of intrinsic cardiac adrenergic cells were observed and quantified in the menopausal left ventricular and apical regions of the heart. This sudden reappearance may account for a higher incidence of takotsubo cardiomyopathies observed in post-menopausal females due to higher local catecholamine release. However, future studies are necessary to determine if this is the pathogenesis of stress-induced cardiomyopathies.

Tables

Table 6 Echocardiography results for 9 month male and female mice at baseline and after EPI (50 mg/kg, i.p.)

	Baseline			**Epinephrine**		
	Males n=28	**Females n=30**	***p*-value**	**Males n=28**	**Females n=30**	***p*-value**
Heart Rate (bpm)	**451.8±7.5**	**484.5±9.0**	**0.007*** **	526.5±5.0	536.0±5.8	0.2
End Systolic LV Volume (µL)	**17.0±0.9**	**12.7±0.7**	**0.0006*** **	12.0±1.0	11.6±0.8	0.8
End Diastolic LV Volume (µL)	**56.7±1.9**	**43.3±1.5**	**<0.0001*** **	48.4±2.3	41.5±1.3	0.01* *
Stroke Volume (µL)	**39.7±1.7**	**30.6±1.2**	**<0.0001*** **	**36.4±1.9**	**29.9±1.1**	**0.004** **
Ejection Fraction (%)	69.6±1.4	70.5±1.4	0.7	75.0±1.9	72.2±1.7	0.3
Fractional Shortening (%)	19.1±1.3	20.1±1.0	0.5	21.1±1.3	19.3±1.2	0.3
Cardiac Output (mL/min)	**18.1±0.9**	**14.7±0.6**	**0.002** **	**19.2±1.0**	**16.1±0.6**	**0.01** **

Data are represented as mean±SEM. **, p<0.05; **, p<0.01; ***, p<0.001*

Table 7 Echocardiography results for 18 month male, cycling and menopausal female mice at baseline and after EPI (50 mg/kg, i.p.)

	Baseline				Epinephrine			
	Males n=6	**Cycling Females n=6**	**Menopausal Females n=12**	***p*-value**	**Males n=6**	**Cycling Females n=6**	**Menopausal Females n=12**	***p*-value**
Heart Rate (bpm)	436.8±13.9	460.3±18.5	443.1±9.2	0.5	**510.6±10.2**	**557.7±9.3**	**537.1±8.1**	**0.02***
End Systolic LV Volume (µL)	**27.3±2.6**	**13.5±2.6**	**23.1±2.4**	**0.01***	11.2±2.2	7.1±0.8	13.6±2.5	0.2
End Diastolic LV Volume (µL)	**66.3±4.8**	**46.2±1.5**	**58.6±2.8**	**0.004****	**57.0±3.1**	**37.9±3.0**	**49.1±3.5**	**0.01***
Stroke Volume (µL)	39.0±3.2	32.7±1.3	35.5±1.7	0.2	**45.8±3.0**	**30.8±2.5**	**35.6±2.1**	**0.004****
Ejection Fraction (%)	59.5±2.9	71.8±4.6	61.5±2.6	0.06	81.1±3.2	82.2±1.6	74.1±3.0	0.1
Fractional Shortening (%)	**14.6±2.9**	**27.0±3.6**	**20.7±2.4**	**0.05***	24.6±3.1	29.2±1.7	25.4±2.5	0.5
Cardiac Output (mL/min)	16.9±1.0	15.1±0.9	15.7±0.8	0.5	**23.3±1.4**	**17.2±1.5**	**19.0±1.0**	**0.02***

Data are represented as mean±SEM. **, p<0.05; **, p<0.01; ***, p<0.001*

Table 8 Echocardiography results for 21 month male, cycling and menopausal female mice at baseline and immobilization stress

	Baseline				Immobilization			
	Males n=6	**Cycling Females n=6**	**Menopausal Females n=11**	***p*-value**	**Males n=6**	**Cycling Females n=6**	**Menopausal Females n=11**	***p*-value**
Heart Rate (bpm)	465.5±33.0	398.4±8.9	416.8±11.0	0.07	**657.7±15.3**	**692.5±7.5**	**687.0±5.8**	**0.05***
End Systolic LV Volume (µL)	44.4±7.6	34.6±6.5	36.1±4.7	0.5	5.1±2.9	1.1±0.4	2.1±0.4	0.2
End Diastolic LV Volume (µL)	85.5±10.1	64.2±9.7	71.8±5.5	0.2	**37.9±4.0**	**24.0±2.8**	**33.6±2.5**	**0.03***
Stroke Volume (µL)	41.1±4.1	29.6±4.3	35.7±3.3	0.2	**32.7±2.3**	**22.9±2.6**	**31.5±2.3**	**0.04***
Ejection Fraction (%)	51.0±6.6	47.8±4.1	51.9±5.1	0.9	88.6±5.2	95.6±1.2	94.1±0.9	0.2
Fractional Shortening (%)	26.8±4.7	24.0±2.5	27.2±3.3	0.8	61.6±5.9	71.8±3.2	68.6±2.2	0.2
Cardiac Output (mL/min)	**18.8±1.6**	**11.6±1.6**	**14.9±1.4**	**0.03***	21.5±1.6	15.9±1.8	21.7±1.6	0.06
LV Mass (mg)	201.3±17.1	194.0±19.9	175.1±10.7	0.4	198.4±27.4	155.4±21.9	158.7±9.0	0.2

Data are represented as mean±SEM. **, p<0.05; **, p<0.01; ***, p<0.001*

Figures

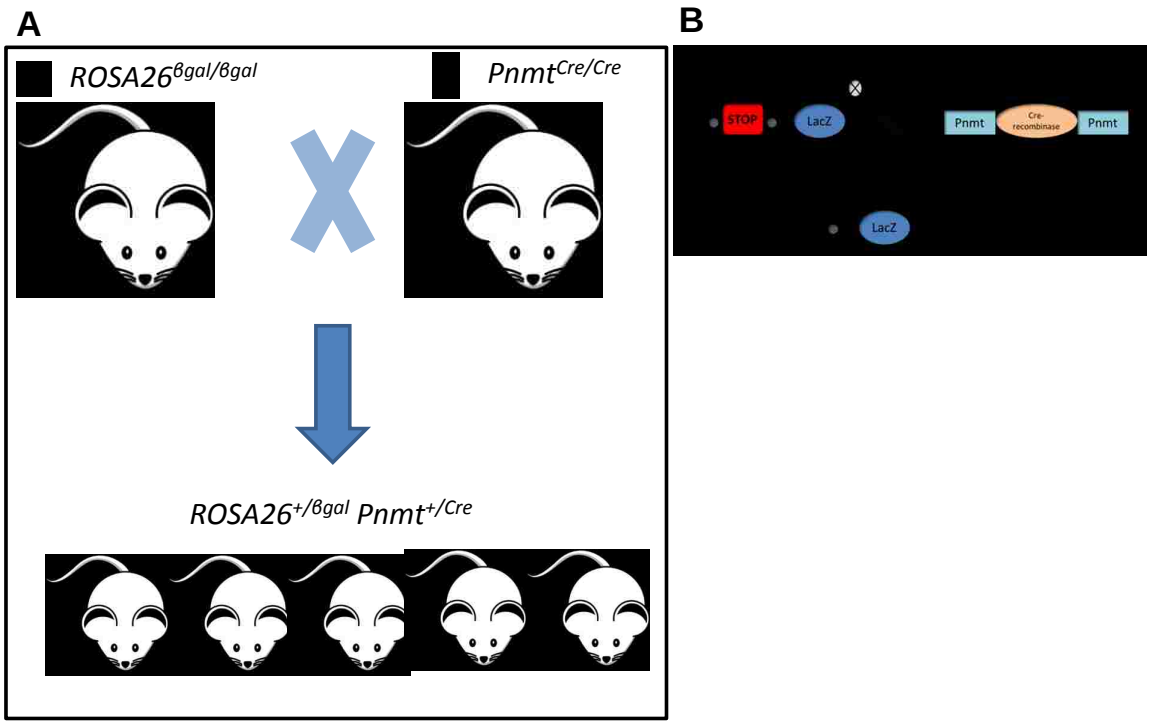

Figure 17 Schematic of mouse model.

(A) Pnmt$^{Cre/Cre}$ and *ROSA26*$^{\beta gal/\beta gal}$ homozygous mice mating scheme and resulting heterozygous offspring genotypes. (B) Recombination of Rosa26 reporter mice and Pnmt-Cre mice results in robust expression of *LacZ* gene.

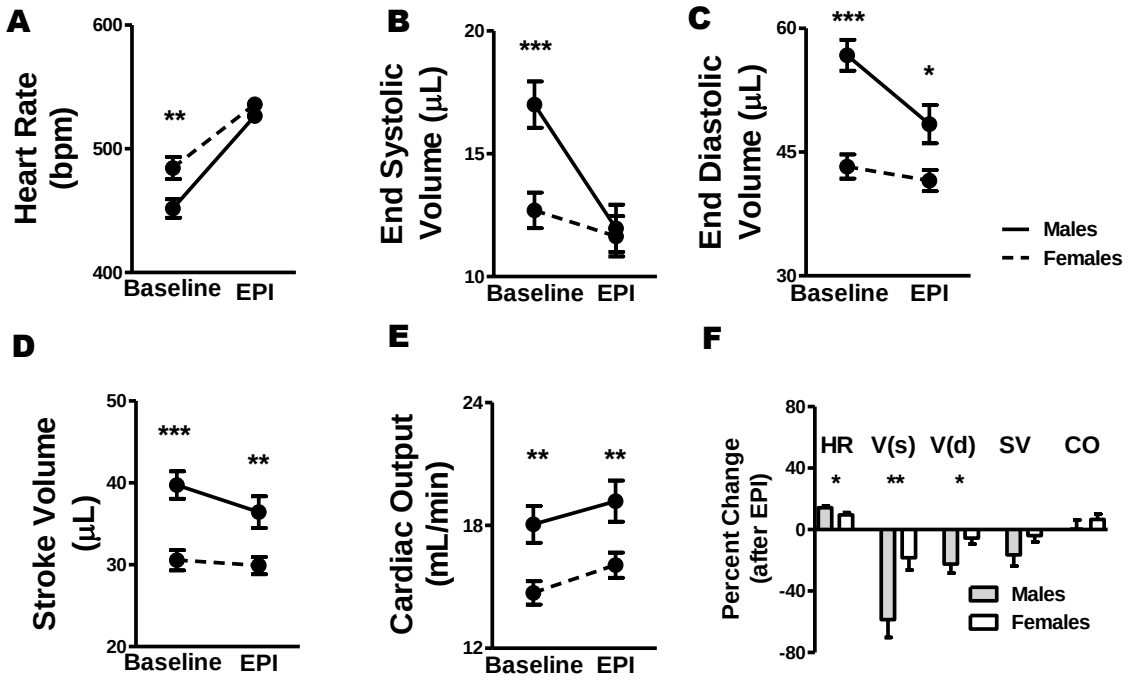

Figure 18 EPI injection of males and pre-menopausal 9 month old mice.

(A) Heart Rate (B) End Systolic Volume (C) End Diastolic Volume (D) Stroke Volume (E) Cardiac Output B-mode ultrasound analysis of 9 month old male and female mice before and after EPI challenge. (F) Percent change calculated in response to EPI in male and female mice. n=28 males and 30 females. Data represented as mean ± SEM. *, p>0.05; **, p>0.01; ***p>0.001.

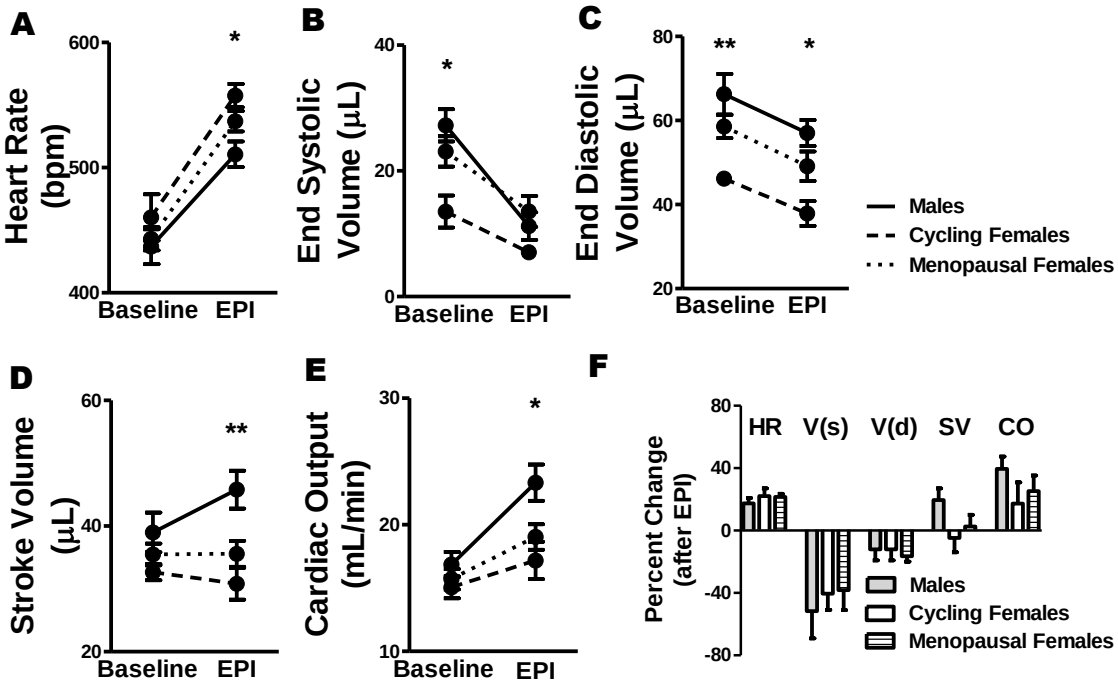

Figure 19 EPI injection of males, pre and post-menopausal females at 18 months.

(A) Heart Rate (B) End Systolic Volume (C) End Diastolic Volume (D) Stroke Volume (E) Cardiac Output B-mode ultrasound analysis of 18 month old male and female (cycling and menopausal) mice before and after EPI challenge. (F) Percent change calculated in response to EPI in male and female (cycling and menopausal) mice. n=6 males, 6 cycling females and 12 menopausal females. Data represented as mean ± SEM. *, $p>0.05$; **, $p>0.01$.

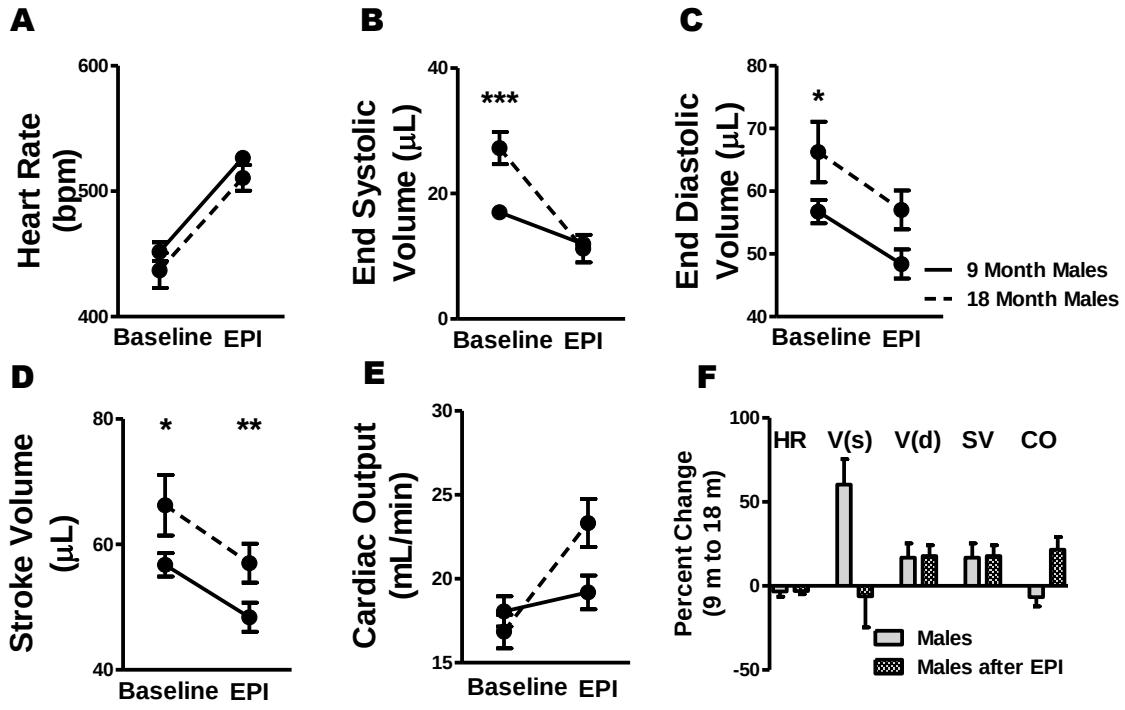

Figure 20 Effects of age and EPI in males.

(A) Heart Rate (B) End Systolic Volume (C) End Diastolic Volume (D) Stroke Volume (E) Cardiac Output B-mode ultrasound analysis of 9 and 18 month old male mice before and after EPI challenge. (F) Percent change calculated from 9 months to 18 months in response to EPI. n=28 at 9 months and 6 at 18 months. Data represented as mean ± SEM. *, p>0.05; **, p>0.01; ***p>0.001

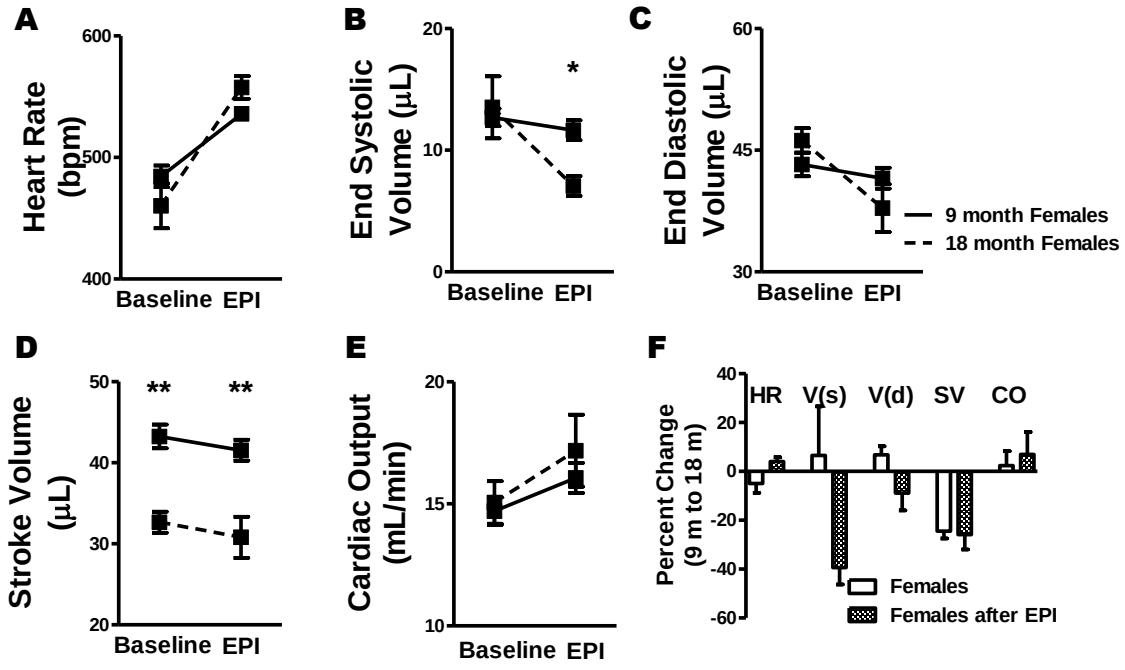

Figure 21 Effects of age and EPI in males.

A) Heart Rate (B) End Systolic Volume (C) End Diastolic Volume (D) Stroke Volume (E) Cardiac Output B-mode ultrasound analysis of 9 and 18 month old male mice before and after EPI challenge. (F) Percent change calculated from 9 months to 18 months in response to EPI. n=30 at 9 months and 6 at 18 months. Data represented as mean ± SEM. *, $p>0.05$; **, $p>0.01$.

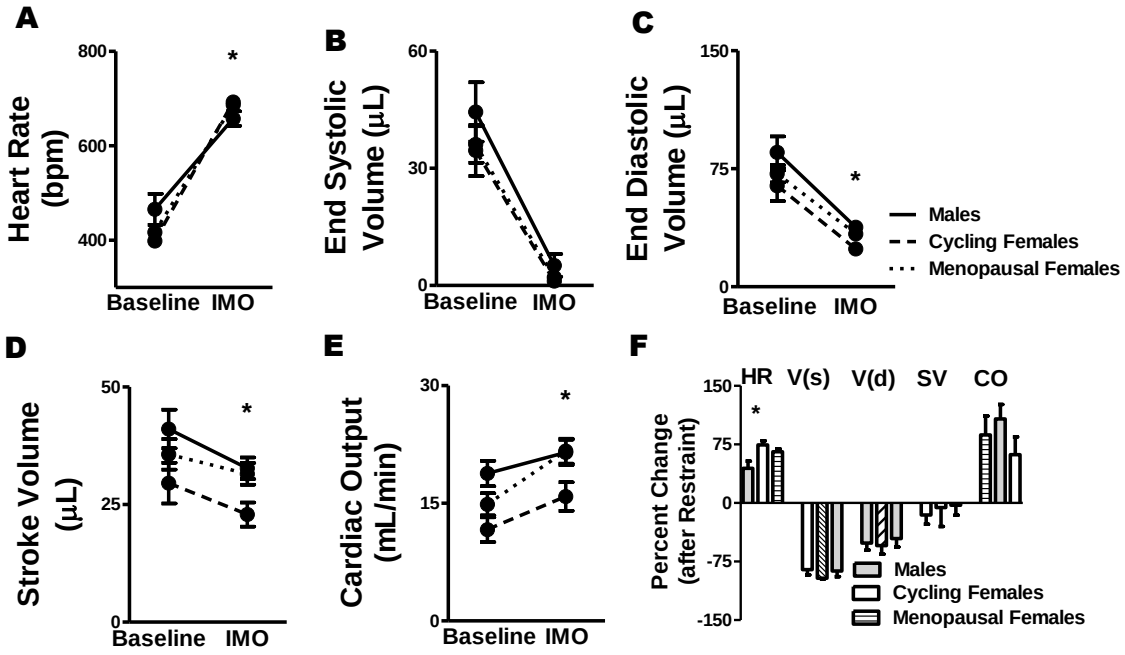

Figure 22 Immobilization stress on males, pre and post-menopausal females at 21 months old.

(A) Heart Rate (B) End Systolic Volume (C) End Diastolic Volume (D) Stroke Volume (E) Cardiac Output B-mode ultrasound analysis of 21 month old male and female (cycling and menopausal) mice before and after immobilization stress. (F) Percent change calculated in response to immobilization in male and female (cycling and menopausal) mice. n=6 males, 6 cycling females and 12 menopausal females. Data represented as mean ± SEM. *, p>0.05.

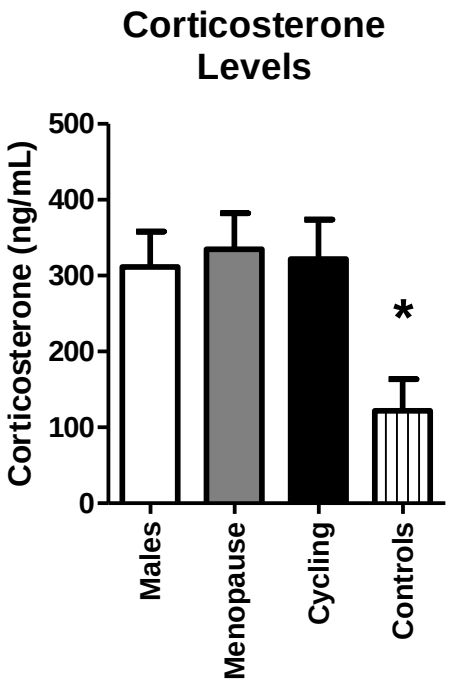

Figure 23 Corticosterone levels of males pre and post-menopausal females compared to unstressed controls.

Plasma corticosterone after immobilization stress in 21 month males, menopausal and cycling females compared to unstressed controls. n=6 males,11 menopausal females, 6 cycling females, and 4 unstressed controls. Data represented as mean ± SEM. *, p>0.05.

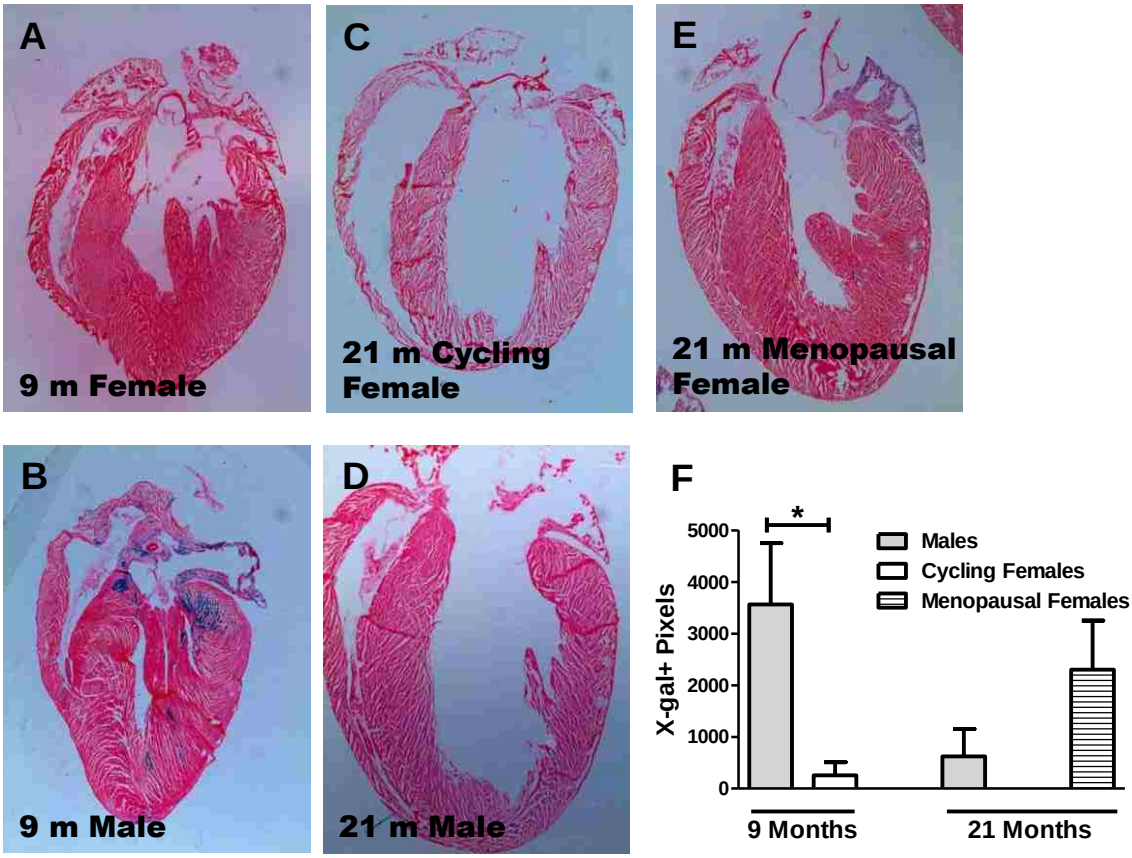

Figure 24 Representative X-gal staining of 9 month males and females and 21 month males and pre and post-menopausal females.

Representative x-gal staining of (A) female 9 month heart section (B) male 9 month heart section (C) 21 month cycling female heart section (D) 21 month male heart section (E) 21 month menopausal female heart section. (F) Quantification of x-gal+ blue pixels. n=7 males at 9 months, 5 females at 9 months, 5 males at 21 months, 4 cycling females at 21 months, 4 menopausal females at 21 months. Data represented as mean ± SEM. *, $p>0.05$.

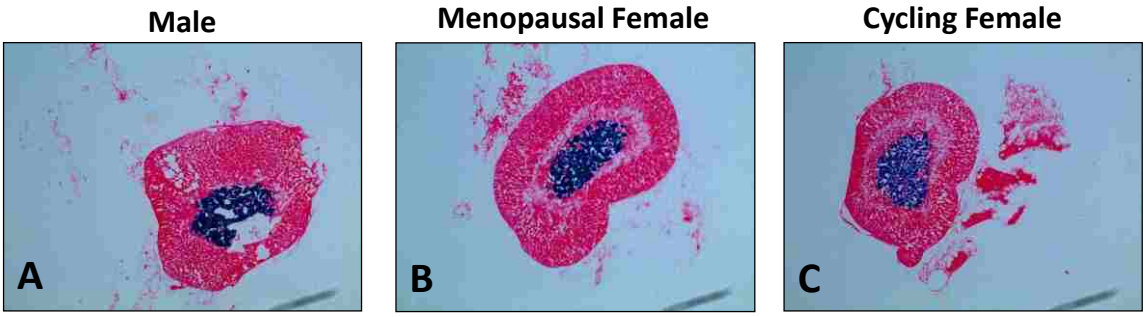

Figure 25 Representative adrenal sections from 21 month mice.

Representative x-gal staining of (A) male 21 month adrenal section (B) menopausal female 21 month adrenal section (C) cycling female 21 month adrenal section.

List of References

Baker, C., Katsandris, Rebekah, Van, Chaunhi and Steven Ebert (2014). Adrenaline and Stress-Induced Cardiomyopathies: Three competing hypotheses for mechanism(s) of action. In Adrenaline: Production, Role in Disease and Stress, Effects on the Mind and Body, A. Bennun, ed. (New York: Nova Science Publishers), pp. 81-116.

Borlaug, B.A., Redfield, M.M., Melenovsky, V., Kane, G.C., Karon, B.L., Jacobsen, S.J., and Rodeheffer, R.J. (2013). Longitudinal changes in left ventricular stiffness: a community-based study. Circulation Heart failure *6*, 944-952.

Cleland, J.G., Swedberg, K., Follath, F., Komajda, M., Cohen-Solal, A., Aguilar, J.C., Dietz, R., Gavazzi, A., Hobbs, R., Korewicki, J.*, et al.* (2003). The EuroHeart Failure survey programme-- a survey on the quality of care among patients with heart failure in Europe. Part 1: patient characteristics and diagnosis. European heart journal *24*, 442-463.

Cocco, G., and Chu, D. (2007). Stress-induced cardiomyopathy: A review. European journal of internal medicine *18*, 369-379.

Du, X.J. (2004). Gender modulates cardiac phenotype development in genetically modified mice. Cardiovascular research *63*, 510-519.

Dubey, R.K., and Jackson, E.K. (2001). Cardiovascular protective effects of 17beta-estradiol metabolites. J Appl Physiol (1985) *91*, 1868-1883.

Gao, X.M., Agrotis, A., Autelitano, D.J., Percy, E., Woodcock, E.A., Jennings, G.L., Dart, A.M., and Du, X.J. (2003). Sex hormones and cardiomyopathic phenotype induced by cardiac beta 2-adrenergic receptor overexpression. Endocrinology *144*, 4097-4105.

Grandi, A.M., Venco, A., Barzizza, F., Scalise, F., Pantaleo, P., and Finardi, G. (1992). Influence of age and sex on left ventricular anatomy and function in normals. Cardiology *81*, 8-13.

H. Sato, H.T., K. Dote, T. Uchida, M. Ishihara (1990). Tako-tsubo-like left ventricular dysfunction due to multivessel coronary spasm (Kagakuhyoronsha Publishing Co., Tokyo), pp. 56-64.

Hinojosa-Laborde, C., Chapa, I., Lange, D., and Haywood, J.R. (1999). Gender differences in sympathetic nervous system regulation. Clinical and experimental pharmacology & physiology *26*, 122-126.

Hogg, K., Swedberg, K., and McMurray, J. (2004). Heart failure with preserved left ventricular systolic function; epidemiology, clinical characteristics, and prognosis. Journal of the American College of Cardiology *43*, 317-327.

Hoyer, P.B., and Sipes, I.G. (2007). Development of an animal model for ovotoxicity using 4-vinylcyclohexene: a case study. Birth defects research Part B, Developmental and reproductive toxicology *80*, 113-125.

Kume, T., Kawamoto, T., Okura, H., Toyota, E., Neishi, Y., Watanabe, N., Hayashida, A., Okahashi, N., Yoshimura, Y., Saito, K.*, et al.* (2008). Local release of catecholamines from the hearts of patients with tako-tsubo-like left ventricular dysfunction. Circulation journal : official journal of the Japanese Circulation Society *72*, 106-108.

Luczak, E.D., and Leinwand, L.A. (2009). Sex-based cardiac physiology. Annual review of physiology *71*, 1-18.

McIntosh, V.J., Chandrasekera, P.C., and Lasley, R.D. (2011). Sex differences and the effects of ovariectomy on the beta-adrenergic contractile response. American journal of physiology Heart and circulatory physiology *301*, H1127-1134.

Olivetti, G., Giordano, G., Corradi, D., Melissari, M., Lagrasta, C., Gambert, S.R., and Anversa, P. (1995). Gender differences and aging: effects on the human heart. Journal of the American College of Cardiology *26*, 1068-1079.

Osuala, K., Telusma, K., Khan, S.M., Wu, S., Shah, M., Baker, C., Alam, S., Abukenda, I., Fuentes, A., Seifein, H.B.*, et al.* (2011). Distinctive left-sided distribution of adrenergic-derived cells in the adult mouse heart. PloS one *6*, e22811.

Regitz-Zagrosek, V., Brokat, S., and Tschope, C. (2007). Role of gender in heart failure with normal left ventricular ejection fraction. Progress in cardiovascular diseases *49*, 241-251.

Regitz-Zagrosek, V., Oertelt-Prigione, S., Seeland, U., and Hetzer, R. (2010). Sex and gender differences in myocardial hypertrophy and heart failure. Circulation journal : official journal of the Japanese Circulation Society *74*, 1265-1273.

Schaible, T.F., Malhotra, A., Ciambrone, G., and Scheuer, J. (1984). The effects of gonadectomy on left ventricular function and cardiac contractile proteins in male and female rats. Circulation research *54*, 38-49.

Schouwenberg, B.J., Rietjens, S.J., Smits, P., and de Galan, B.E. (2006). Effect of sex on the cardiovascular response to adrenaline in humans. Journal of cardiovascular pharmacology *47*, 155-157.

Schwertz, D.W., Vizgirda, V., Solaro, R.J., Piano, M.R., and Ryjewski, C. (1999). Sexual dimorphism in rat left atrial function and response to adrenergic stimulation. Molecular and cellular biochemistry *200*, 143-153.

Scott, J.M., Esch, B.T., Haykowsky, M.J., Isserow, S., Koehle, M.S., Hughes, B.G., Zbogar, D., Bredin, S.S., McKenzie, D.C., and Warburton, D.E. (2007). Sex differences in left ventricular function and beta-receptor responsiveness following prolonged strenuous exercise. J Appl Physiol (1985) *102*, 681-687.

Shao, Y., Redfors, B., Stahlman, M., Tang, M.S., Miljanovic, A., Mollmann, H., Troidl, C., Szardien, S., Hamm, C., Nef, H.*, et al.* (2013). A mouse model reveals an important role for catecholamine-induced lipotoxicity in the pathogenesis of stress-induced cardiomyopathy. Eur J Heart Fail *15*, 9-22.

Thawornkaiwong, A., Preawnim, S., and Wattanapermpool, J. (2003). Upregulation of beta 1-adrenergic receptors in ovariectomized rat hearts. Life sciences *72*, 1813-1824.

Ueyama, T. (2004). Emotional stress-induced Tako-tsubo cardiomyopathy: animal model and molecular mechanism. Annals of the New York Academy of Sciences *1018*, 437-444.

Vizgirda, V.M., Wahler, G.M., Sondgeroth, K.L., Ziolo, M.T., and Schwertz, D.W. (2002). Mechanisms of sex differences in rat cardiac myocyte response to beta-adrenergic stimulation. American journal of physiology Heart and circulatory physiology *282*, H256-263.

Wittstein, I.S., Thiemann, D.R., Lima, J.A., Baughman, K.L., Schulman, S.P., Gerstenblith, G., Wu, K.C., Rade, J.J., Bivalacqua, T.J., and Champion, H.C. (2005). Neurohumoral features of myocardial stunning due to sudden emotional stress. The New England journal of medicine *352*, 539-548.

Yoshida, T., Hibino, T., Kako, N., Murai, S., Oguri, M., Kato, K., Yajima, K., Ohte, N., Yokoi, K., and Kimura, G. (2007). A pathophysiologic study of tako-tsubo cardiomyopathy with F-18 fluorodeoxyglucose positron emission tomography. Eur Heart J *28*, 2598-2604.

CHAPTER FIVE: CONCLUSIONS

Cardiovascular disease is the primary cause of death in adults in the United States and accounts for 26.6 percent of all infants that die of congenital birth defects. Adrenergic hormones are known regulators of cardiovascular function in both embryos and adults, they are mediators of stress responses and have profound stimulatory effects on cardiovascular function. My thesis addressed critical questions regarding the involvement of catecholamines in the embryonic heart and the role of catecholamines in cardiac function in young and aged male and female hearts. I explored the roles of adrenergic hormones in the development of the embryonic conduction system as well as showed a link between adrenergic-hormones and mitochondrial functional maturation during embryogenesis. Further, I performed longitudinal high-resolution echocardiography on male and female mice incorporating menopausal status as a variable and tested the effect of stress on heart function by the injection of epinephrine and immobilization.

The major conclusions found from the second chapter of work presented here include:

1. Adrenergic deficiency leads to decreased connexin 43 in embryonic (E)10.5 atrioventricular junctional regions but not E9.5 mouse hearts
2. Atrioventricular conduction is significantly slower in adrenergic-deficient hearts
3. Arrhythmic activity is significantly induced in adrenergic-deficient hearts compared with adrenergic-competent controls

These findings indicate that adrenergic hormones are critical for the development of the cardiac conduction system. Disruption of this key signaling pathway either by genetic anomalies or pharmacological intervention could result in permanent cardiovascular conduction defects. To further understand the nature of the atrioventricular delay observed in the adrenergic-deficient hearts and the association, if any, of decreased Cx43 the use of CRISPR (clustered regularly interspaced short palindromic repeats)/Cas9 modeling could provide a powerful genetic tool (Mali et al., 2013). The *Dbh* gene could easily be disrupted in a Cx43 overexpression mouse model (Ewart et al., 1997) using these new technologies and creating a novel transgenic colony. Again, utilizing the microelectrode arrays we would determine if the loss of adrenergic hormones slow the propagation of the conduction system from the atrium to the ventricle through the A-V region in this unique model. Further, the characterization of Cx43 protein levels at E9.5-E11.5 in the adrenergic-deficient embryonic hearts will prove incredibly informative. While, we do see a decrease in immunofluorescence staining of Cx43, a direct measure of protein content would elucidate if there is true down regulation of this important gap junction protein in an adrenergic-deficient state. Lastly, as mentioned previously the gene and protein levels of connexin 45, 40, and 37.5 would provide information if there is any compensation by other gap junction proteins that are known to be expressed in the early heart.

The major conclusions found from the third chapter of work presented here include:

1. Adrenergic hormones are necessary to maintain sufficient ATP/ADP ratios
2. Extracellular acidification rates and oxygen consumption rates are significantly decreased in adrenergic-deficient hearts during late periods of embryonic development
3. Metabolic steady-state substrate levels are unaffected due to the loss of adrenergic hormones
4. Mitochondrial biogenesis genes are unaffected due to the loss of adrenergic hormones
5. Mitochondrial membrane potential is similar between adrenergic-deficient and competent embryonic hearts
6. Adrenergic hormones influence embryonic cardiac mitochondrial morphology

The loss of adrenergic hormones results in a severe energy deficiency in the developing embryonic heart during the critical transition from embryonic to fetal development. This period coincides with the “embryonic shift” from mainly glycolytic mechanisms to oxidative phosphorylation energy production. Thus adrenergic hormones could be a major driving factor for this shift in energy production modalities.

Potential exploration into the involvement of catecholamines and the mechanism(s) that drive this shift will provide knowledge of the basic organization of the energy metabolism system within mammalian development. Possible explanations for the necessity of adrenergic hormones in up regulation mitochondrial activity could involve the assembly of the supercomplexes composed of the electron transport complex. While the machinery of each

complex (I-V) is maternally inherited, and present from fertilization, the organization of these individual complexes is a multifaceted and understudied field. It could conceivably be the presence and PKA stimulation driven by adrenergic hormones that facilitates the joining of the complexes into a functional supercomplex.

Additionally, a prominent feature of the work discussed in this chapter includes irregularly shaped and elongated mitochondria. The mechanistic rationale behind this intriguing finding is currently unknown, however, future studies involve the examination of mitochondrial fission and fusion genes. The fission genes include *dynamin-related protein 1* (*Drp1)* and *fission 1 (Fis1)* and the mitochondrial fusion genes localized to the outer membrane are *mitofusin 1* (*Mfn1*) and *mitofusion 2* (*Mfn2*). Additionally, the inner membrane fusion gene is *optic atrophy 1* (*Opa1*) (Knott et al., 2008). While the gene expression levels of these fission/fusion regulators may be informative in determining a causal nature of the mitochondrial morphological abnormalities observed in the adrenergic-deficient embryonic heart, protein levels, as well of phosphorylation status could be of greater enlightenment. Drp1 for example is known to be regulated by PKA phosphorylation on residue S656 in rats. This phosphorylation negatively regulates Drp1 and thus inhibits fission (Chang and Blackstone, 2007). Similarly, Mfn2 was discovered to contain a PKA phosphorylation site, S442 in rats. While the rate of fusion was not examined in the phospho-deficient of phospho-mimetic states the effects of vascular smooth muscle cell proliferation as a result of Mfn2

was found to be highly correlated with the phosphorylation status (Zhou et al., 2010).

An interesting feature of the *Dbh*$^{-/-}$ embryos is the subviability seen in the maternal heterozygous as compared to the complete embryonic lethality observed in the maternal homozygous state. It has been hypothesized the explanation for this phenomenon is due to maternal adrenergic hormonal influence (Thomas et al., 1995). However, mitochondria and the mitochondrial genome, containing any mutations, are inherited solely from the maternal egg. Within all mitochondrial dysfunction models a threshold effect occurs wherein the mutational load reaches a point the phenotype presents itself and under this level the phenotype is muted. A potential future direction would be to perform a microinjection of eggs that have undergone *in vitro* fertilization from heterozygous (*Dbh*$^{+/-}$) dam and sire into a homozygous (*Dbh*$^{-/-}$) pseudopregnant female. Within this investigation one could test if the lack of maternal hormones cause the early embryonic lethality or if the incomplete penetrance of the mitochondrial mutational load inherited from a heterozygous mother is the explanation for the subviability

The major conclusions found from the fourth chapter of work presented here include:

1. Differential left ventricular response to epinephrine and immobilization stressors in males versus females

2. Similar left ventricular responses to epinephrine and immobilization stressors were seen between males and menopausal females as compared to age-matched cycling females
3. A drastic reappearance of intrinsic cardiac adrenergic cells were observed and quantified in the menopausal left ventricular and apical regions of the heart

The differential responses to stressors in combination with the pattern of intrinsic adrenergic myocardium could provide useful information for the clinical syndrome known as takotsubo cardiomyopathy. The creation of a mouse model for this stress induced cardiomyopathy yields a powerful tool for understanding the currently undefined pathophysiology. Much work has been conducted regarding the design of an animal model, with little understanding of the mechanisms driving this syndrome (Shao et al., 2013a; Shao et al., 2013b).

The modes of stress induction in the mouse model presented here, in addition to menopausal induction, provide a scenario quite similar to the human condition. However, a potential pitfall in utilizing the mouse as a surrogate for the human cardiovascular system is the over stimulated nature of the mouse in a basal state. The conscious mouse heart rate ranges from 500-650 beats per minute were as the average human heart rate is 60-100 beats per minute. The mouse is already in a “stressed” state and external stimuli (i.e. epinephrine and or restraint) may not have the complete desired outcome. For this reason the use of larger animal models that are more akin to human cardiovascular function, such as rabbits, dogs, or cats, may be a suitable alternative to the use of rodents.

The mouse model utilized here, *Pnmt*$^{+/Cre}$ *ROSA26*$^{+/\beta gal}$, provided the opportunity to investigate the intrinsic adrenergic myocardium over time and in response to menopausal status. However, the LacZ staining observed here is a historical representation of cells that are capable of producing stress hormones. Within this study we have not measured the production of epinephrine or norepinephrine in the heart in response to menopause or stress. A potential experiment to test the levels of NE/EPI produced would involve culturing the area(s) most heavily stained (i.e. the left ventricle and atrium) in the aged and menopausal hearts as compared to controls. While the use of restraint stress would not be feasible, provocation with isoproterenol could induce increased beating activity in the cultured myocytes and allow for quantification of the NE and EPI that is being produced in response to stres. While these experiments could be informative, they would require a new cohort of mice and reproduction of the colony.

Alternatively, the current samples available from the study performed here can be sectioned and stained directly for norepinephrine, epinephrine or other markers such as Dbh and Pnmt. While quantification is certainly a challenge with immunofluorescence, differences can be readily observed, especially if the intensity is electronically quantified using 3D software such as Volocity® (Perkin Elmer). By employing this method both functional data, via echocardiography, and biochemical depiction of the levels of adrenergic hormones present in the areas that stain heavily with LacZ.

The work performed here demonstrates the importance of adrenergic hormones in both the developing cardiovascular system as well as the adult heart. Additionally, this work provides a unique perspective on the effect adrenergic hormones have on cardiovascular function, heart failure, and sudden cardiac death. These adult cardiac disease states are often capable of prevention through manipulation of life style, congenital malformations however, presents at a stage so early in the pregnancy that most women do not realize they are even pregnant and have the ability to alter the course of gestation. Surgical intervention is commonly the only treatment option available to correct these congenital heart defects. Thus understanding the typical embryogenesis and organogenesis patterns and the downstream implications these hormones have is of critical importance to developing new treatment options and potentially prevention of congenital heart disease.

List of References

Chang, C.R., and Blackstone, C. (2007). Drp1 phosphorylation and mitochondrial regulation. EMBO Rep *8*, 1088-1089; author reply 1089-1090.

Ewart, J.L., Cohen, M.F., Meyer, R.A., Huang, G.Y., Wessels, A., Gourdie, R.G., Chin, A.J., Park, S.M., Lazatin, B.O., Villabon, S.*, et al.* (1997). Heart and neural tube defects in transgenic mice overexpressing the Cx43 gap junction gene. Development *124*, 1281-1292.

Knott, A.B., Perkins, G., Schwarzenbacher, R., and Bossy-Wetzel, E. (2008). Mitochondrial fragmentation in neurodegeneration. Nat Rev Neurosci *9*, 505-518.

Mali, P., Esvelt, K.M., and Church, G.M. (2013). Cas9 as a versatile tool for engineering biology. Nature methods *10*, 957-963.

Shao, Y., Redfors, B., Scharin Tang, M., Mollmann, H., Troidl, C., Szardien, S., Hamm, C., Nef, H., Boren, J., and Omerovic, E. (2013a). Novel rat model reveals important roles of beta-adrenoreceptors in stress-induced cardiomyopathy. Int J Cardiol.

Shao, Y., Redfors, B., Stahlman, M., Tang, M.S., Miljanovic, A., Mollmann, H., Troidl, C., Szardien, S., Hamm, C., Nef, H.*, et al.* (2013b). A mouse model reveals an important role for catecholamine-induced lipotoxicity in the pathogenesis of stress-induced cardiomyopathy. Eur J Heart Fail *15*, 9-22.

Thomas, S.A., Matsumoto, A.M., and Palmiter, R.D. (1995). Noradrenaline is essential for mouse fetal development. Nature *374*, 643-646.

Zhou, W., Chen, K.H., Cao, W., Zeng, J., Liao, H., Zhao, L., and Guo, X. (2010). Mutation of the protein kinase A phosphorylation site influences the anti-proliferative activity of mitofusin 2. Atherosclerosis *211*, 216-223.